

NUMERICAL ANALYSIS ON THE BEHAVIOUR
OF CFRP SHEAR-STRENGTHENED RC DEEP
BEAMS WITH LARGE SQUARE AND
CIRCULAR OPENINGS

SHIM CHEE WEI

B.ENG (HONS.) CIVIL ENGINEERING
UNIVERSITY MALAYSIA PAHANG

UNIVERSITI MALAYSIA PAHANG

DECLARATION OF THESIS AND COPYRIGHT

Author's full name : **SHIM CHEE WEI**

Date of birth : **29 MAY 1991**

Title : **NUMERICAL ANALYSIS ON THE BEHAVIOUR OF CFRP SHEAR –
STRENGTHENED RC DEEP BEAMS WITH LARGE SQUARE AND
CIRCULAR OPENINGS**

Academic Session : **2014/2015**

I declare that this thesis is classified as :

CONFIDENTIAL (Contains confidential information under the Official Secret Act 1972)*

RESTRICTED (Contains restricted information as specified by the organization where research was done)

OPEN ACCESS I agree that my thesis to be published as online open access (Full text)

I acknowledged that Universiti Malaysia Pahang reserves the right as follows :

1. The thesis is the property of Universiti Malaysia Pahang.
2. The Library of Universiti Malaysia Pahang has the right to make copies for the purpose of research only.
3. The Library has the right to make copies of the thesis for academic exchange.

Certified By:

(Student's Signature)

(Signature of Supervisor)

910529-14-5131
(New IC / Passport Number)

DR. CHIN SIEW CHOO
Name of Supervisor

Date :

Date :

NOTES :

* If the thesis is CONFIDENTIAL or RESTRICTED, please attach with the letter from the organization with period and reasons for confidentiality or restriction

NUMERICAL ANALYSIS ON THE BEHAVIOUR OF CFRP SHEAR-
STRENGTHENED RC DEEP BEAMS WITH LARGE
SQUARE AND CIRCULAR OPENINGS

SHIM CHEE WEI

Report submitted in partial fulfilment of the requirements
for the award of the degree of
Bachelor Eng. (Hons.) Civil Engineering

Faculty of Civil Engineering and Earth Resources
UNIVERSITI MALAYSIA PAHANG

JUNE 2015

SUPERVISOR'S DECLARATION

We hereby declare that we have checked this thesis and in our opinion, this thesis is adequate in terms of scope and quality for the award of the degree of Bachelor of Civil Engineering (Hons.).

Signature :
Name of Supervisor : DR. CHIN SIEW CHOO
Position : LECTURER
Date :

STUDENT'S DECLARATION

I hereby declare that the work in this thesis is my own except for quotations and summaries which have been duly acknowledged. The thesis has not been accepted for any degree and is not concurrently submitted for award of other degree.

Signature :

Name : SHIM CHEE WEI

ID Number : AA11048

DATE :

Specially dedicated to my parents,

ACKNOWLEDGEMENTS

I am grateful and would like to express my sincere gratitude to my supervisor Dr. Chin Siew Choo for her germinal ideas, invaluable guidance, continuous encouragement and constant support in making this research possible. She has always impressed me with her outstanding professional conduct and her strong conviction for science. I appreciate their consistent support from the first day I applied to graduate program to these concluding moments. I am truly grateful for her progressive vision about my study in science, tolerance of my careless mistakes, and her commitment to our research studies.

My sincere thanks go to all my friends and members of the staff of the Civil Engineering Department (Design Laboratory), UMP, who helped me in many ways and made my stay at UMP pleasant and unforgettable.

I acknowledge my sincere indebtedness and gratitude to my parents for their love, dream and sacrifice throughout my life. I acknowledge the sincerity of my parents-in-law, who consistently encouraged me to carry on my higher studies in Malaysia.

ABSTRACT

This study presents a finite element analysis to investigate the behaviour of reinforced concrete deep beams with square and circular openings. Deep beams are always constructed at the lower floors as transfer beams to transfer the loads from the entire building to the foundations. Reinforced concrete (RC) acts as one of the most essential building materials and it is widely used in the construction due to its low pricing, efficiency and strength of the reinforced concretes as well as its stiffness. Openings are inevitable for the architectural and mechanical purpose to accommodate the conduits. However, presence of openings in the deep beams will significantly reduce the load capacity of the deep beams, as well as excessive cracking and deflection. Strengthening by Carbon Fibre Reinforced Polymer helps in regain the load bearing capacity of the deep beams. Researches were focus on the experimental work and hence this study conducted in terms of the numerical aspects and finite element analysis. ANSYS CivilFEM 12.0, a finite element modelling and analysis software, was used to analysis the deep beams. Three – dimensional modelling of RC deep beams was adopted in this study. A total of 14 beams including one control beam were modelled as simply supported beam with openings where the locations of the openings were at the support which was 300 mm from the edge of the beams. Two incremental loads were applied at the 800 mm from the edge of the beams. The beams was symmetrical in shape. The beams had the cross sections of 120 mm x 600 mm and 2400 mm in length with square and circular openings. The objectives of this study were to determine the most effective strengthening method by using CFRP in terms of load-deflection behaviours, crack patterns, stress and strain contours. This study was validated by experimental results. Various strengthening methods were used to identify the most effective method of strengthening which included orientation of CFRP in vertical alignment (90°), horizontal alignment (0°), whole piece, cut strips, surface strengthening and U-wrap strengthening. Deep beams with openings failed due to shear cracks because of the sharp edges of the openings. From the finding, the square opening and circular opening experienced a reduction of 62.0% and 51.3% in beam capacity, respectively. From the various strengthening configurations of CFRP, configuration with vertical alignment, whole piece and U-wrap strengthening method was the most effective method. CFRP restored the load bearing capacity with most effective method by 63.0% and 85.0% for deep beams with square and circular openings respectively. A comparison between the numerical and experiments results showed that a comparable agreement on the load deflection behaviours and strong agreement on the crack patterns.

ABSTRAK

Kajian ini membentangkan satu analisis unsur terhingga untuk mengkaji sifat/kelakuan rasuk konkrit bertetulang dalam dengan pembukaan segi empat tepat dan bulat. Rasuk konkrit bertetulang dalam sentiasa dibina di tingkat yang lebih rendah untuk memindahkan beban daripada seluruh bangunan kepada asas-asas. Konkrit Bertetulang (RC) sebagai salah satu bahan binaan yang paling penting dan ia digunakan secara meluas dalam pembinaan disebabkan oleh harga yang rendah, kecekapan dan kekuatan konkrit bertetulang serta kekejangan yang tinggi. Bukaannya adalah tidak dapat dielakkan bagi tujuan senibina dan mekanikal untuk menampung konduit. Walaubagaimanapun, kewujudan bukaan pada gelombang-gelombang yang mendalam dengan ketara akan mengurangkan kapasiti beban gelombang-gelombang yang mendalam, serta berlebihan keretakan dan pesongan. Pengukuhan dengan polimer diperkukuh gentian karbon membantu dalam pemulihan kekuatan dalam kapasiti konkrit bertetulang. Walau bagaimanapun, penyelidikan sebelum adalah lebih fokus kepada kerja-kerja eksperimen dan oleh yang demikian kajian ini dijalankan dari segi aspek berangka dan analisis unsur terhingga. ANSYS CivilFEM 12.0, satu unsur terhingga pemodelan dan analisis perisian, telah digunakan untuk analisis gelombang-gelombang yang mendalam. Tiga – pemodelan dimensi rasuk mendalam RC telah digunakan dalam kajian ini. Sejumlah 14 rasuk yang termasuk satu rasuk kawalan adalah peringkat sebagai rasuk semata-mata disokong dengan bukaan di mana lokasi yang bukaan berada pada penyokong yang seluas 300 mm dari tepi gelombang-gelombangnya. Dua beban kenaikan akan dikenakan pada dalam 800 mm dari tepi gelombang-gelombangnya. Rasuk dalam adalah simetri dalam bentuk. Rasuk dalam yang mempunyai bahagian cross 120 mm x 600 mm dan 2400 mm panjang dengan pembukaan segi empat tepat dan bulatan. Objektif kajian ini adalah untuk menentukan kaedah pengukuhan yang berkesan dengan menggunakan CFRP dari segi beban-pesongan tingkah laku, corak retak, kontur tekanan dan ketegangan. Kajian ini telah disahkan oleh keputusan eksperimen. Pelbagai kaedah pengukuhan telah digunakan untuk mengenal pasti kaedah yang paling berkesan bagi pengukuhan yang merangkumi orientasi CFRP di jajaran menegak (90°), penjajaran mendatar (0°), seluruh bahagian, memotong jalur, permukaan pengukuhan dan pemantapan U-Balut. Rasuk yang mendalam dengan bukaan gagal kerana retak ricih kerana tepi tajam bukaan. Daripada kajian, pembukaan segi empat tepat dan bulatan mengalami penurunan sebanyak 62.0% dan 51.3% dalam rasuk kapasiti masing-masing. Dari pelbagai konfigurasi pengukuhan daripada CFRP, konfigurasi dengan jajaran menegak, seluruh bahagian dan kaedah pengukuhan U-Balut adalah kaedah yang paling berkesan. CFRP semula keupayaan galas dengan kaedah paling berkesan 85.0% dan 63.0% bagi rasuk dalam yang mendalam dengan pembukaan Pekeliling dan bukaan persegi masing-masing. Perbandingan antara yang berangka dan keputusan ujikaji menunjukkan bahawa keputusan setanding beban pesongan sifat rasuk dan keputusan yang kukuh pada pola retak.

TABLE OF CONTENTS

	Page
SUPERVISOR’S DECLARATION	ii
STUDENT’S DECLARATION	iii
ACKNOWLEDGEMENTS	iv
ABSTRACT	v
ABSTRAK	vi
TABLE OF CONTENTS	viii
LIST OF TABLES	xi
LIST OF FIGURES	xii
LIST OF SYMBOLS	xviii
LIST OF ABBREVIATIONS	xix
CHAPTER 1 INTRODUCTION	
1.1 BACKGROUND OF THE STUDY	1
1.1.1 Reinforced Concrete Deep Beams	2
1.1.2 Reinforced Concrete Deep Beams with Openings	2
1.1.3 Finite Element Analysis by ANSYS CivilFEM 12.0	3
1.1.4 Carbon Fibre Reinforced Polymer (CFRP)	4
1.1.5 Importance of Strengthening	5
1.2 PROBLEM STATEMENT	6
1.3 OBJECTIVES OF STUDY	7
1.4 SCOPES OF STUDY	7
1.5 SIGNIFICANCES OF STUDY	9
CHAPTER 2 LITERATURE REVIEWS	
2.1 INTRODUCTION	10
2.2 STRUCTURAL BEHAVIOUR OF RC DEEP BEAM	11
2.3 STRUCTURAL BEHAVIOUR OF RC DEEP BEAM WITH OPENINGS	12

2.3.1	Effects of Openings on Sizes, Shapes and Locations	12
2.4	FINITE ELEMENT ANALYSIS BY NUMERICAL APPROACH	14
2.4.1	Finite Element Analysis by ANSYS	16
2.5	MATERIAL MODELLING	17
2.5.1	Concrete	17
2.5.2	Reinforcement Steel Bar	21
2.5.3	Carbon Fibre Reinforced Polymer	21
2.5.4	Modelling Interface of FRP and Concrete	22
2.6	BEHAVIOUR OF RC DEEP BEAMS WITH OPENINGS STRENGTHENED BY CFRP	25
2.6.1	Behaviour and Performance of CFRP	26
2.6.2	Advantages and Disadvantages of Using CFRP	27
2.6.3	Method and Application of CFRP	28
2.7	SUMMARY	29
CHAPTER 3 RESEARCH METHODOLOGY		
3.1	INTRODUCTION	35
3.2	RC BEAM MODELS	36
3.2.1	Control Beam	36
3.2.2	RC Deep Beams with Square and Circular Openings	37
3.3	MATERIAL PROPERTIES	39
3.4	DETAILS OF STUDY	42
3.4.1	Control Beam	45
3.4.2	RC Deep Beam with Square Opening without Strengthening of CFRP	47
3.4.3	RC Deep Beam with Square Opening Strengthened by CFRP	48
3.4.4	RC Deep Beam with Circular Opening without Strengthening of CFRP	51
3.4.5	RC Deep Beam with Circular Opening Strengthened by CFRP	52
3.4.6	Configuration of CFRP	53
3.5	ANALYSIS OF RC DEEP BEAM BY USING ANSYS CIVILFEM	57
	12.0	
3.5.1	Pre-processing	57
3.5.2	Material Parameters	57
3.5.2.1	Geometrical Nodes	63
3.5.2.2	Geometrical Lines	65
3.5.2.3	Mesh Generation	66
3.5.2.4	Steel Reinforcement Bar	67
3.5.2.5	Supports and Actions	68

3.5.2.6	Loading History and Solution Parameters	70
3.5.2.7	Monitoring Points	70
3.5.3	Finite Element Non-Linear Analysis	71
3.5.3.1	Starting Analysis	71
3.5.3.2	Interactive Window	71
3.6	SUMMARY OF PROCEDURES	72
3.7	METHODOLOGY CHART	73

CHAPTER 4 RESULTS AND DATA ANALYSIS

4.1	INTRODUCTION	74
4.2	LOAD – DEFLECTION BEHAVIOUR	74
4.2.1	Control beam	75
4.2.2	RC Deep Beams with Openings	76
4.2.3	RC Deep Beams with Openings Strengthened by CFRP	77
4.2.3.1	Surface Strengthening for Deep Beams with Square Openings	77
4.2.3.2	Surface Strengthening for Deep Beams with Circular Openings	78
4.2.3.3	U-wrap strengthening (Square & Circular Openings)	81
4.3	CRACK PATTERN	82
4.3.1	Control beam	83
4.3.2	RC Deep Beams with Square and Circular Openings	85
4.3.3	RC Deep Beams with Openings Strengthened by CFRP	87
4.3.3.1	Surface strengthening – Deep Beams with Square Openings (Initial Step)	87
4.3.3.2	Surface strengthening – Deep Beams with Square Openings (Critical Step)	89
4.3.3.3	Surface strengthening – Deep Beams with Circular Openings	90
4.3.3.4	U-wrap strengthening	91
4.4	STRAIN CONTOUR	93
4.4.1	Control Beam	93
4.4.2	RC Deep Beams with Openings (DBS and DBC)	94
4.4.3	RC Deep Beams with Openings Strengthened by CFRP	97
4.5	STRESS CONTOUR	102
4.5.1	Control beam	102
4.5.2	RC Deep Beams with Openings	103
4.5.3	RC Deep Beams with Openings Strengthened by CFRP (Surface Strengthening)	105
4.6	VALIDATION OF FINITE ELEMENT ANALYSIS RESULTS WITH EXPERIMENTAL RESULTS	108
4.6.1	Control Beam	108

4.6.2	RC Deep Beams with Openings (Square and Circular)	109
4.6.3	Strengthened RC Deep Beams	112
4.6.3.1	Surface Strengthening for RC Deep Beams with Circular Openings (DBCS1)	112
4.6.3.2	U-wrap strengthening of DBSS7 and DBCS3	113
4.7	SUMMARY OF THE RESULTS	116

CHAPTER 5 CONCLUSION AND RECOMMENDATIONS

5.1	CONCLUSION	117
5.2	RECOMMENDATION FOR THE FUTURE RESEARCH	119

REFERENCES	120
-------------------	-----

APPENDICES

A	Types of crack patterns in ANSYS	123
B	Extra result of DBSS7	124
C	Gantt chart of the study	126

LIST OF TABLES

Table No.	Title	Page
2.1	Geometrical characteristics of tested beams	29
2.2	FRP shear-strengthening details	30
2.3	Details and results of various finite element analysis	31
3.1	Test parameters	44
3.2	Element types used in ANSYS CivilFEM 12.0	58
3.3	Summary of material properties assigned to the eleme	60
3.4	Real constants of steel reinforcements by area of reinforcements	62
3.5	Geometrical nodes for steel reinforcement	63
4.1	Comparison of FEA and experimental results and percentage of the beams	116

LIST OF FIGURES

Figure No.	Title	Page
2.1	Detailed of the tested crushed stone concrete deep beams	13
2.2	Stress-strain curve for concrete	19
2.3	Crack patterns at failure	20
2.4	Bilinear bond-slip model	23
2.5	Finite element model	24
2.6	A typical FE model	28
3.1	Schematic diagram of control beam	36
3.2	Arrangement of steel reinforcement in control beam	36
3.3	Schematic diagram of deep beam with square openings	37
3.4	Arrangement of steel reinforcements in deep beam with square openings	37
3.5	Schematic diagram of deep beam with circular openings	38
3.6	Arrangement of steel reinforcements in deep beam with circular openings	38
3.7	Type of elements that represented the materials used in experimental	40
3.8	Material properties of all the elements needed in ANSYS	40
3.9a	Elements that can be chosen to set for the real constant	41
3.9b	Total of five sets real constant had been set for all the elements needed	41
3.10	Initiation of CivilFEM 12.0	42
3.11	International standards and SI units	43
3.12	Control beam in ANSYS CivilFEM 12.0	46
3.13	Steel reinforcement modelling	46

3.14	Model of deep beam with square opening and the locations of steel reinforcement	47
3.15	CFRP laminate to strengthen the deep beam with square opening	49
3.16	CFRP was pasted in four different pieces	49
3.17	U-wrap strengthening method	50
3.18	Modelling of alignment of CFRP (shown in circle)	50
3.19	RC deep beam with circular opening	51
3.20	RC deep beam with circular opening strengthened by surface-strengthening	52
3.21	RC deep beam with circular opening strengthened by U-wrap	53
3.22	CFRP with whole piece in vertical alignment for deep beams with square opening (DBSS1, DBSS5)	54
3.23	CFRP with whole piece in horizontal alignment for deep beams with square opening (DBSS2, DBSS6)	54
3.24	Four pieces of CFRP with square opening in vertical alignment (DBSS3)	55
3.25	Four pieces of CFRP with square opening in vertical alignment (DBSS4)	55
3.26	CFRP with circular opening in vertical alignment (DBCS1 & DBCS3)	56
3.27	CFRP with circular opening in horizontal alignment (DBCS2 & DBCS4)	56
3.28	SOLID65, material code for concrete strength G35	58
3.29	All the elements types chosen for this study	59
3.30	Example on choosing the materials properties	60
3.31	Summary of materials assigned to the elements in ANSYS	61
3.32	Input of area of the steel to define the real constant	62
3.33	Geometrical nodes on the Cartesian plane along x, y and z directions	64

3.34	Geometrical lines of examples of shear link in ANSYS	65
3.35	CFRP attribute was assigned to the layer during meshing	66
3.36	Steel reinforcement in ANSYS CivilFEM 12.0	67
3.37	Support with all degree of freedom are restrained	68
3.38	Support with restrained y-direction	69
3.39	Pressure (area loads) was applied on the deep beam	69
3.40	Interaction window to set the option for load applying	70
3.41	Interactive window of initializing the analysis	71
3.42	Methodology chart of work flow	73
4.1	Load-deflection curve of control beam (CB)	75
4.2	Load-deflection curves for CB, DBS and DBC	76
4.3	Load-deflection curve of deep beams with square openings	78
4.4	Differences in the recovery of load capacities of DBCS1 and DBCS2	79
4.5	Comparison of control beam and all the beams strengthened by surface strengthening method in circular and square openings	80
4.6	Load-deflection curves of DBSS5, DBSS6, DBCS3 and DBCS4	81
4.7	Symbols of crack pattern	83
4.8a	Crack pattern of control beam	84
4.8b	Crack pattern of control beam at the last load step	84
4.9a	Crack pattern of DBS at the initial step	85
4.9b	Crack pattern of DBS at the last load step	86
4.10a	Crack pattern of DBC at the first load step	86
4.10b	Crack pattern of DBC at the last load step	87
4.11a	Crack pattern of DBS at the initial step	88

4.11b	Crack pattern of DBSS1 at the initial step	88
4.11c	Crack pattern of DBSS2 at the initial step	88
4.11d	Crack pattern of DBSS3 at initial step	88
4.11e	Crack pattern of DBSS4 at initial step	88
4.12a	Crack pattern of DBSS1 at the final step	89
4.12b	Crack pattern of DBSS2 at the final step	89
4.12c	Crack pattern of DBSS3 at the final step	89
4.12d	Crack pattern of DBSS4 at the final step	89
4.13a	Crack pattern of DBCS1 at the initial step	90
4.13b	Crack pattern of DBCS1 at the final step	90
4.14a	Crack pattern of DBCS2 at the initial step	90
4.14b	Crack pattern of DBCS2 at the final step	90
4.15a	Crack pattern of DBSS5 at the initial step	91
4.15b	Crack pattern of DBSS5 at the final step	91
4.15c	Crack pattern of DBSS6 at the initial step	92
4.15d	Crack pattern of DBSS6 at the final step	92
4.16a	Crack pattern of DBCS4 at the initial step	92
4.16b	Crack pattern of DBCS4 at the final step	92
4.17a	Strain contour of control beam at initial load step	93
4.17b	Strain contour of control beam at ending load step	94
4.18a	Strain contour of DBS at initial load step	95
4.18b	Strain contour of DBS at critical load step	95
4.18c	Strain contour of DBC at initial load step	96
4.18d	Strain contour of DBC at critical load step	96

4.19a	Strain contour of DBSS1 at initial load step	97
4.19b	Strain contour of DBSS1 at critical load step	98
4.19c	Strain contour of DBSS5 at initial load step	98
4.19d	Strain contour of DBSS5 at critical load step	99
4.19e	Strain contour of DBCS1 at initial load step	100
4.19f	Strain contour of DBCS1 at critical load step	100
4.19g	Strain contour of DBCS3 at initial load step	101
4.19h	Strain contour of DBCS3 at critical load step	101
4.20a	Stress contour of CB at initial load step	102
4.20b	Stress contour of CB at critical load step	103
4.21a	Stress contour of DBS at initial load step	104
4.21b	Stress contour of DBC at initial load step	104
4.22a	Stress contour of DBSS1 at critical load step	106
4.22b	Stress contour of DBSS5 at critical load step	106
4.22c	Stress contour of DBCS1 at initial load step	107
4.22d	Stress contour of DBCS3 at critical load step	107
4.23	Comparison of the load-deflection curve of control beam between FEA and experimental results	108
4.24	Validation of crack pattern in experiment (a) and FEA (b)	109
4.25	Load-deflection curve of deep beams with square openings without strengthening of CFRP	110
4.26	Load-deflection curve of deep beams with square openings without strengthening of CFRP	110
4.27	Load-deflection curve comparison for deep beams with circular openings in FEA result and experimental result	111
4.28	Crack patterns between FEA and experiment	111

4.29	Load-deflection curve between experimental and FEA results	112
4.30	Crack patterns between experimental and FEA results	112
4.31a	Load-deflection curves of DBSS7 as compared to experimental result	113
4.31b	Crack pattern of DBSS7 in FEA and experimental crack	114
4.32a	Crack pattern of DBCS3 and experimental crack	114
4.32b	Load-deflection curve of DBCS3 and experimental crack	115
A1	Types of crack patterns in ANSYS	123
B1	Crack pattern of DBSS7 at initial step	124
B2	Strain contour of DBSS7 at initial step	124
B3	Stress contour of DBSS7 at initial step	125
C1	Gantt chart of the study	126

LIST OF SYMBOLS

D	Depth
E	Modulus of elasticity
f'_c	Maximum concrete strength
f_t	Tensile strength
\emptyset	Diameter
ε	Strain
L	Span
s	Displacement
τ	Bond stress
τ_{max}	Maximum bond stress
$<$	Less than
$>$	Greater than

LIST OF ABBREVIATION

2D	2 – dimensional
3D	3 – dimensional
CB	Control beam
CFRP	Carbon Fibre Reinforced Polymer
DBC	RC Deep beams with circular openings
DBCS	RC deep beams with circular openings strengthened by CFRP
DBS	RC deep beams with square openings
DBSS	RC deep beams with square openings strengthened by CFRP
FE	Finite element
FEA	Finite element analysis
FEM	Finite element modelling
FRP	Fibre Reinforced Polymer
kN	Kilo-Newton
m	metre
mm	Millimetre
RC	Reinforced concrete

CHAPTER 1

INTRODUCTION

1.1 BACKGROUND OF THE STUDY

Rapid development in some developing nations has encouraged the construction of high-rise buildings and sky scrapers. Due to the heavy load from the enormous buildings, deep beams are always constructed at the lower floors as transfer beams to transfer the load from the entire building to the foundations. Reinforced concrete (RC) as one of the most essential building materials and it is widely used in the construction due to its low pricing, efficiency and strength of the reinforced concrete as well as its stiffness (Dadvar, 2014). Thus, RC deep beams are playing an important role in tall buildings, offshore structures, and foundations (Kong, 2006). Sometimes, the creation of openings on the reinforced concrete (RC) deep beams is needed to accommodate the utility services conduits such as electrical wiring and piping (Hawileh et. al., 2012a).

Some of the researches and studies have been done on the RC deep beams with openings recently. Dadvar (2014) tested the behaviour of reinforced concrete beams and high walls with finite element analysis. Campione and Minafò (2012) experimentally and analytically evaluated the influence of circular openings in reinforced concrete deep beams with low shear span-to-depth ratio. Hemanth (2012) studied the behaviour of FRP strengthened deep beams with openings through experiments and numerical study by using ANSYS. Five deep beams with openings without shear reinforcements were tested under three-point loading. Another finite element analysis on simply supported RC beams with circular openings had been conducted by Hafiz et. al. in 2014. Alsaeq (2014) investigated

the usage of Carbon Fibre Reinforced Polymer (CFRP) to increase the structural strength of RC deep beams with openings.

1.1.1 Reinforced Concrete Deep Beams

RC deep beam which means the depth of the beam is comparable to the span length of the RC beam itself. However, the Eurocode 2 (1984) (draft): *Common Unified Rules for Concrete Structures* does not directly provide guidelines for the design of the deep beams. Instead, it is required to refer to clauses 18.18 of the CEB-FIP Model Code (1978). Moreover, the design is not covered in BS 8110 as well, this can be known from the statement that “*for the design of deep beams, reference should be made to specialist literature*”. This is similar to the Draft Eurocode 2 which explicitly states that “*it does not apply however to deep beams...*” and refer to CEB-FIP Model Code. The main design documents, recently, available are the American code ACI 318-83 (revised 1986), CIRIA Guide 2, the CEB-FIP Model Code and the Canadian code CAN-A23.3-M84 (Kong, 2006). However, American Concrete Institute (ACI) states that, in the ACI 318-08 code, specification of deep beam should have either clear spans equal to or less than four times of the overall member depth or regions with concentrated loads within twice the member depth from the face of the support.

1.1.2 Reinforced Concrete Deep Beams with Openings

In recent decade, techniques used on the openings in deep beams are improving and much advanced. Openings are needed nowadays to allow the installation of conduits for utility pipelines such as electricity, air conditioning, gas pipeline, fire-rescues system, and computer networks. Opening in deep beam sometimes is not constructed together during casting of the RC deep beam but it is necessary to be made from core boring method on the RC deep beam on the existing building. The load path will be changed and shear capacity of the RC deep beam will be reduced if the openings intercept the stress field of the loading and the reaction point (Campione & Minafò, 2012). Several of shapes and

sizes of openings could be found on the openings of RC deep beams, generally, the openings in the area where shear is dominant which is near to the support (Hafiz et. al., 2014). Openings are inevitable now due to its convenience for the utility pipelines and most important it can reduce the overall story heights of buildings by creating openings on the RC deep beams.

1.1.3 Finite Element Analysis by ANSYS Civil FEM 12.0

ANSYS CivilFEM 12.0, a structural modelling and analysis software, is used for finite element analysis by numerical method and modelling of RC deep beams with openings is done in 3-Dimensional. ANSYS CivilFEM 12.0 is a high-end solutions for advanced civil engineering projects. ANSYS CivilFEM 12.0 can be used for creating engineering solutions spanning static, dynamics, linear and non-linear problems. This civil structural software is capable for structural elements and the checking code included Eurocode, Russian SP, ACI, Brazilian Code, ASTM, British Code, AISC and Chinese Code (<https://caei.com/ansys-software-support/civilfem-ansys-software>). Moreno et. al. quoted that “CivilFEM is at the present time one of the most advanced tools that engineers can embrace, a project that is committed with a time and with a permanent vocation of investigation and development.” (Moreno et. al., 2001).

Finite element analysis is a numerical method to solve some complicated problems. Numerical solutions can now been obtained through finite element analysis for even very complicated stress problems (Royslance, 2001). Finite element analysis can be applied in many areas of studies, e.g. structure analysis, solid mechanics, dynamics, thermal analysis, electrical analysis, biomaterials and etc. Finite element analysis is originally developed for solving solid mechanics problem. At first, input such as boundary conditions will be set into ANSYS CivilFEM 12.0 and the software will provide output, for examples, stress, strain, displacements, load-deflection diagram and deformation of the models.

1.1.4 Carbon Fibre Reinforced Polymer (CFRP)

Carbon Fibre Reinforced Polymer (CFRP), also *Carbon Fibre Reinforced Plastic*, and it is similar to fibre glass. *Fibre-reinforced polymer* (FRP) is a composited polymer matrix reinforced with fibre while CFRP is polymer matrix composite material reinforcing by carbon fibre. Carbon fibre is woven into a textile material and resin such as epoxy resin is applied and allowed to cure. The polymer used in the material usually will be epoxy, vinylester or polyester thermosetting plastic and phenol formaldehyde resins (Masuelli, 2013). CFRP gains its popularity recently due to its best strength to weight ration among all the construction materials so it is very strong. CFRP can be considered as the improvement on glass fibre reinforced polymer although CFRP is much more expensive than glass fibre reinforced polymer. The advantages of light weight, resistance to corrosion and high strength of CFRP made this material to be an excellent option for use as external reinforcing for construction elements. Recently, CFRP material is showing a continuous great promise in using as strengthening material in reinforced concrete structures (Khalifa et. al., 1998). At the early stage, CFRP tends to be used in the sport car manufacturing production line. Strong and lightweight materials are needed for the car racing. CFRP is used in air craft production as well because CFRP is honoured with its minimum weight but great strength (<http://www.technologystudent.com/joints/carfib1.html>). CFRP is introduced to strengthen the beam so that the weakening done by the opening can be improved. CFRP material is distinguished by its extremely high strength and rigidity and differ so much from that of their matrix material. Unlike Glass Fibre Reinforced Polymers, CFRP exhibit considerably greater rigidity, sharply enhanced electrical and thermal conductivity and a lower density, due to its advantages in physical properties, which lead CFRP to the application in aerospace engineering when CFRP is introduced. CFRP is not being used in Civil Engineering field until 1991. This material was first applied in the Civil Engineering field in the strengthening of the Ibach Bridge near Lucerne in Switzerland in 1991. CFRP, embedded in polyester resin, is reinforced and composed from very thin carbon fibres with diameter only 5 – 10 μm (Flaga, 2000).

1.1.5 Importance of Strengthening

Increasing in safety requirements, changing of social needs, more stringent design standards and the deterioration of existing reinforced concrete infrastructures are requesting the demands in strengthening of the structures (Godat et. al., 2007).

FRP repairs work by reducing the stress range experienced in the metal substrate, this method should be effective before and after crack initiation, as long as the bond between the FRP and the underlying metal is maintained (Alemdar et al., 2012). Safety of residents and users in a particular building can only be guaranteed if the damaged or vulnerable reinforced concrete structures have been repaired and strengthened. Beams, as the vital structural elements to withstand loads, laterally and vertically, so investigation on the efficient method to repair and strengthen the beams are necessary in terms of maintaining the safety of the structures, users and residents. In this study, several of strengthening methods will be tried out in the ANSYS modelling until the two most effective methods are determined.

As the infrastructures continue to age, there is an increase of need for effective maintenance, repair, rehabilitation, and retrofit. As the time passes by, many aging structural members is not providing the load capacity as compared to the original design. This situation is due to the cracking of concrete, corrosion of steel or insufficient deformation capacity to withstand the lateral and vertical load. These older structural members may not have sufficient strength, stiffness or load capacity for the applied load (Sezen, 2012). Inadequate of strength in these structures and components may risk the lives of users and residents and damage to property of public.

1.2 PROBLEM STATEMENT

The use of deep beams at lower levels for high rise buildings is more common nowadays due to the rapid development. Usage of deep beams with openings in the high rise buildings for both residential and commercial properties and purposes has increased significantly due to the convenience and economic considerations. Openings are convenient to be created for the utilities purpose and without increasing the stories overall height. However, creating openings in fulfilling the architectural or mechanical requirements to achieve the building's function would result in the reduction of shear capacity of the particular elements, thus it leads to the questioning of safety of the building. Whenever the openings are inevitable, safety precautions step should be taken to ensure the recovery of strength capacity of the elements (Hemanth, 2012). The strength capacity reduced is not only to withstand the vertical and self-weight of the building but also needed to withstand the lateral load, wind load, and bending moment force. The reduction in the shear capacity is more significant when opening fully interrupts the natural load path (Hawileh et al., 2012a). Different shapes, percentages of reduction, and locations of the openings will have different degree of strength reduction in the RC deep beams.

Traditionally, externally bolting and steel plates are practiced in civil industry to strengthen the structural elements. Additional reinforcements are added externally to the surfaces of the structural members for additional capacity. The success of this technique is that attached as new reinforcement for the structural members and relieves heavily on the physical properties of long-term durability of the reinforcement materials (Shaw, n.d.). However, there are some disadvantages for the bolting and steel plates thus leading this technique to a less common practice in the industry. The main disadvantages of using bolting plates are the steel plates are not protected by concrete as the same ways of internal reinforcement, the durability and corrosion effects remain questioned, precaution steps should be taken before installing the steel plates, surface of the steel plates should be carefully prepared to resist the corrosion, weight of the steel plates make the transportation difficult and etc.

Due to the unsuitability of the bolting and steel plates system in the industry, modelling and finite element analysis on the CFRP should be carried out to investigate the shear capacity recovery on the RC deep beams with openings for further development

in the civil industry. Finite element analysis can be used to predict the behaviour of the RC deep beams with openings through modelling and meshing.

1.3 OBJECTIVES OF STUDY

- i. To determine the behaviour of deep beams with openings without strengthening and strengthening using CFRP in terms of load deflection behaviour, crack pattern, stress and strain contours.
- ii. To identify the effect of openings with different shapes, i.e. circular and square, in deep beam.
- iii. To identify the most effective strengthening method to strengthen the RC deep beam with opening by CFRP.

1.4 SCOPE OF STUDY

In this particular study, a commercial finite element analysis software, ANSYS CivilFEM 12.0, was adopted to run the numerical analysis of finite element method to solve the approximate solutions of stresses, strains and displacements at each node of elements. Numerical analysis was adopted to identify the behaviour of RC deep beams with openings as well as the behaviours of beams after strengthening using CFRP. Three fundamental type deep beams (control beam, deep beams with openings and deep beams with openings strengthened by CFRP) were considered in this investigation for each shapes. A deep beam without any opening acted as a control beam while the remaining modelled deep beams were with openings. One of the modelled deep beams with opening was not strengthened while the remaining deeps beams were modelled with different strengthening methods to identify the most effective strengthening method by applying CFRP around the openings. The simply – supported deep beams were tested by applying four point loading to evaluate the load deflection failure, crack pattern, stress and strain contours. The deep beams were tested to failure by constantly increased the force on the both point loads. The results from the modelling simulation were compared with the

experimental result to determine the similarities and differences between the behaviours of deep beams.

The dimensions of the deep beam with opening that being studied are $120\text{ mm} \times 600\text{ mm}$ for the cross section of width and height and length of 2400 mm . The size of opening had been decided to be around 45% of reduction from the depth of the RC deep beam which is 270 mm in diameter for the circular opening while 270 mm for each side of the square opening. Meanwhile, the diameter of steel reinforcement for the RC deep beams with openings at tension region, which were bottom reinforcement, was 16 mm with a total of two reinforced steel bars. The diameter of steel reinforcement for the compression region, which was top region, is 10 mm with the number of two reinforcement steel bars. Four horizontal reinforcement bars with six millimetre were installed as well with 150mm from centre to centre each side. The shear link being used for this study was decided to be mild steel with six millimetres in diameter.

1.5 SIGNIFICANCE OF STUDY

The building overall height will significantly increase if deep beams without openings are constructed for the sky scrapper. The increase in the story height is to ensure that there is enough clear story height. Furthermore, it will delay the process of construction as higher floor is needed and the cost of construction will increase as well to ensure the building could be built by following all the requirements. This problem becomes more concern when the rapid development path in Malaysia is more obvious recently and openings in the deep beams are increasing in its popularity to ensure cost and time efficiency. Deep beams with openings are needed to overcome these problems, e.g. cost and time, and shear capacity reduction in the deep beams can be solved by using CFRP wrap externally. Thus, through finite element analysis, the behaviour of RC deep beams with openings strengthened with CFRP and without strengthening of CFRP could be determined and analysed. This finite element analysis is essential before the construction starts to prevent any unfavourable or unpredictable structural failure during opening drilling process. This process may significantly help in reducing the loss of time and cost during the construction process. Indeed, the effective and proper wrapping method of CFRP may improve the life span and durability of the structural members as well as increase the shear bearing capacity of the RC deep beams. Moreover, the process of installation of CFRP will not damage the physical and chemical properties of the deep beams as compared to the installation of bolting and steel plates. In short, RC deep beams with openings strengthened by CFRP is not only the wise solution for reducing the building overall height but also save the construction cost at the same time improving the safety during construction.

CHAPTER 2

LITERATURE REVIEW

2.1 INTRODUCTION

Reinforced concrete can be considered as one of the most important materials in the construction (Dadvar, 2014). Beam which is constructed from the reinforced concrete acts an important role in the building structural members. A beam can be defined as an element that has horizontal span between the supports where the beams support mainly vertical load which acting in right angle to the length of the beam. The cross section of the beam is small compared to the span length (“What is a beam? | Tata Steel Construction,” n.d.). A beam primarily resists bending to withstand the load from the building. The loads always come from the building, external load, own weight, span and bending moment which is external reactions to the loads. Deep beam which is referring to a structural member whose behaviour is dominated by shear deformation can be considered as a deep beam. For the practice of designing, civil engineers always design deep beam for girders, transfer beam, pile foundation, bridge bents and etc (Birrcher et al., 2008). Moreover, deep beam is also defined as the horizontal member which has a clear span that is equal to or less than four times of the overall of the overall member depth (Seo et. al., 2004).

It is a need to often carefully pay great attention to the shear capacity of a reinforced concrete beam because there is no advance warning typically for catastrophic nature of shear failure. There are various reasons that shear strengthening is required such as remediation in design or construction errors or because of changes in functions of the original idea of design or due to the environmental considerations. Sometimes, shear

strengthening is needed due to the result in a shear capacity that is less than the enhanced flexural strength (Godat et al., 2007). While, it is a fact that these materials are gaining the wide acceptance by the civil community by proving from the large body literatures in the field of FRP rehabilitation, along with the corresponding increase in the level of activity (Neale, 2000).

2.2 STRUCTURAL BEHAVIOUR OF RC DEEP BEAM

A deep beam is a reinforced concrete structural member whose behaviour is dominated by shear deformation (Birrcher et al., 2008). Furthermore, a number of authors have mentioned the similar definition for the RC deep beam, which is a deep beam is a member whose shear span-to-depth, a/h , ration is relatively small, typically, a region of beam with ratio of a/h smaller than 2.0 to 2.5 will be considered as deep beam.(Amin et al., 2013; Birrcher et al., 2008; Birrcher et. al., 2009; Campione & Minafò, 2012; Seo et al., 2004).

Transfer girder is always being used to transfer the heavy load from the upper floor to the lower part, thus it is always under high shear stress. The load from the building system that composed of bearing wall or shear wall and moment frame as upper and lower part is always very high the requirement in the depth of the transfer girder has to be increased because high stress with the demand for the bulky and high-rise building. The bonding of reinforcement and the anchor is important in this type of beam due to the high stress thus the depth of the beam has to be increased as well (Seo et al., 2004).

Birrcher et. al. (2008) questioned the behaviour of RC deep beam which exposed to the environment and public view, the serviceability of the structure is significantly arguably for its strength. Commonly, the width and spacing between the diagonal cracks formed by the load will quantify the serviceability performance of RC deep beam. During the design stage, by adjusting the section and distance between the shear links to limit the cracking by comparing the cracking load to the service load. Typically, the shear and flexural forces are resisted by reinforced concrete during the design based on the assumption that strains vary linearly at a section. By referring to the *Bernoulli hypothesis* or *beam theory*, the plane section is always assumed to be remained plane for the

mechanical behaviour. Undoubtable, design for a deep beam must be different from the ordinary deep beam because assumption for the derivation of the sectional theory will be different and no longer valid.

2.3 STRUCTURAL BEHAVIOUR OF RC DEEP BEAM WITH OPENINGS

From the experiment done by Campione & Minafò (2012), all the tested beams (deep beams with circular openings and low shear span to depth ratio) had failed due to the diagonal cracking or to concrete strut failure. Failure load values varied from 225 kN to 1250 kN and the first visual cracking load was observed from 250 kN to 750 kN. The load was periodically paused to observe the crack on the deep beams and the patterns of cracks were examined by visual inspection. Deep beams with openings in the middle section or without any openings and openings are located within the shear span had distinct failure mode. Moreover, deep beam with opening with plain concrete exhibited very brittle failure.

2.3.1 Effects of Openings on Sizes, Shapes and Locations

The failure mode was not that depending by the reinforcement but mainly depended on the location and the presence of the opening (Campione & Minafò, 2012). Amin et al. (2013) conducted investigation by using CivilFEM 12.0 to investigate the effect of opening sizes and locations on the shear strength behaviour of RC deep beams without web reinforcement. Eleven models of RC deep beams were modelled with different sizes and at different locations as shown in Figure 2.1.

Name of specimen	h (mm)	b (mm)	d (mm)	(l/d) ratio	(a/d) ratio	f_c (MPa)	Dagg. (mm)	Long. A_s	f_y (MPa)
S1-1	450	120	414	2.42	1	30.85	9.5	3Ø22	430
S1-2	350		313	3.2	1.25	29.36	9.5	2Ø25	395
S1-3	250		217	4.61	1.5	29.24	9.5	3Ø16	486
S1-4	150		119	8.4	2.5	26.25	9.5	3Ø12	416
S1-5	350		313	3.2	1.25	42.3	9.5	3Ø16	486
S1-6	250		217	4.61	1.5	43.5	9.5	3Ø16	486
S1-7	250		217	4.61	1.5	32.07	12.5	3Ø16	486
S1-8	250		217	4.61	1.5	31.81	19	3Ø16	486
S1-9	250		217	4.61	1	32.86	9.5	3Ø16	486
S1-10	250		217	4.61	2	33.23	9.5	3Ø16	486
S1-11	250		217	4.61	2.25	28.9	9.5	3Ø16	486

Figure 2.1: Detailed of the tested crushed stone concrete deep beams

(Amin et al., 2013)

From the result obtained by Amin et al. (2013), it was found that the ultimate shear was significantly decreased by about 53.6% when opening was provided at the shear zone but when opening was located at the mid-span, then it had the minimum effect where the average reduction in shear stress is about 8%. For the square opening, bigger sizes of the dimensions of the square showed the higher reduction in the shear stress. Decreasing of shear strength of RC deep beam when the ratio of shear span to depth is increased. Amin et al. (2013) found that by increasing the shear span to depth ratio from 1.5 to 2.25, with constant length to depth ratio and maximum size of aggregate, shear strength reduced by about 4.7%, 5.43%, and 12.03% for shear zone, support and mid-span opening locations respectively.

2.4 FINITE ELEMENT ANALYSIS BY NUMERICAL APPROACH

The advantages of FRPs as external strengthening result in extensive of experimental research for strengthening externally for reinforced concrete members in the area of FRP shear strengthening. In contrast, there is a limited number of numerical studies for this application to date, especially with regard to the interfacial behaviour between the concrete and bonded FRPs (Godat et al., 2007). One of the powerful method for simulating complex structural behaviour is through finite element analysis (Ottosen & Petersson, 1992). It is better in economical consideration that model FRP shear-strengthened beams than conducting laboratory tests on beams strengthened by FRP. The aim of conducting finite element analysis is to determine the load-deflection behaviour of the strengthened beams.

Arduini et. al. (1997) developed a finite element analytical model to predict the behaviour of two-span beams with bonded carbon FRP (CFRP) sheets and at the same time tested in laboratory. The concrete beam was modelled in three-dimensional by using meshing of eight-node brick elements while CFRP was modelled directly to be applied on the beam to simulate the perfect bonding condition in finite element analysis. The analysis from the finite element model showed that the load-deflection behaviour was stiffer and less ductile than the result from experiment and the CFRP sheets were considered to be linear elastic until rupture. The attribute to the assumption of perfect bond between the reinforced concrete beam and CFRP might cost this slightly overestimated of the peak loads and mid-span deflection.

Kachlakev and McCurry (2000) showed another numerical model in three-dimensional. For the research, the model was analysed by ANSYS finite-element package to simulate the behaviour of the concrete beam. The behaviour studied was behaviour of concrete beam after strengthening externally. Similarly to research done by Arduini et. al. (1997) that the concrete was modelled by three-dimensional eight-node elements with a non-linear behaviour in ANSYS. Steel bars were modelled by adopting the elastic-perfectly plastic behaviour element with two-node bar. The FRP laminates also applied directly to the concrete elements to assume a perfect bonding between the FRP and concrete elements. FRP composite used layered solid elements with a linear elastic response. The result was also slightly overestimated by finite element analysis in ANSYS

but very good agreement in the result before debonding of FRP between experimental and numerical result. The assumption of perfect bonding between concrete and FRP as well as limited number of concrete nodes attributed to the slightly overestimation of the result.

Drucker-Prager yield criterion was used with regard to the non-linear response of the concrete compressive behaviour (Al-Mahaidi et. al., 2001). Al-Mahaidi et. al. (2001) studied the behaviour of shear-strengthening beams in two-dimensional by using DIANA, finite element analysis software. Concrete tensile strength was considered in the study. Behaviour of perfect elasticity plastic was assumed for the steel reinforcements. FRP composites also assumed to have elastic-perfect plastic behaviour although FRP composites showed elastic behaviour until rupture. The numerical predictions showed a convincing result that the numerical result gave less load carrying capacity than the experimental results. The tensile strain in the FRPs were also showed lower than the ultimate tensile strain in the analysis.

Wong (2001) conducted a two-dimensional non-linear finite element analysis for the numerical analysis of strengthened beams. The numerical program was based on the modified compression field theory, which was based on a smeared, rotating crack model for the concrete. Orthotropic material was used to represent the cracked concrete in this analysis and the steel reinforcement was also assumed to have elastic-plastic manner with strain-hardening effects. FRP composites were also assumed as other journal above that behaved linear elastic with brittle rupture in tension. An elastic model and elastic-plastic relation were used for bond interface to characterize the bond stress-slip behaviour between the surface of concrete and FRP composites. The shear stiffness of the epoxy and the adhesive thickness affected the slope of the linear relationship of the strengthened concrete beams. The numerical model still giving a reasonable result after doubling the concrete compressive strength while keeping the strain at peak stress unchanged (Wong, 2001). The numerical result secured a more accurate result by applying elastic-plastic bond relation at the same time linear elastic bond relation led to a pre-mature shear failure.

Complex behaviour of the beams such as bond-slip behaviour, concrete non-linearity and the different failure modes of the concrete and FRPs are taken into account in the study of an appropriate three-dimensional model to accurately simulate the shear-strengthened by FRP in a finite element package ADINA 8.1 (Godat et al., 2007).

Different shear-strengthened beam applications such as side-bonded laminates and U-shaped wrapping configurations were investigated to show the validity of the finite element model. The published test data was used to validate the numerical predictions.

2.4.1 Finite Element Analysis by ANSYS CIVLFEM 12.0

Moreno et al. (2001) claimed that at the year of 2001, CivilFEM was the most advanced tools that engineers could embrace, this is due to the capabilities of CivilFEM included an extra ordinary and extensive materials and sections library for the construction material of concrete and steel structures. Moreno et al. also stated that CivilFEM also performed concrete and steel code checking and design according to Eurocodes 2 and Eurocodes 3, American (ACI318), British (BS8110 and BS5950-1995 and 2001) and etc. Moreover, CivilFEM conducted for the aforementioned codes cracking analysis with regards to serviceability.

CivilFEM is integrated with ANSYS which is working inside ANSYS program. This means that all the ANSYS tools can be easily used in CivilFEM. The CivilFEM menus, help system, commands, log files and so on are integrated in the ANSYS. Users may switch between processors of ANSYS and CivilFEM at any moment (Moreno et al., 2001).

There are two approaches in finite element analysis to simulate the de-bonding of FRP. The first approach is that by modelling the cracking pattern and failure of the concrete elements adjacent to the adhesive layers. However, this approach required very fine meshing which is with element sizes of 0.2 mm – 0.5 mm which referred as mesoscale model. This approach required large computational resources (Lu et. al 2005a,b). Utilization of interface of elements is used to predict the nonlinear behaviour between the FRP and concrete (Wong, 2001; Wu & Yin, 2003).

2.5 MATERIAL MODELLING

2.5.1 Concrete

SOLID65 which is the material code that used in ANSYS CivilFEM 12.0, 3-D modelling for concrete strength of 35 N/mm². Concrete block can be modelled by defining eight nodes and having three degree of freedom for all the nodes. Nonlinear material properties should be used for the elements of concrete. The concrete in the modelling is capable of cracking, crushing, plastic deformation and creep in three orthogonal directions (Hafiz et al., 2014). Poisson's ratio of 0.2 should be used for the concrete.

After the primary diagonal crack fully developed between the load and support region and the yielding of tension reinforcement only the failure of RC deep beam took place. Primary diagonal crack was observed that it was parallel to the axis of compression struts. Besides that, from the experiment, it was also found that the crack pattern was more scattered in the specimens with both horizontal and vertical reinforcements as compared to only either horizontal or vertical reinforcements. The final failure mode from the experiment conducted could be further categorized into three types of failure pattern which were diagonal splitting failure, compression strut failure and shear compression failure (Seo et al., 2004). Various crack patterns for failure had been shown in Figure 2.3.

Multi-linear isotropic stress-strain curve for the concrete non-linear was computed from the following equations to obtain the compressive uniaxial stress-strain relationship and as shown in Eq. (2.1) to Eq. (2.4)

$$f_c = \varepsilon E_c \quad \text{for } 0 \leq \varepsilon \leq \varepsilon_1 \quad (2.1)$$

$$f_c = \frac{\varepsilon E_c}{1 + \left(\frac{\varepsilon}{\varepsilon_0}\right)^2} \quad \text{for } \varepsilon_1 \leq \varepsilon \leq \varepsilon_0 \quad (2.2)$$

$$f_c = f'_c \quad \text{for } \varepsilon_0 \leq \varepsilon \leq \varepsilon_{cu} \quad (2.3)$$

$$\varepsilon_0 = \frac{2f'_c}{E_c} \quad (2.4)$$

The curve should start at zero stress and strain. For all the material obeyed Hook's law which stated that within the elastic limit, stress is proportional to strain, thus, elastic zone where stress is proportional to strain (Patel & Tank, 2014).

In finite element package ADINA 8.1, the concrete behaved fully defined in compression and tension. The elastic limit is taken as 30% of the maximum concrete compressive strength in the elastic limit. It is then followed by non-linear behaviour where the maximum concrete strength was reached. This followed by the behaviour softenings until concrete crushing occurred. Tension of concrete is shown by an ascending–descending behaviour. The slope of the ascending branch is equal to the concrete modulus of elasticity. In the descending part of the stress–strain curve, the fixed smeared crack model is used, in which the plane of failure occurs perpendicular to the corresponding principal stress direction. The normal and shear stiffness across the plane of failure are reduced, and plane stress conditions are assumed to exist in the plane of tensile failure. Figure 2.2 shows the uniaxial stress–strain curve for the concrete. For the finite-element implementation, the values of the tensile strength, f_t , and elastic modulus, E , if not given in the respective references, are approximated based on the following CSA 2004 Eq. (2.5) and Eq. (2.6)

$$f_t = 0.6\sqrt{f'_c} \text{ (MPa)} \quad (2.5)$$

$$E = 3300\sqrt{f'_c + 6900} \text{ (MPa)} \quad (2.6)$$

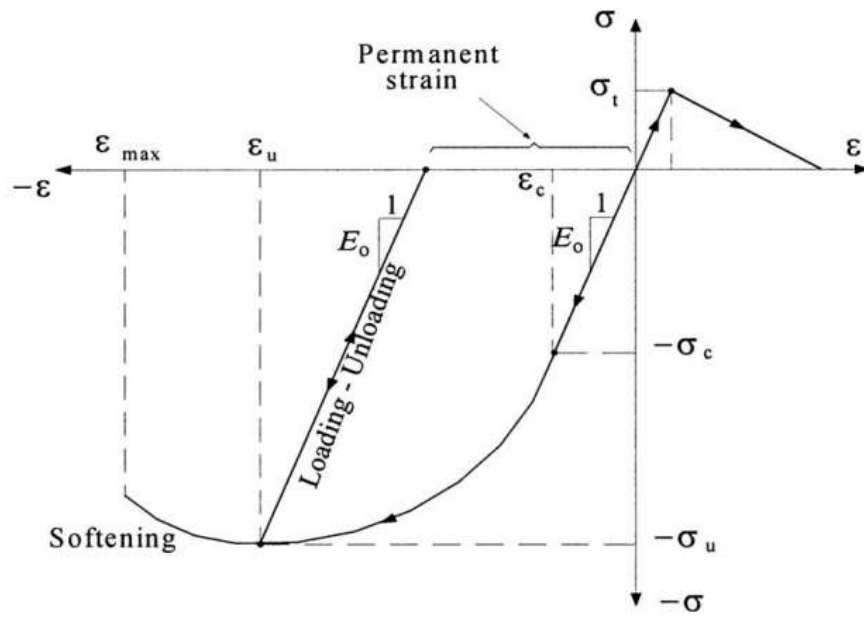


Figure 2.2: Stress-strain curve for concrete

(Godat et al., 2007)

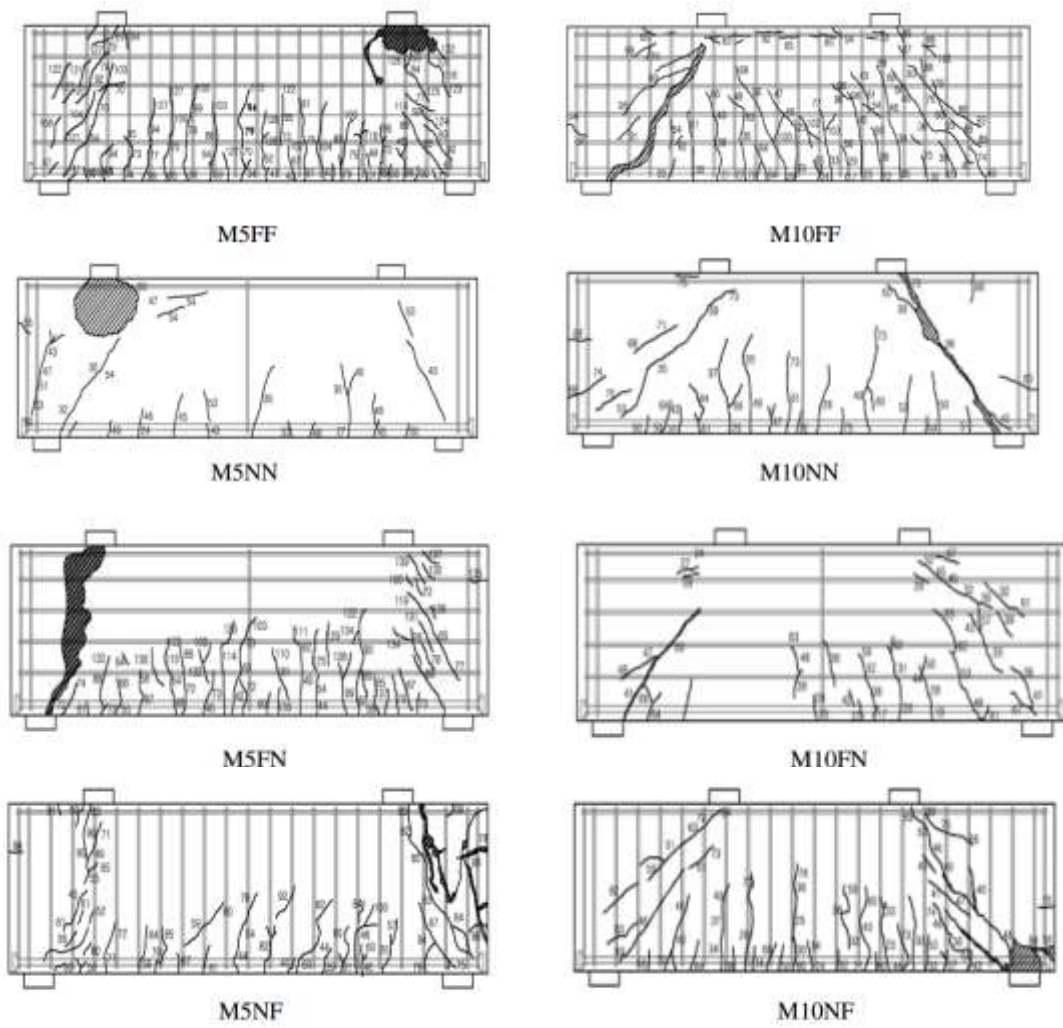


Figure 2.3: Crack patterns at failure

(Seo et al., 2004)

2.5.2 Reinforcement Steel Bar

LINK8 was being defined and used for the steel reinforcement for the modelling of RC deep beam. For 3-D modelling, 3-D spar element was being used for the steel reinforcement and it was a uniaxial tension-compression element with three degrees of freedom at each nodes. The modelling of the steel reinforcement also included plasticity, creep, swelling, stress stiffening and large deflection capabilities. Moreover, both linear elastic and bilinear inelastic were assumed for the modelling of steel reinforcement bar. Yield strength of longitudinal reinforcements and stirrups were 400 MPa and 240 MPa respectively. Poisson's ratio for the steel reinforcement should be kept at 0.3.

Steel reinforcement is modelled in finite element modelling representing by an elastic-plastic constitutive relation with linear strain hardening. Godat et. al. (2007) modelled the strengthened beams by considering that the stresses transferred from the steel to surrounding concrete were in the tension-stiffening model of concrete. The value for shear retention was increased a factor of 0.5 to indirectly include the effect of steel dowel action. For the study from Godat et. al., the ratio between the slopes in the elastic range to the plastic range was taken from 100 to 200.

2.5.3 Carbon Fibre Reinforced Polymer

The material in ANSYS CivilFEM 12.0 that represents CFRP is SHELL99. CFRP sheets should be modelled by element SHELL99. This element SHELL99 can be modelled by multiple layers up to 250 layers. It is also same as element of concrete that it has eight nodes and each node will have six degree of freedom (Hawileh et al., 2012a). An epoxy layer, element INTER205, was introduced to be the interface between the concrete surface and the CFRP composites sheet. The epoxy layer is simulated as the interfacial bond-slip action between concrete surface and CFRP layer and it is zero thickness.

The use of FRP for external strengthening for shear recovering have been shown by experiments that it is viable (Khalifa et al., 1998). Khalifa et. al. also mentioned that the

FRP reinforcement is an excellent option for external reinforcement due to its resistivity to chemicals, the properties of non-corrosive and non-magnetic. Furthermore reinforcement by CFRP also has its advantages of lightweight and convenience of instalment due to the formability of CFRP.

FRP composites in Godat et. al (2007) was assumed as a linear elastic orthotropic constitutive relationship. A rupture point on the stress–strain relationship for the fiber direction defines the ultimate stress and strain of the FRP.

Two different constituents of materials were consisted in the FRP composites. The constituents were combined at a macroscopic level and are not soluble in each other. One of the constituents was the reinforcement, which embedded in the second constituent, a continuous polymer called the matrix. Moreover, the reinforcing material was in the form of carbon fibres, which were typically stiffer and stronger than the matrix. The FRP composites which combined with carbon was Carbon Fibre Reinforcing Polymer (CFRP). The CFRP composites were one type of orthotropic material. Hence both the materials had different material properties (Patel & Tank, 2014).

2.5.4 Modelling interface of FRP and Concrete

Lu et. al. (2005a,b) proposed one of the most accurate bond stress-slip models that can be done by numerical analysis in finite element analysis software. The relationship between local shear stress and the relative displacement were used to simulate the behaviour of the interface of FRP and concrete. Three differences of relations between bond and slip had also been suggested that the relation was classified according to their level of sophistication. The relation was also referred to as the precise, simplified and bilinear model. Figure 2.4 shows the adoption of the simplified relation.

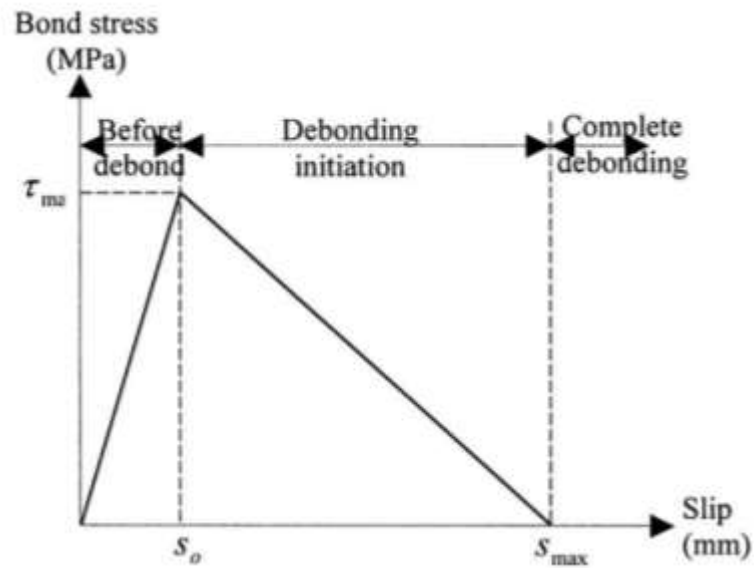


Figure 2.4: Bilinear bond-slip model

(Lu et. al., 2005a, b)

τ_{max} was considered to be the maximum bond stress and s_0 was considered to be the corresponding slip. Eq. (2.7) to Eq. (2.12) show the relationship of the interface between bond and slip. Figure 2.5 shows the finite element that modelled for the equations below. Therefore, for the ascending part ($s \leq s_0$).

$$\tau = \frac{\tau_{max}}{s_0} s \quad (2.7)$$

$$\tau_{max} = 1.5\beta_w f_t \quad (2.8)$$

$$s_0 = 0.0195\beta_w f_t \quad (2.9)$$

$$\beta_w = \sqrt{(2.25 - b_f/b_c)/(1.25 + b_f/b_c)} \quad (2.10)$$

For the descending part ($s_0 < s \leq s_{max}$)

$$\tau = \tau_{max} \frac{(s_{max}-s)}{(s_{max}-s_0)} \quad (2.11)$$

$$s_{max} = 2G_f/\tau_{max} \quad (2.12)$$

where

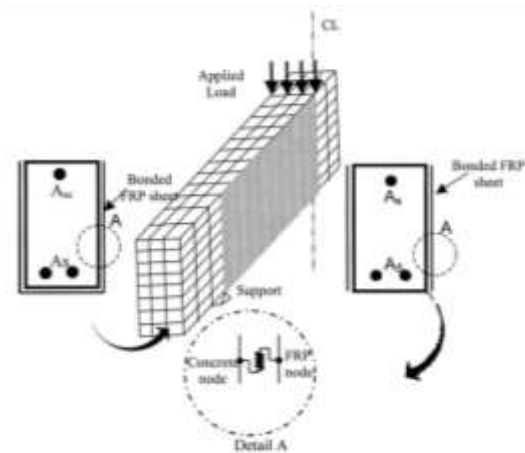


Figure 2.5: Finite element model

(Lu et. al., 200a, b)

FRP composites were always bonded to the surface of concrete by using epoxy as the bond material between the surface of concrete and FRP. The modelling of the bond of interface between the FRP and concrete was important to accurately simulating the contribution of the FRP composites to shear resistance. The bond modelling in numerical analysis had to be appropriately reflected the physical of the bond interface as nearer as could. The two most common elements to represent the bond element were link element as well as contact elements. Contact element was a linear-dimensional element with four nodes whereas the link element is a non-dimensional element with two nodes (Kim & Vecchio, 2008). The study used the formulae of bilinear bond stress-slip relationship

proposed by Sato & Vecchio (2003) in the research. The fracture energy of concrete were shown by the Eq. (2.13) to Eq. (2.16).

$$\tau_{bFy} = (54f'_c)^{0.19} \quad (2.13)$$

$$G_f = \left(\frac{\tau_{bFy}}{6.6}\right)^2 \quad (2.14)$$

$$s_{Fy} = 0.057G_f^{0.5} \quad (2.15)$$

$$s_{Fu} = 2G_f/\tau_{bFy} \quad (2.16)$$

where

τ_{bFy} = maximum bond shear stress;

f'_c = compressive strength of the concrete;

s_{Fy} = bond slip at the maximum bond shear stress;

s_{Fu} = ultimate bond slip;

2.6 BEHAVIOUR OF RC DEEP BEAMS WITH OPENINGS STRENGTHENED BY CFRP

Performance of fibre reinforced polymer being used in reinforced concrete members was not only mentioned by (Saiedi et. al., 2013), but also mentioned in the journal by Badawi & Soudki (2010) that fibre reinforced polymer could effectively repair and improve the structural performance of reinforced concrete members such as beams, walls, columns and etc. Corrosion of the steel reinforcement may shorten the service life of the reinforced concrete structure due to the reduction of the cross-sectional area of the steel reinforcement and destruction of mechanical interlock of the corroded steel reinforcements (Badawi & Soudki, 2005, 2010). Several experiments and investigations have been conducted to study the effectiveness of FRP laminates on the recovery of

strength of the RC members (Alemдар et al., 2012; Badawi & Soudki, 2010; Ban & Abduljalil, 2014; El Maaddawy & Sherif, 2009; El-maaddawy & El-ariss, 2012; Elsafty & Graeff, 2013; Farghaly & Benmokrane, 2013). It was found that the effect of strengthening by CFRP laminates not only increase the strength and flexural stiffness of the RC members but also to a higher level than that of the control beam. CFRP also being identified that confinement of CFRP minimized the expansion of the span during corrosion at the same time reduced the crack width for both sides of the shear-span corrosion beam.

2.6.1 Behaviour and Performance of CFRP

One of the most effective solutions to overcome corrosion of steel reinforcement is by using fibre reinforced polymer reinforcement in the concrete structures. Carbon Fibre Reinforced Polymer, due to its high resistance to alkalinity and excellent long-term and fatigue characteristics, thus it is good for the pre-stressing construction structural elements (Badawi & Soudki, 2005, 2010; Saiedi et. al., 2013). Performance of CFRP had been discussed in Badawi & Soudki (2010) that the beam without strengthening of CFRP failed by concrete crushing after the tensile steel reinforcement yielded while the beams strengthened by CFRP failed by a rupture in the flexural CFRP laminate then only followed by concrete crushing under the condition that the original beams were corroded beams to a specified degree.

Badawi & Soudki (2005) investigated that the expansion in shear-span corrosion beam can be reduced up to a 70% when load was applied by confining the cross section of the RC beam with CFRP laminates.

2.6.2 Advantages and Disadvantages of Using CFRP

Carbon fibre reinforced polymer is a type of composite material that made of a polymer matrix reinforced with fibres. Fibres used are usually glass, carbon or aramid. The polymer is usually epoxy, vinylester or polyester thermosetting plastic. FRPs are commonly used in aerospace, automotive and recently in construction industries. Composite materials are usually made from two or more constituent materials with separate and distinct within the finished structure although there are significant different in physical and chemical properties which are engineered or naturally occurring materials. Most composites have strong, stiff fibres in a matrix which is weaker and less stiff. Making the components to be strong, stiff and low density are always the main objective. FRP materials increased in its demand recently due to the high performance resin system and new styles of reinforcement. Furthermore, FRP composites are lightweight, corrosive-less, high tensile strength, ease of handling, high specific strength and high specific stiffness thus enables it to be much advantageous than other traditional civil engineering materials e.g. concrete and steel (Masuelli, 2013).

However, CFRP has a characteristic of brittle failure which is linear elastic response in tension up to failure. CFRP is also relatively poor resistance to transverse or shear resistance and they are weak when exposed to high temperature. Cost of CFRP is always higher than the traditional steel reinforcement and concrete as well as pre-stressing tendons. The characteristics of lack of plastic behaviour and the very low shear strength in the transverse direction easily lead to premature tendon rupture and sometimes combined effects are present such as shear cracking planes in reinforced concrete beam where dowel action exists (Masuelli, 2013).

2.6.3 Method and Application of CFRP

A cured CFRP composite sheet was modelled up to failure and the properties for the modelled CFRP should be elastic orthotropic material. The elastic orthotropic material properties used were as follow:-

$$E_x(\text{elastic modulus in direction of fibres}) = 65 \text{ GPa}$$

$$E_{y,z}(\text{elastic modulus perpendicular to the direction of fibre}) = 5.87 \text{ GPa}$$

$$v_{xy,xz}(\text{Poisson's ratio in the } xy \text{ – and } xz \text{ – planes}) = 0.28$$

$$v_{yz}(\text{Poisson's ratio in the } yz \text{ – planes}) = 0.42$$

$$G_{xy,yz}(\text{shear modulus in the } xy \text{ – and } yz \text{ – planes}) = 2.9 \text{ GPa}$$

$$G_{yz}(\text{shear modulus in the } yz \text{ – plane}) = 2.2 \text{ GPa}$$

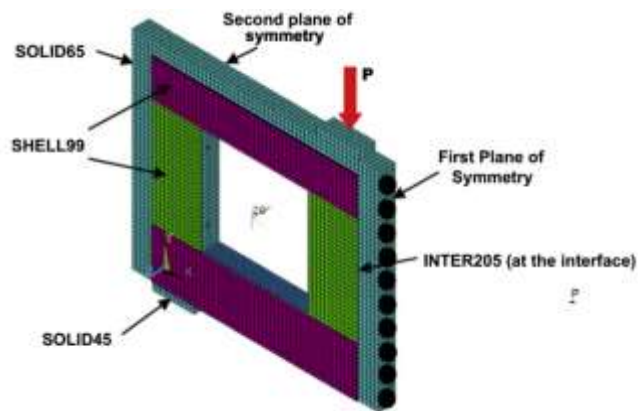


Figure 2.6: A typical FE model

(Hawileh et al., 2012a)

2.7 SUMMARY

Many researchers had carried out numerical approach to determine the shear-strengthening of beams to recover the beam capacity with different methods to determine the effective method to strengthen the beams in terms of shear. Table 2.2 lists the methods of strengthening from different researchers of their work in numerical analysis with different dimensions and parameters listed in Table 2.1.

Table 2.1: Geometrical characteristics of tested beams

Beam set	Section type	Beam dimensions (mm)				Steel stirrups
		L	b _c	h	a/d	
Adhikary & Mutsuyoshi (2004)	Rectangular	2,600	150	200	3.0	-
Pellegrino & Modena (2002)	Rectangular	2,700	150	300	3.0	8 nos @ 200 mm
Khalifa & Nanni (2000)	Rectangular	3,050	150	405	2.8	-
Chaallal et. al. (1998)	T section	1,300	150	250	2.5	6 nos @ 200 mm

Shear-strengthening could be done in different methods. The two most common methods of strengthening were side bonded and U-wrap, moreover, the number of layers of CFRP sheets used for strengthening was also taken into account. Table 2.2 summarizes the strengthening method used by the researchers in their analysis modelling.

Table 2.2: FRP shear-strengthening details

Beam set	Specimen	Strengthening type	Strengthening details
Adhikary & Mutsuyoshi (2004)	B-1	-	-
	B-8	U-wrap	Continuous sheet
Pellegrino & Modena (2002)	TR30D1	-	-
	TR30D3	Side bonded	One continuous ply
	TR30D4	Side bonded	Two continuous plies
	TR30D2	Side bonded	Three continuous plies
Khalifa & Nanni (2000)	BT1	-	-
	BT2	U-wrap	One continuous ply
	BT3	U-wrap + H ^a	Two continuous plies
	BT4	U-wrap	Vertical strips
	BT5	Side bonded	Vertical strips
	BT6	U-wrap	Continuous sheet ^b
Chaaallal et. al. (1998)	US	-	-
	RS90	Side bonded	Vertical strips
	RS135	Side bonded	Inclined strips

Finite element analysis on deep beams and normal simply supported beams had been studied by researchers to study the behaviour of reinforced concrete beams with openings after the strengthening by CFRP. The presence of CFRP in the strengthening of the beams with opening. CFRP would greatly recovered the beam capacity of the beams with opening. Table 2.3 shows the details and result of the beams with opening from different researchers.

Table 2.3: Details and results of various finite element analysis

Authors (year)	Parameters					Result	
	Type of beam	Beam size	Opening shape	Opening size	Software		
(Campione & Minafò, 2012)	RC deep beam	200 mm × 480 mm × 820 mm	Without opening	Circular opening with different locations	100 mm in diameter	ATENA 2D	All tested beams failed due to diagonal cracking or to concrete strut failure
(Amin et al., 2013)	RC deep beam	120 mm × 450 mm × 1300 mm	Square		0.45h, 0.30h, 0.15h	ANSYS CIVILFE M 12.0	Effect is largest when opening is provided at shear zone. Shear increase with decrease with the size of opening
(Hafiz et al., 2014)	Simply supported RC beam	100 mm × 250 mm × 2050 mm	Square and circular		133 mm in width and diameter	ANSYS CIVILFE M 10.0	Opening size with less than 44% of depth of beam has no effect on the ultimate load capacity. For more than 44% reduces the ultimate load at least 34.29%.

(Mohamed, Shoukry, & Saeed, 2014)	RC deep beam	500 mm × 2000 mm × 6000 mm	Rectangular and square. Different number of opening	Different opening sizes: 120 mm × 600 mm 600 mm	ABAQUS	Web openings along load path reduced about 35% of beams capacity.
(Hemanth, 2012)	Simply supported RC deep beam	150 mm × 460 mm × 1200 mm	Circular opening	N.A.	ANSYS	Ultimate load carrying capacity of all the strengthened beams is higher when compared to control beam. Initial shear crack appeared at higher loads. Strength gain caused by GFRP sheets was in the range 68 – 125%.
(Alsaeq, 2014)	RC deep beam	110 mm × 600 mm × 2400 mm	Large opening, square and circular opening	240 mm in width and diameter	ANSYS 12.1	Using a circular opening instead of a square one with the same size can save a 19% of structural strength. CFRP laminaes enhances the strength by an amount of up to 29% for beams.

(Hawileh, El-Maaddawy, & Naser, 2012b)	RC deep beam	80 mm × 500 mm × 1200 mm	Square openings at middle of shear span or top of the shear span near support	150 mm × 150 mm & 200 mm × 200 mm & 250 mm × 250 mm	ANSYS	The load capacity of the CFRP-strengthened FE models was up to 74% higher than that of the unstrengthened FE models.
(El Maaddawy & Sherif, 2009)	RC deep beam	80 mm × 500 mm × 1200 mm	Square openings	250 mm in width	Experimental research	Externally bonded CFRP shear strengthening around the openings was found very effective in upgrading the shear strength of RC deep beams. The strength gain caused by the CFRP sheets was in the range of 35 – 73%.

From the literature review that had been studied and summarised in Table 2.3, the gap of researches was found that the opening for the analysis were mostly focused on small opening and the location was not in the critical shear zone. Circular and square openings were mostly done by researchers to investigate the behaviour of the beams before and after strengthening by CFRP, but large openings, which are more than 44%, have limited sources of researches. Thus, in this study, large opening size about 45% for square and circular in shapes was adopted and the location of the opening was at the support which was at the critical shear zone.

CHAPTER 3

RESEARCH METHODOLOGY

3.1 INTRODUCTION

ANSYS CivilFEM 12.0 performs advanced customization for the ANSYS in the finite element analysis. Actually, ANSYS and CivilFEM are the combination of two programs and they are integrated well and thoroughly with providing Construction and Civil Engineering fields in a wide range of projects with the possibility by applying high-end technology. CivilFEM is being widely used due to its capabilities of including a unique and extensive materials and sections library for both concrete and steel structures. Finite element analysis can be done and analysed through its postprocessor. Code checking is the system provided in the postprocessor for users to analyse the modelling by referring to the code that is chosen for analysis (Moreno et al., 2001). ANSYS CivilFEM 12.0 is an engineering simulation software for the finite element modelling and analysis.

3.2 RC BEAM MODELS

3.2.1 Control Beam

Figure 3.1 and 3.2 show the schematic diagram of the control beam that being used in this study. The cross-section of the control beam was 120 mm x 600 mm with a length of 2400 mm as shown in the figures. Figure 3.2 also shows the arrangement of steel reinforcements in the control beam.

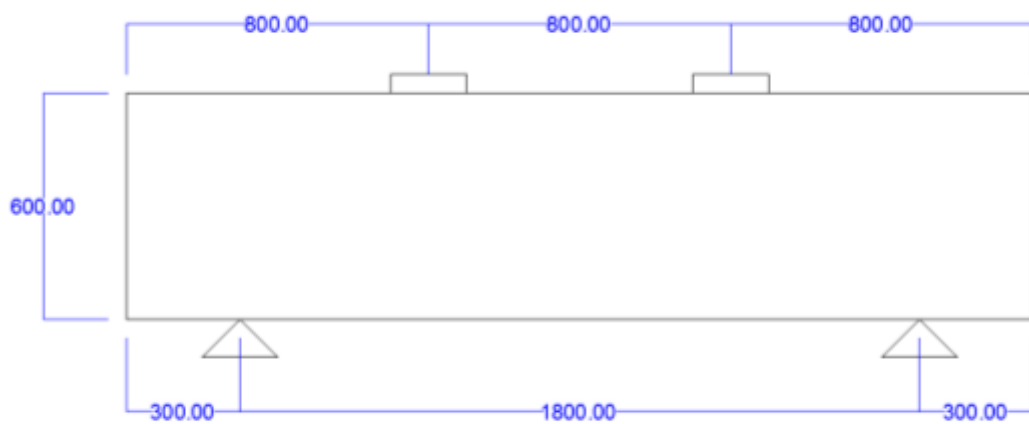


Figure 3.1: Schematic diagram of control beam

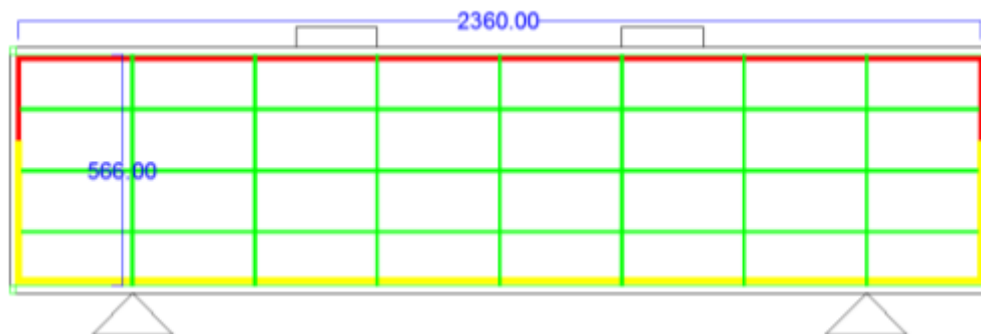


Figure 3.2: Arrangement of steel reinforcement in control beam

3.2.2 RC Deep Beams with Square and Circular Openings

i. Opening shape: Square

Opening size: 120 mm x 270 mm x 270 mm

- a. RC Deep beam with square opening without strengthening (45% of reduction)
- b. RC Deep beam with square opening with CFRP strengthening (45% of reduction)

Figure 3.3 and 3.4 show the schematic diagram of RC deep beams with square openings. The opening is 300 mm from the side of the beam as shown in Figure 3.3 while Figure 3.4 shows the arrangement of the steel reinforcements.

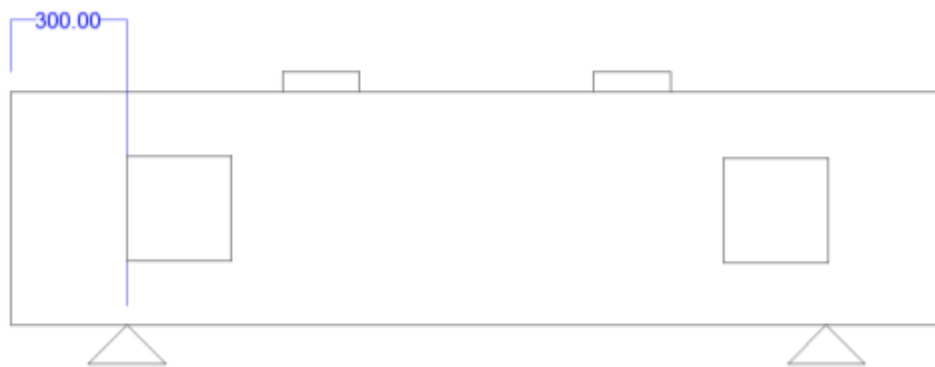


Figure 3.3: Schematic diagram of deep beam with square openings

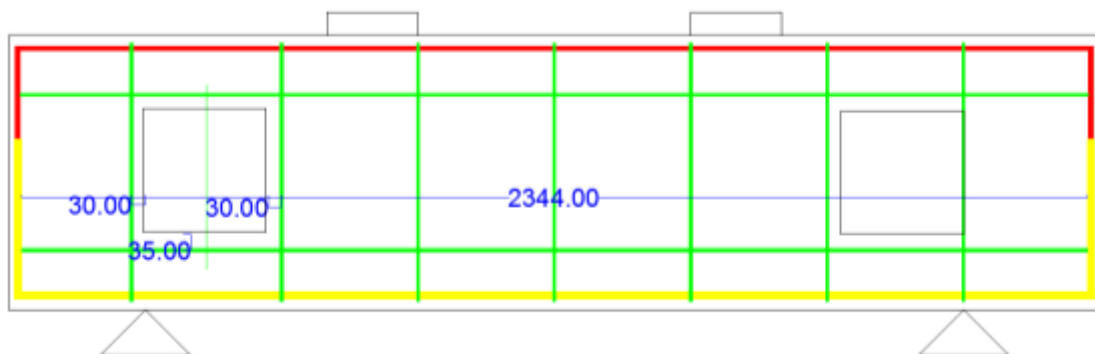


Figure 3.4: Arrangement of steel reinforcements in deep beam with square openings

ii. Opening shape: Circular
 Opening size: 270 mm in diameter

- a. RC Deep beam with circular opening without strengthening (45% of reduction)
- b. RC Deep beam with circular opening with CFRP strengthening (45% of reduction)

Figure 3.5 and 3.6 show the schematic diagram of RC deep beams with circular openings. The opening is 270 mm from the edge of the beam as shown in Figure 3.5 while Figure 3.6 shows the arrangement of the steel reinforcements.

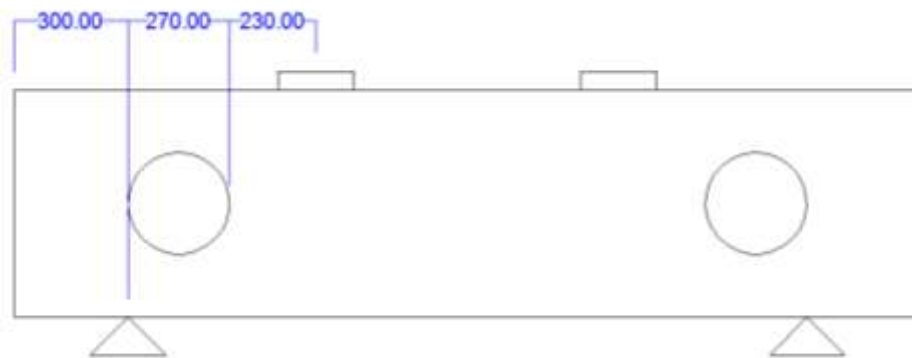


Figure 3.5: Schematic diagram of deep beam with circular openings

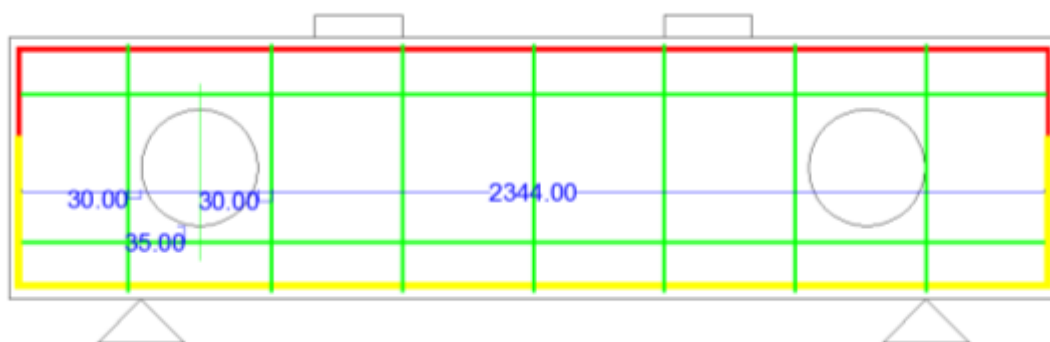


Figure 3.6: Arrangement of steel reinforcements in deep beam with circular openings

3.3 MATERIAL PROPERTIES

The material properties used in ANSYS had to be appropriate to the physical properties of the materials being used in experimental work and the material codes had been shown in Figure 3.7. The SOLID65 represents the concrete of GRADE 35 in experimental work.

There were three types of steel reinforcements being used in the analysis which included steel reinforcements with diameter in 16 mm, 10 mm and shear link with 6 mm. The steel reinforcements had the same properties, LINK8, for the steel of 16 mm and 10 mm but different real constants. The real constants defined the difference between the steel in 16 mm and 10 mm. The shear link also had the same material properties but different value of yielding and real constant.

CFRP which was the strengthening material used to recover the load capacity of the RC deep beams in this study was modelled by the material with code of SOLID46 in ANSYS. Figure 3.8 shows the materials properties that had been set for all the element types. Figure 3.9a and Figure 3.9b show the real constants that had to be set for all the elements so that ANSYS could differentiate the elements that have same element types. There were a total of three types of elements which had been set for the real constant while a total of four sets of material properties had been configured for different type of elements. Set 1 represented concrete, while Set 2, Set 3 and Set 4 represented steel reinforcement with 16 mm, steel reinforcement with 10 mm and shear link with 6 mm respectively. Set 5 was the real constant for CFRP.

The thickness of the CFRP used in this study was 0.0014 m and the maximum length of the CFRP in each element was only 20 mm for each side. The dimension for the model of CFRP was small in scale since CFRP was very fine and it had a very narrow and neat arrangement. The properties was similar to the physical properties of CFRP in experimental work.

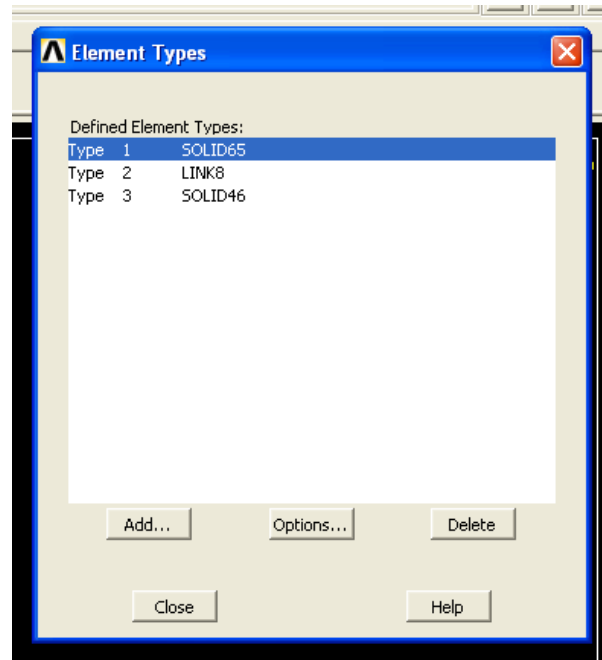


Figure 3.7: Type of elements that represented the materials used in experimental

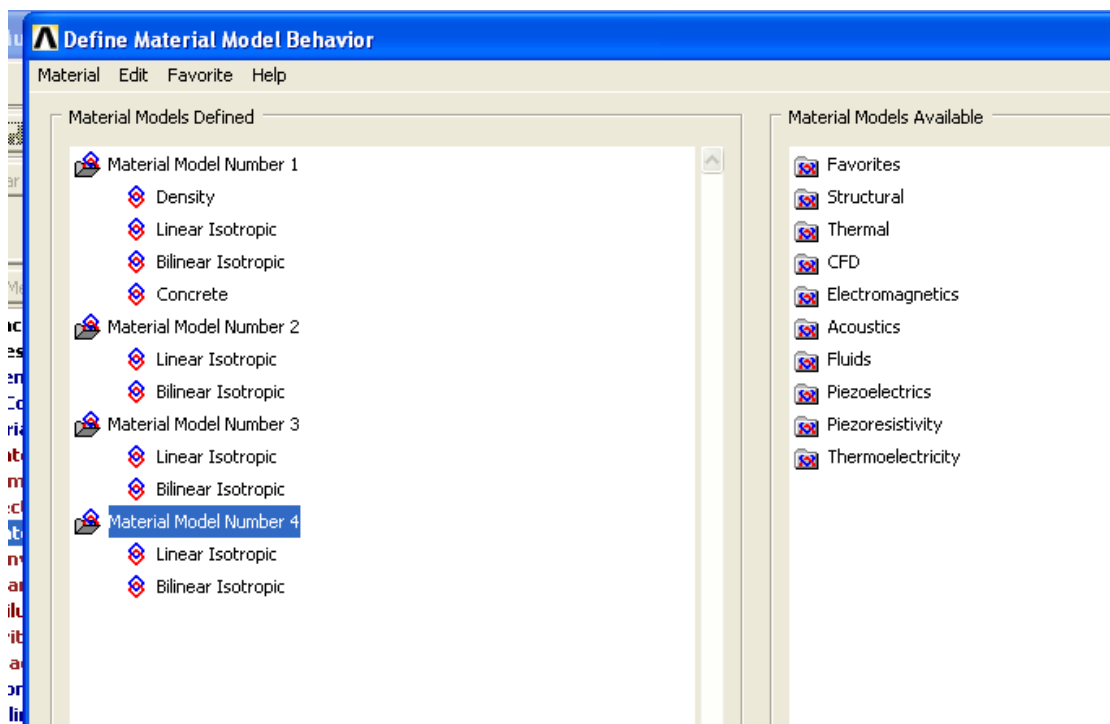


Figure 3.8: Material properties of all the elements needed in ANSYS

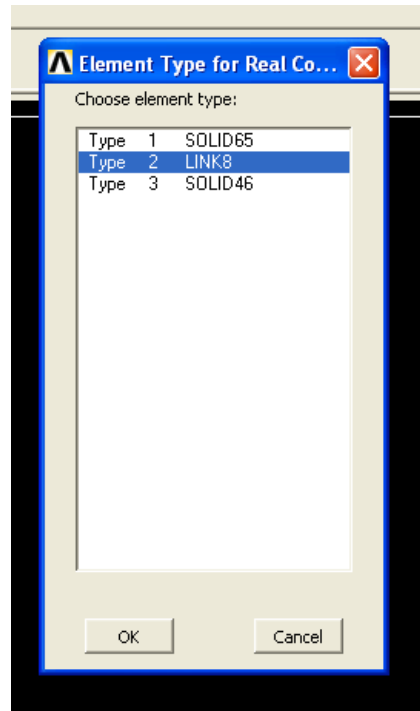


Figure 3.9a: Elements that can be chosen to set for the real constant

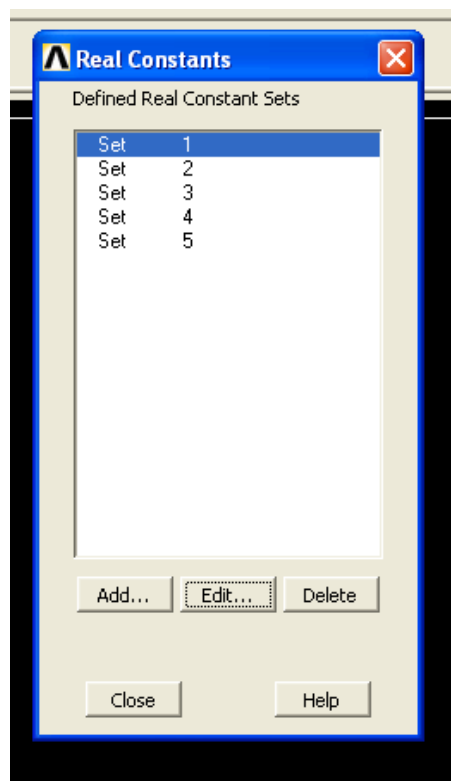


Figure 3.9b: Total of five sets real constant had been set for all the elements needed

3.4 DETAILS OF STUDY

In this study, thirteen deep beams with and without openings were modelled as four-point loading (simply supported) beams by using ANSYS CivilFEM 12.0 in 3-dimensional. Incremental load was used to test the modelled RC deep beam until the beams experienced serviceability failure. All the typical RC deep beams had the same dimensions of 120 mm x 600 mm and 2400 mm in length. CivilFEM 12.0 had to be activated manually so that it was initiated and ready to be used together with ANSYS. Figure 3.10 shows the initiation of CivilFEM 12.0. International standard, Eurocode 3 had been chosen for the steel standard and Eurocode 2 for the concrete as shown in Figure 3.11, and SI units had to be chosen to ensure the dimensions were in standard form. All the beams were modelled in half of the length in ANSYS. The beams were modelled in half-length to ease the analysis of the beams. Shorter time was required to run for the analysis and it had the same result with the beam in full length. The beams were constrained in all direction at the mid-end of the beams to ensure the beams acted same as full-length beams. At the support of the beams, it was fixed for all degree of freedom. Load was applied on the beams directly with incremental load.

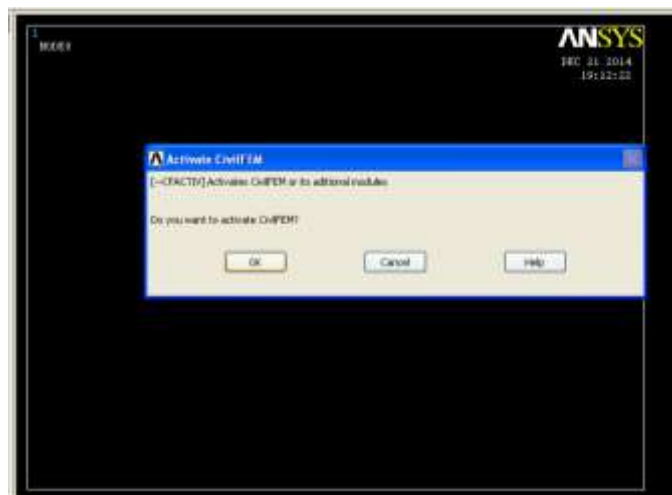


Figure 3.10: Initiation of CivilFEM 12.0

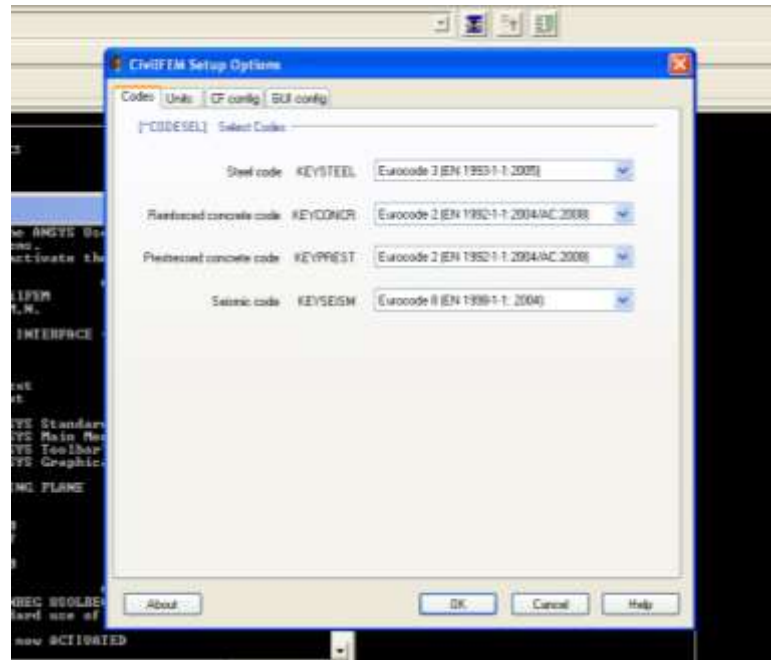


Figure 3.11: International standards and SI units

Steel reinforcement bar was modelled for tension, compression and shear link reinforcement. Tension reinforcement bars which consisted of two steel reinforcement bars with diameter of 16 mm. Compressive reinforcement which made up of two 10 mm steel reinforcement bars and the diameter for the shear link reinforcement was 6 mm. The shear links were spaced 300 mm from centre to centre. Horizontal links were also modelled in the RC deep beams by regularly 150 mm apart from the top and bottom of the beams and from centre to centre of the steel reinforcements. Concrete cover was maintained at 20 mm for all the modelled beams.

One of the thirteen beams acted as control beam without opening and strengthening had been set as the reference for all the other beams. The study parameters were set at two different shapes and the presence of strengthening. The details of the modelled RC deep beam were given in Table 3.1. All the strengthening CFRP laminate was only pasted with one layer.

Table 3.1: Test parameters

Beams	Opening Shape	Wrapping Method	Alignment of CFRP	No. of pieces of CFRP	Opening Size (mm)
CB	-	-	-	-	-
DBS	Square	-	-	-	270 × 270
DBSS1	Square	Surface Strengthening	Vertical	1	270 × 270
DBSS2	Square	Surface Strengthening	Horizontal	1	270 × 270
DBSS3	Square	Surface Strengthening	Vertical	4	270 × 270
DBSS4	Square	Surface Strengthening	Horizontal	4	270 × 270
DBSS5	Square	U-wrap Strengthening	Vertical	-	270 × 270
DBSS6	Square	U-wrap Strengthening	Horizontal	-	270 × 270
DBSS7	Square	U-wrap strengthening	Vertical	Cut strip	270 × 270
DBC	Circular	-	-	-	Ø 270
DBCS1	Circular	Surface Strengthening	Vertical	1	Ø 270
DBCS2	Circular	Surface Strengthening	Horizontal	1	Ø 270
DBCS3	Circular	U-wrap Strengthening	Vertical	-	Ø 270
DBCS4	Circular	U-wrap Strengthening	Horizontal	-	Ø 270

3.4.1 Control Beam

The first beam that needed to be modelled was control beam (CB) which did not have opening and absence of strengthening. Figure 3.12 shows the details modelling of the control beam in ANSYS CivilFEM 12.0. The beam was modelled in half of its length for ease of analysis. The control beam was modelled by blocks of concrete elements which was SOLID65. Eight of the nodes were joined together to be a block of element. When all the elements joined together and it would be a beam with reinforced concrete properties. The tension steel reinforcement which consisted of two 16 mm – diameter steel bars and two 10 mm – diameter steel reinforcements for the compression zone as shown in Figure 3.13. Eight vertical shear reinforcements with 6 mm – diameter and two horizontal shear reinforcements with 6 mm – diameter for each side were modelled to prevent failure due to cracking. Steel reinforcements were modelled by joining two nodes together and the steel reinforcement was shown in a line. Two incremental loading were applied to the control beam until the beam is failed.

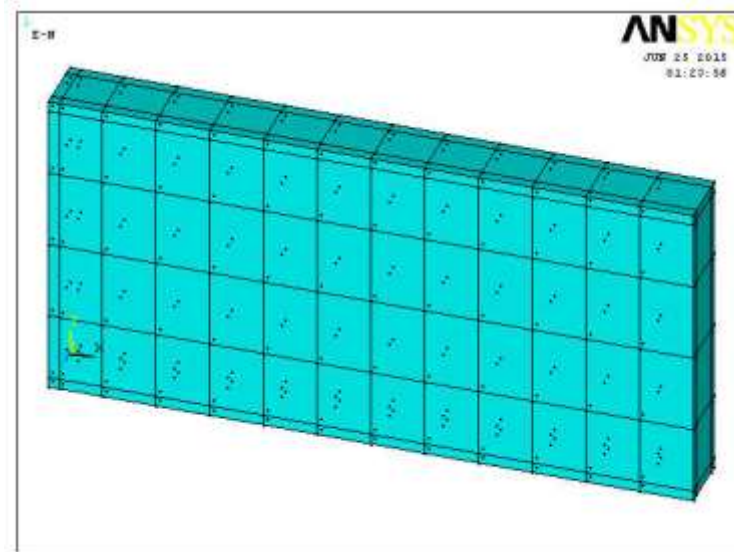


Figure 3.12: Control beam in ANSYS CivilFEM 12.0

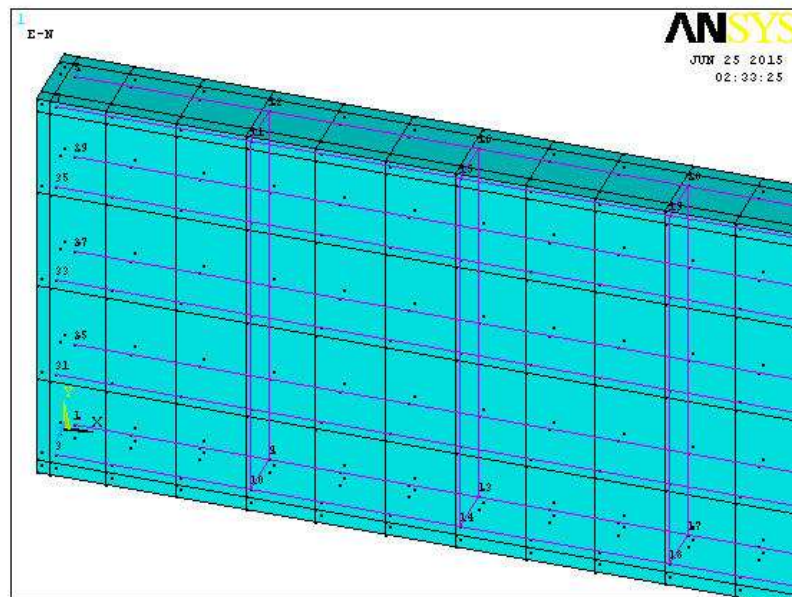


Figure 3.13: Steel reinforcement modelling

3.4.2 RC Deep Beam with Square Opening without Strengthening Of CFRP

Reinforced concrete deep beam with square opening (DBS) without any strengthening was modelled to determine the percentage of reduction in load capacity of the deep beams with openings. The size of the opening was 270 mm for each side. The side of the square opening was placed just at the support and extended towards the mid span of the beam. Two incremental loadings were applied at the distance of 500 mm from the supports. The steel reinforcement bars for this model were different from the control beam. The steel reinforcement had to be adjusted around the opening so that the location of opening could be started exactly at the support. Modelling of the beam with square opening was almost similar to the modelling of the control beam. The concrete elements were joined by eight nodes to form a block and the steel reinforcements were modelled by joining two nodes. Figure 3.14 shows the model of deep beam with square opening. The locations of steel reinforcement also shown in figure 3.14.

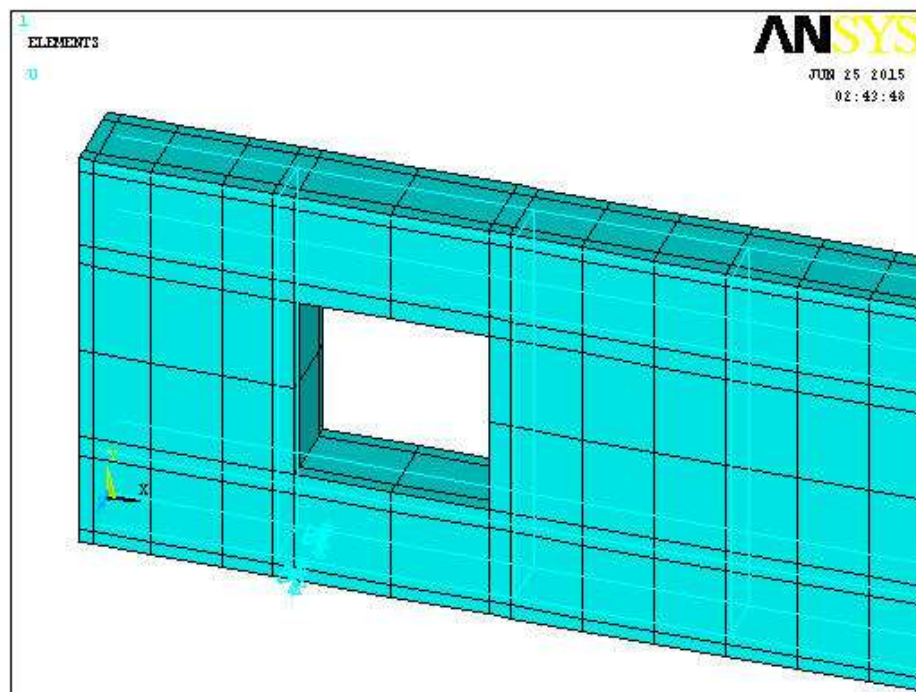


Figure 3.14: Model of deep beam with square opening and the locations of steel reinforcement

3.4.3 RC Deep Beam with Square Opening Strengthened by CFRP

The deep beams with openings being modelled need to be strengthened so that the most effective method of strengthening could be identified. There are a number of methods had been modelled to identify the percentage of recovery and at the same time to determine the best strengthening method to recover the load capacity of the deep beams with openings. The strengthening was focused at the shear zone because the beams were assumed to have shear failure as the large opening was placed at the support.

The deep beam with square opening, DBSS1, was strengthened by surface strengthening method as shown in Figure 3.15. One whole piece of the CFRP was pasted on the RC deep beam and then the square opening was cut on the CFRP laminate. The CFRP was in red colour when modelled in ANSYS to differentiate it with concrete elements as shown in Figure 3.15. Only one layer of CFRP was pasted on the beam. DBSS1 was modelled in vertical alignment and DBSS2 was in orientation of 0° . DBSS1 had the vertical direction while DBSS2 had the horizontal direction. DBSS3 and DBSS4 had the surface strengthening by CFRP. The overall dimensions of CFRP same as DBSS1 and DBSS2. DBSS3 and DBSS4 had the CFRP pasted on the beam with four different pieces. CFRP was cut into four pieces and pasted around the opening. Figure 3.16 shows that the CFRP was pasted in four different pieces and the boundary of the CFRP obviously could be seen between the top piece and the side piece.

The other method of strengthening was U-wrap strengthening where covered the both side and bottom of the beam. DBSS5 and DBSS6 had the U-wrap strengthening with vertical and horizontal direction of CFRP respectively. Figure 3.17 shows the deep beam strengthened by U-wrap method. By switching on the wire frame function, the CFRP laminates could be clearly seen that it was pasted at both side and bottom of the beam.

The direction of the alignment of the CFRP had to be set in the material properties to ensure the CFRP was modelled accordingly. The horizontal alignment would be set in zero degree while vertical direction was set as 90° as shown in Figure 3.18. The alignment of CFRP would alter the recovery of load capacity. All the beams were tested by incremental load. The RC deep beam was tested to failure as well and the crack pattern, load-deflection, stress and strain contours were obtained and analysed.

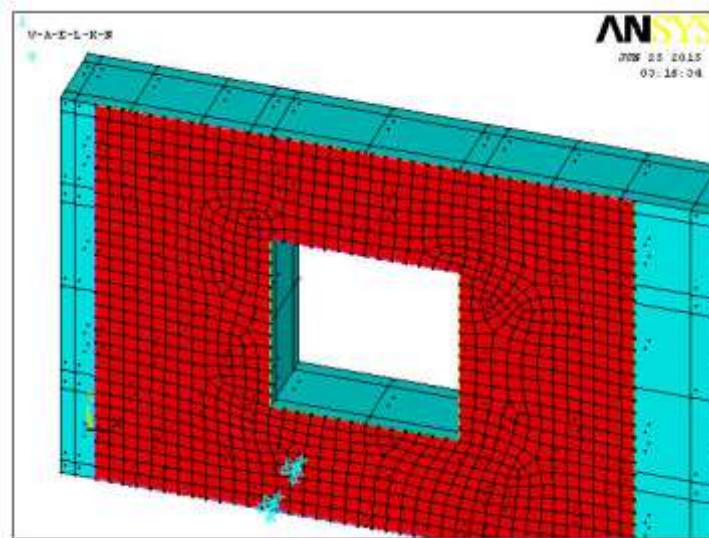


Figure 3.15: CFRP laminate to strengthen the deep beam with square opening

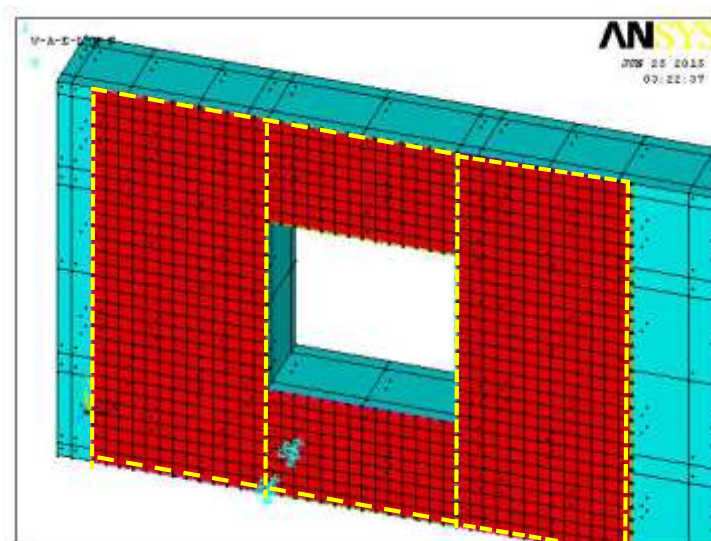


Figure 3.16: CFRP was pasted in four different pieces

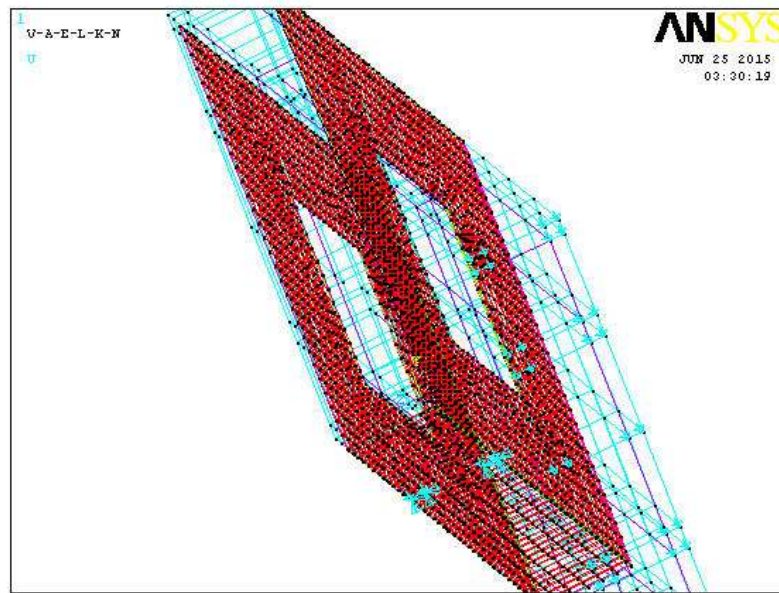


Figure 3.17: U-wrap strengthening method

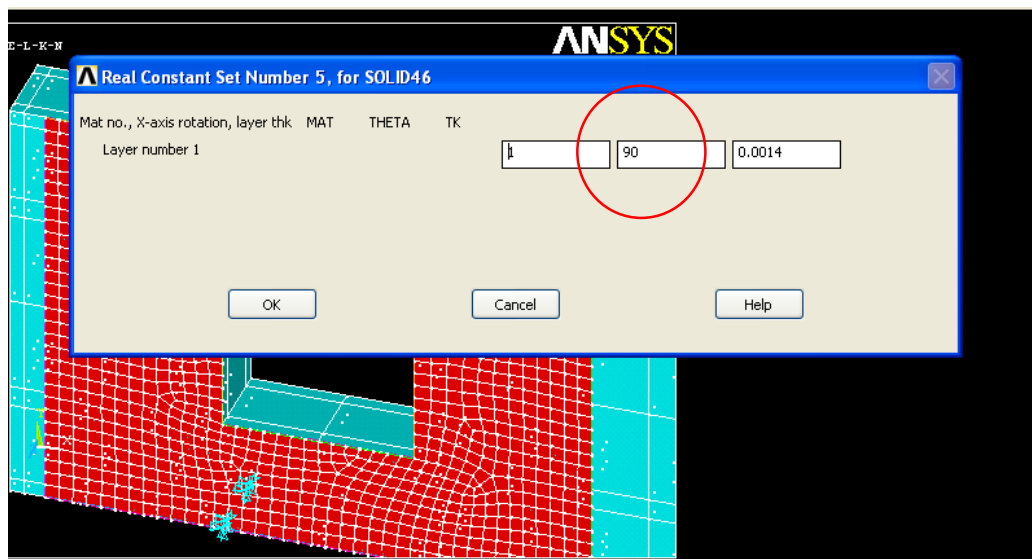


Figure 3.18: Modelling of alignment of CFRP (shown in circle)

3.4.4 RC Deep Beam with Circular Opening without Strengthening Of CFRP

The other parameter that need to be carried out in this study was the different shape of opening. Circular opening was created on the RC deep beam (DSC1). The diameter for this opening would be 270 mm in diameter. The circumference of the circle was aligned with the support and extended towards the shear span. This modelled RC deep beam with circular opening will not strengthened by any material and it was also be tested to fail by two incremental loads.

The circular opening was modelled by an icosagon, a regular polygon with 20 sides, to illustrate the circular opening at the beam. The deep beams with circular opening were also modelled by joining eight nodes to form an element. Icosagon was the best shape to model the circular opening to be analysed in ANSYS. Figure 3.19 shows the model of deep beam with circular opening in ANSYS.

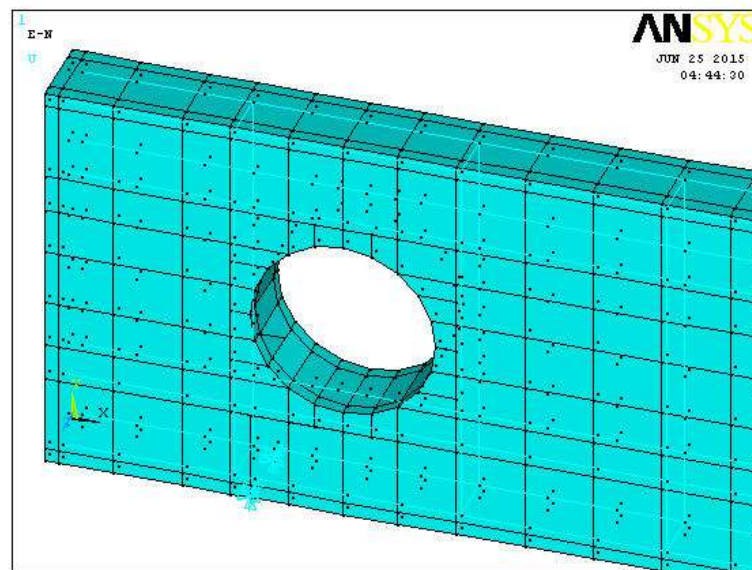


Figure 3.19: RC deep beam with circular opening

3.4.5 RC Deep Beam with Circular Opening Strengthened by CFRP

DBCS1 and DBCS2 were the beams that had been modelled to recover the load capacity by surface-strengthening. Both direction of alignment had been modelled for DBCS1 and DBCS2. DBCS3 and DBCS4 were strengthened by U-wrap method as shown in Figure 3.21. The modelling of CFRP for circular opening was totally different from CFRP for square opening as the CFRP for circular opening was also modelled one by one by joining eight nodes together to form a CFRP element and CFRP for square opening was modelled by blocks and auto-meshing was generated for the CFRP material. Figure 3.20 shows the surface bonded CFRP to strengthen the RC deep beams with circular openings.

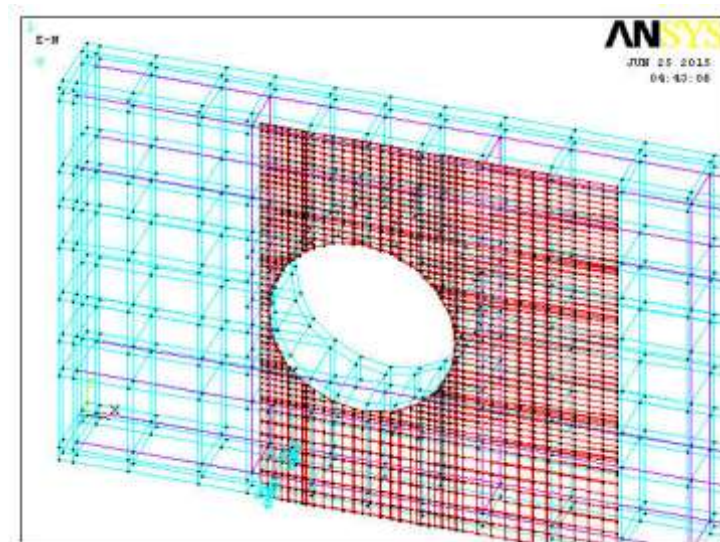


Figure 3.20: RC deep beam with circular opening strengthened by surface-strengthening

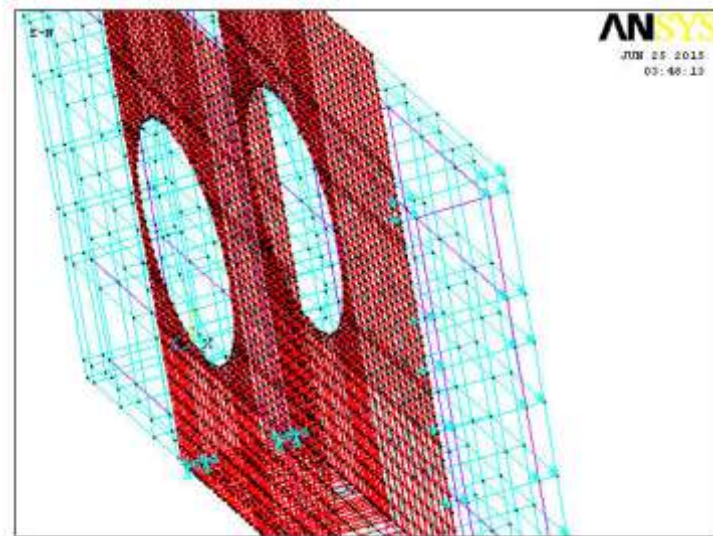


Figure 3.21: RC deep beam with circular opening strengthened by U-wrap

3.4.6 Configuration of CFRP

Carbon fibre reinforced polymer had been modelled in various orientation and method of attaching the CFRP onto the reinforced concrete beam models. Different methods of strengthening gave different results for the analysis and then the most effective strengthening method could be determined. Six deep beams with square opening strengthened by CFRP had been modelled to determine the load capacity recovery of the deep beams. DBSS1 and DBSS2 were strengthened by one whole piece of CFRP and then square opening was cut from the CFRP. Both of them have different orientation of CFRP which were horizontal and vertical alignment. Figure 3.22 and Figure 3.23 illustrate the alignment of CFRP in vertical and horizontal alignment.

Another strengthening method being carried out in this study was by U-wrap method. U-wrap strengthening method indicated the beams were wrapped in three sides included the bottom side. The CFRP also modelled in two directions of alignment which were vertical (DBSS5) and horizontal (DBSS6). In 2-dimensional view, the strengthening of CFRP by surface bonded and U-wrap would look exactly the same. Thus, Figure 3.22 and

Figure 3.23 also indicate the deep beams with square openings strengthened by U-wrap method in both alignment.

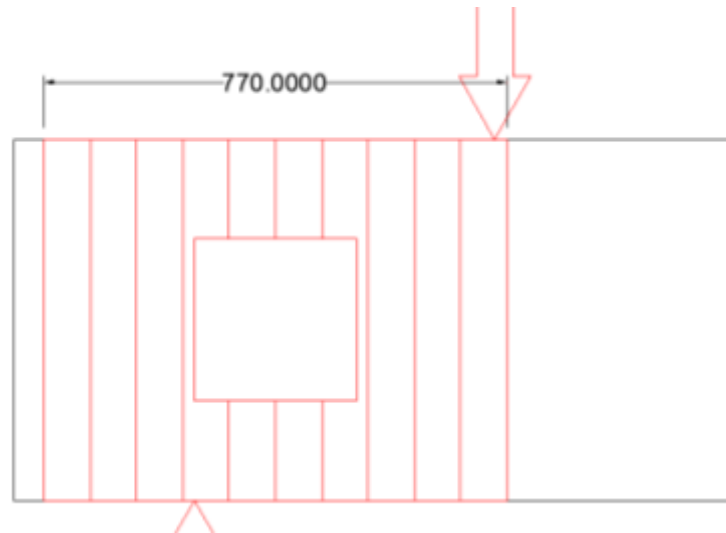


Figure 3.22: CFRP with whole piece in vertical alignment for deep beams with square opening (DBSS1, DBSS5)

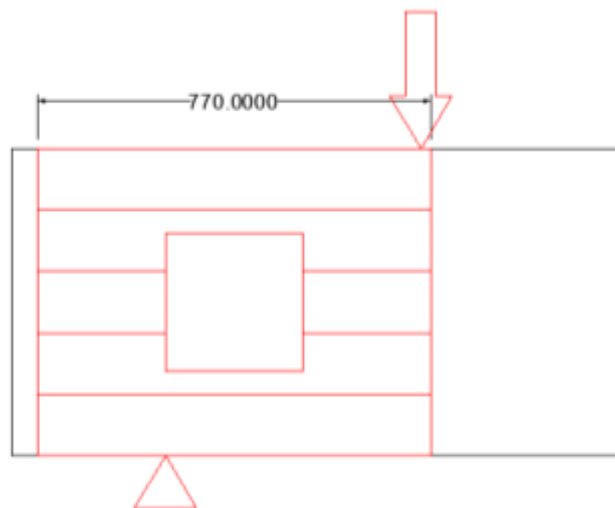


Figure 3.23: CFRP with whole piece in horizontal alignment for deep beams with square opening (DBSS2, DBSS6)

The finite element result had to be validated with experimental result, thus the configuration of CFRP had to be similar with the experimental work. For square opening, the CFRP was pasted onto the beam separately by four pieces. Each sheet on each side of the opening. This method was compared with previous strengthening method to determine the most effective way to strengthen the weakened beams. DBSS3 gave vertical alignment while DBSS4 was model in horizontal alignment. Figure 3.24 and Figure 3.25 show clearly the arrangement of CFRP around the opening.

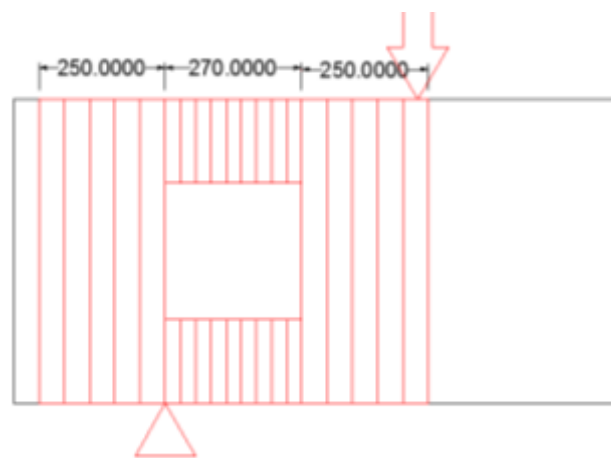


Figure 3.24: Four pieces of CFRP with square opening in vertical alignment (DBSS3)

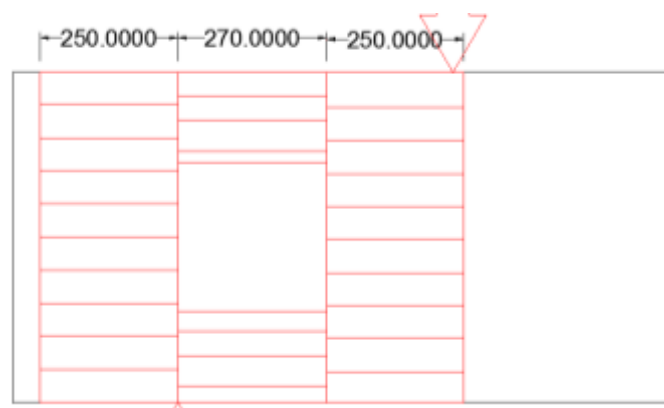


Figure 3.25: Four pieces of CFRP with square opening in vertical alignment (DBSS4)

Similar to deep beams with square openings, deep beams with circular openings also been modelled in various type of strengthening methods to determine the most effective strengthening method to recover the load capacity of deep beams with circular openings. Each method of strengthening would be modelled in two directions of alignments which were vertical and horizontal in direction. Schematic diagram of beams DBCS1 and DBCS3 are shown in Figure 3.26 while DBCS2 and DBCS4 are shown in Figure 3.26 to Figure 3.27, respectively. DBCS1 and DBCS2 were strengthened by surface bonded while DBCS3 and DBCS4 were strengthened by U-wrap method.

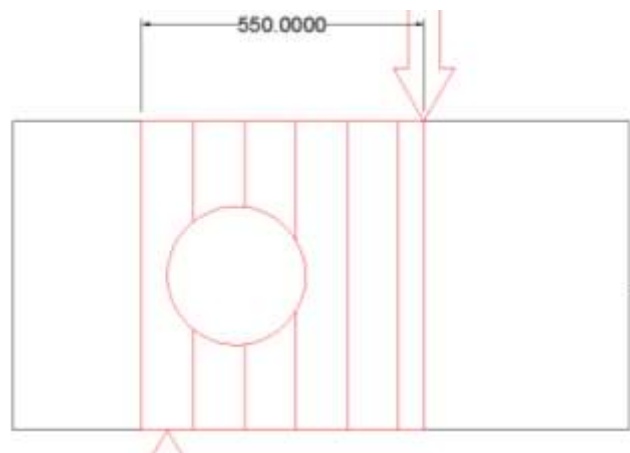


Figure 3.26: CFRP with circular opening in vertical alignment (DBCS1 & DBCS3)

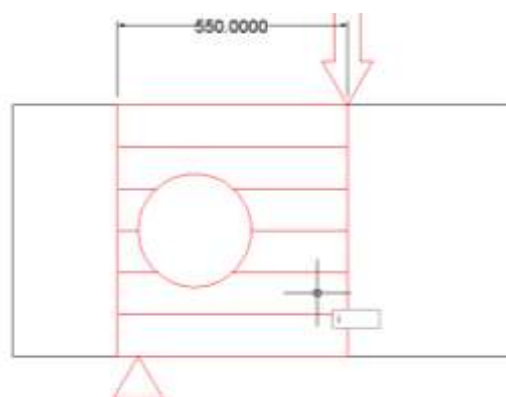


Figure 3.27: CFRP with circular opening in horizontal alignment (DBCS2 & DBCS4)

3.5 ANALYSIS OF RC DEEP BEAM BY USING ANSYS CIVILFEM 12.0

In this study, a 3-dimensional (3D) nonlinear finite element was conducted by using the finite element analysis software, ANSYS CivilFEM 12.0. There were three main steps involved in this research methodology e.g. pre-processing, finite element nonlinear analysis and finally post-processing. The details of every steps were discussed further in the sub-topic.

3.5.1 Pre-processing

Pre-processing stage of the geometrical modelling in ANSYS CivilFEM 12.0 could be considered as defining the materials, elements, nodes and methods to analyse the modelling. These defining steps were important for the modelling because it defined the input data for geometrical nodes, geometrical lines as elements, mesh generation, steel reinforcement bar definition, supports, loads, reactions, incremental loads and lastly definition of monitoring points.

3.5.2 Material Parameters

Before starting any modelling, there were some parameters prior to be defined. Selection of elements types would be the initial step for this study. Parameters in the modelling should be tallied with the parameters for the experimental deep beam. Thus, for example, concrete grade for experimental work is Grade 35, thus the material code for the concrete grade 35 is SOLID65, as shown in the Figure 3.28, shows the material selected for concrete in ANSYS CivilFEM 12.0.

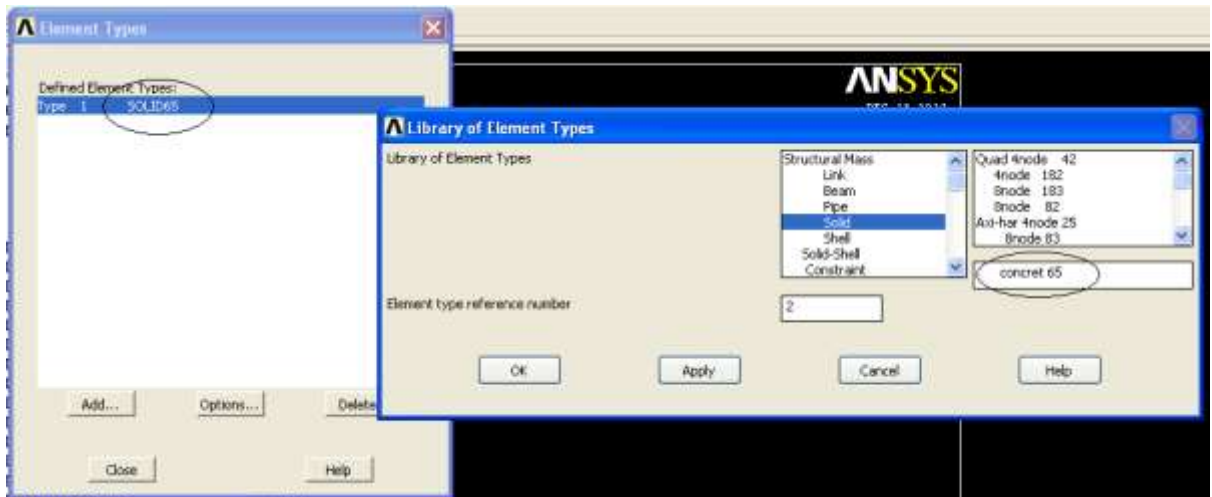


Figure 3.28: SOLID65, material code for concrete strength G35

The elements types for the construction could be chosen from the Element Types in the panels, then chose the desired materials from the pop out window. For choosing the material for concrete, ‘Solid’ was chosen and the concrete 65 was the material that need for this study. SOLID65 would be shown at the Element Types to show that this material had been chosen for the modelling. The other elements types selected for this study were listed in the Table 3.2. Elements types were important because it influenced the result later and affect the failure mode. Finite element analysis result had to be validated as compared to the experimental result, thus the materials chosen had to be identical to the experimental work. Figure 3.29 shows the elements that had been used in analysis.

Table 3.2: Element types used in ANSYS CivilFEM 12.0

Material	Element types
Concrete Grade 35 (35 N/mm ²)	SOLID65
Steel reinforcement bar	LINK8
Carbon fibre reinforced polymer	SOLID46

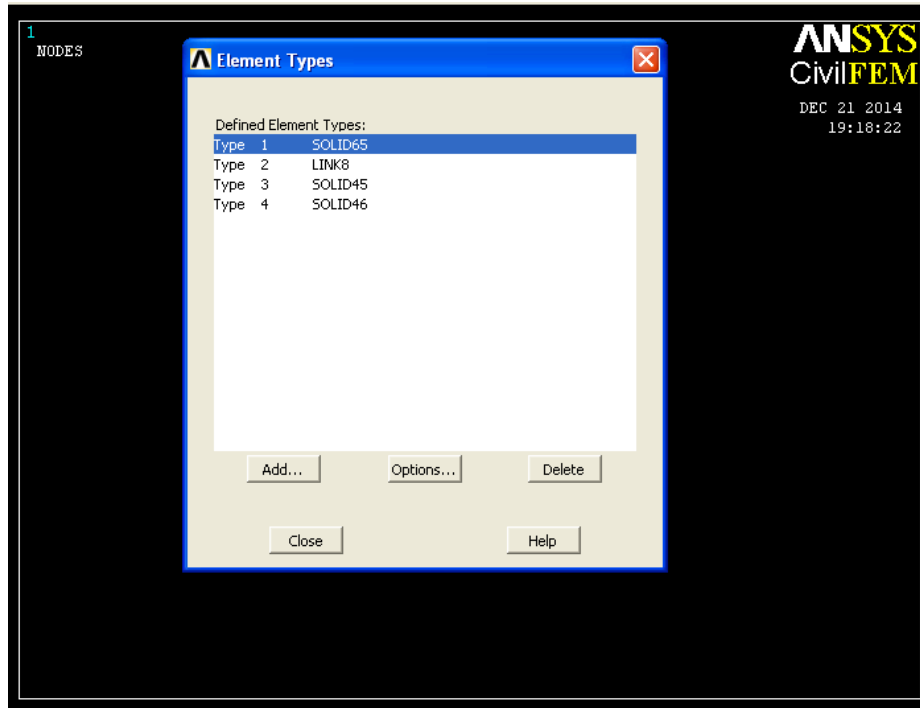


Figure 3.29: All the elements types chosen for this study

Materials properties had to be assigned to the elements so that the analysis could be done according to the behaviour of the materials. This study could only show the convincing result by choosing the correct materials properties for all the elements. Figure 3.30 shows one of the examples on choosing the materials properties accordingly and correctly.

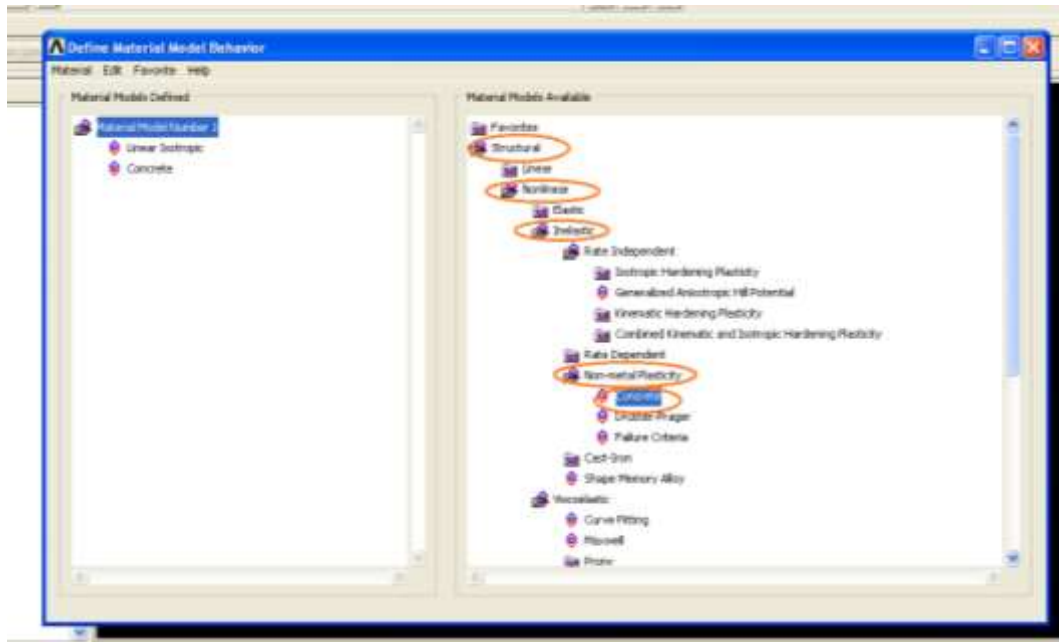


Figure 3.30: Example on choosing the materials properties

Material properties of all the elements had been summarized in the Table 3.3. The elements had to be determined whether it was elastic during assigning the materials properties. Linear or non-linear also had to be specified because it could significantly affect the result. Figure 3.31 shows the overall materials that assigned for each element.

Table 3.3 Summary of material properties assigned to the elements

Elements	Materials Properties	Values	Units
Concrete	Elastic Modulus	32.3	GPa
	Poisson's ratio	0.2	-
	Open Shear Transfer Coefficient	0.2	-
	Closed Shear Transfer Coefficient	1	-

	Uniaxial Tensile Cracking Stress	29.75	MPa
	Uniaxial Crushing Stress	210669	GPa
Steel reinforcement	Elastic Modulus	210	GPa
	Poisson's Ratio	0.3	-
	Yield Strength	410	MPa
Shear link	Elastic Modulus	210	GPa
	Poisson's Ratio	0.3	-
	Yield Strength	410	MPa
CFRP	Elastic Modulus	170	GPa
	Poisson's Ratio	0.3	-
	Yield Strength	930	MPa
Steel plate	Elastic Modulus	200	GPa
	Poisson's Ratio	0.3	-

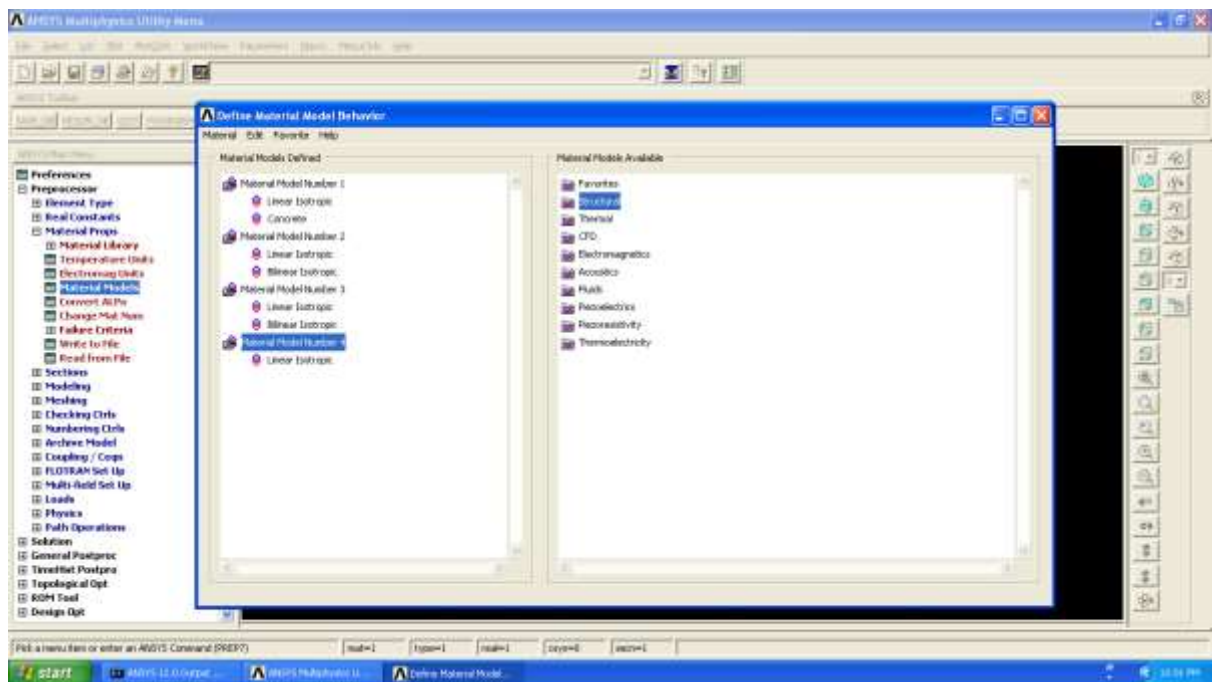


Figure 3.31: Summary of materials assigned to the elements in ANSYS

The diameter of the steel reinforcement bars were 16 mm for the tension zone and 10 mm for the compression zone as well as 6 mm for the steel stirrups. Thus, the real constants of the steel reinforcement bars had to be defined by defining the area of the reinforcements since three of the steel reinforcements had the same element type. Table 3.3 below lists the real constant used for the three types of steel reinforcement bars and Figure 3.32 shows the input of area of the steel to define the real constants.

Table 3.4: Real constants of steel reinforcements by area of reinforcements

Steel Reinforcement Bars	Real Constant
16 mm	201.06 mm ²
12 mm	113.10 mm ²
6 mm	28.27 mm ²

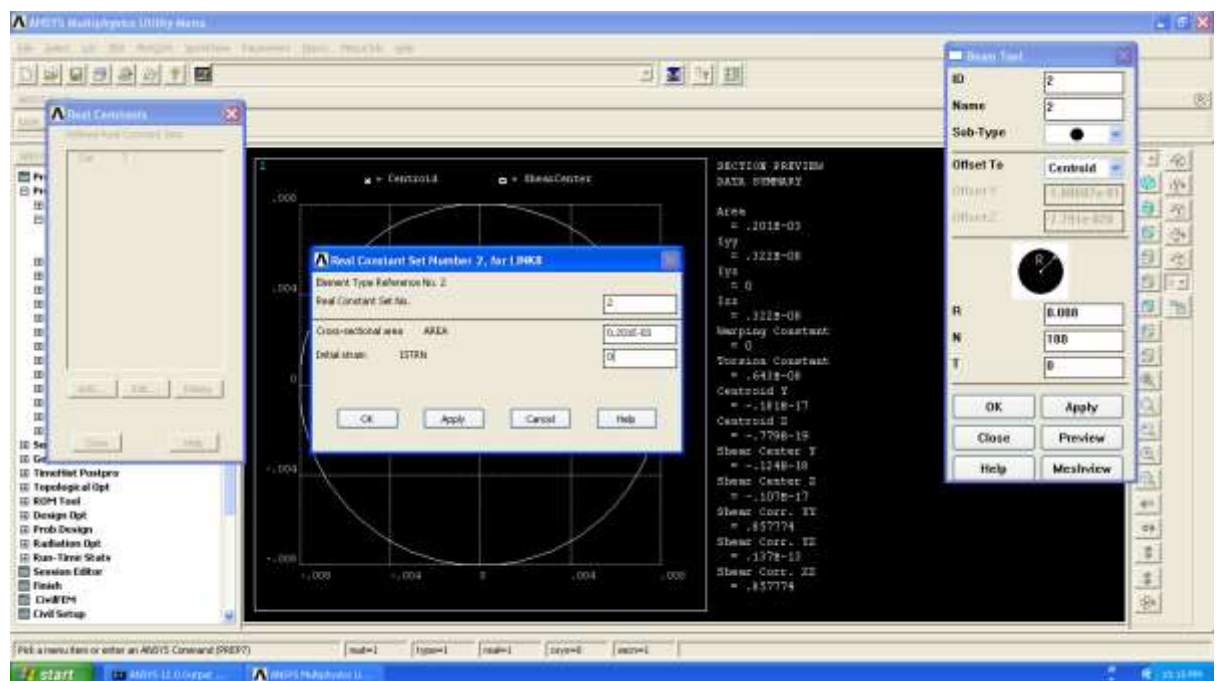


Figure 3.32: Input of area of the steel to define the real constant

3.5.2.1 Geometrical Nodes

Geometrical nodes had to be defined in the Cartesian plane to allow the modelling of steel reinforcements. The geometrical nodes were defined through the command pad because this was the simplest method to model the reinforcements. Table 3.4 lists the nodes for the steel reinforcements in control beam and Figure 3.33 shows the geometrical nodes on the Cartesian plane along x, y and z directions.

Table 3.5: Geometrical nodes for steel reinforcement

No. of nodes	X	Y	Z
1	0.02	0.02	0.02
2	1.2	0.02	0.02
3	0.02	0.02	0.1
4	1.2	0.02	0.1
5	0.02	0.58	0.02
6	1.2	0.58	0.02
7	0.02	0.58	0.1
8	1.2	0.58	0.1
9	0.3	0.58	0.02
10	0.3	0.02	0.02
11	0.3	0.02	0.1
12	0.3	0.58	0.1
13	0.6	0.58	0.02
14	0.6	0.02	0.02
15	0.6	0.02	0.1
16	0.6	0.58	0.1
17	0.9	0.58	0.02
18	0.9	0.02	0.02
19	0.9	0.02	0.1
20	0.9	0.58	0.1
21	1.2	0.58	0.02
22	1.2	0.02	0.02
23	1.2	0.02	0.1
24	1.2	0.58	0.1
25	0.02	0.15	0.02
26	1.2	0.15	0.02
27	0.02	0.3	0.02
28	1.2	0.3	0.02

29	0.02	0.45	0.02
30	1.2	0.45	0.02
31	0.02	0.15	0.1
32	1.2	0.15	0.1
33	0.02	0.3	0.1
34	1.2	0.3	0.1
35	0.02	0.45	0.1
36	1.2	0.45	0.1

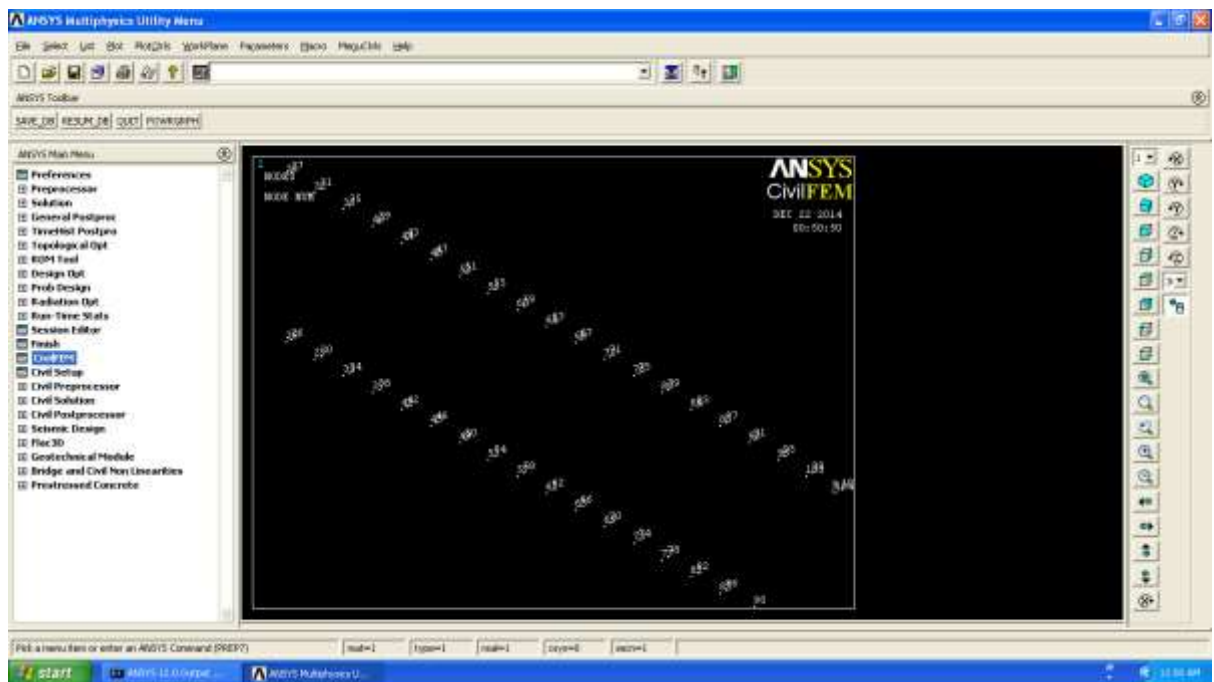


Figure 3.33: Geometrical nodes on the Cartesian plane along x, y and z directions

3.5.2.2 Geometrical Lines

Geometrical lines connected the desired nodes together to form a model. Geometrical lines were not simply a line but defined the elements and materials. Before connecting the nodes by the geometrical lines, element type had to be assigned to the geometrical line so that ANSYS CivilFEM 12.0 could recognize the types of elements wished to be used. Figure 3.34 shows the element that connected all the nodes together to form the RC deep beam.

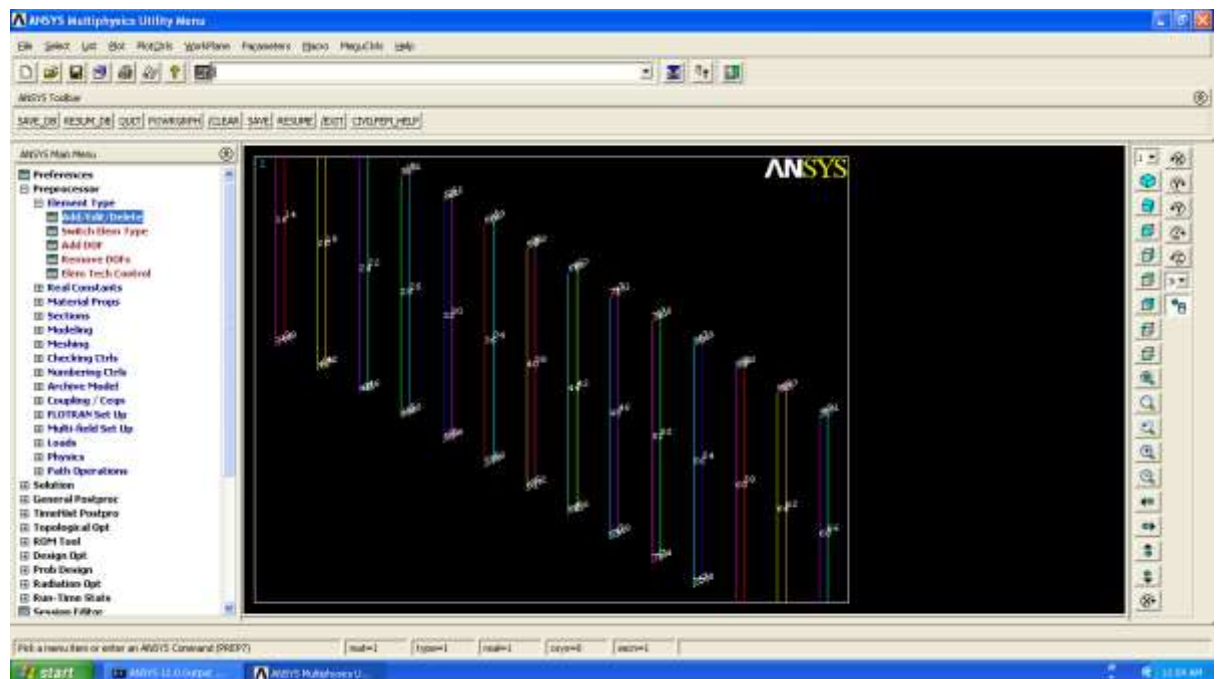


Figure 3.34: Geometrical lines of examples of shear link in ANSYS

3.5.2.3 Mesh Generation

In this study, the mesh generation only used for defining the CFRP in the models of deep beams with square openings. The meshing was done after defining all the elements to the nodes and geometrical lines. Mesh generation had to be done step by step in ANSYS CivilFEM 12.0 because every command had to be completed by the user. The mesh generation in ANSYS CivilFEM 12.0 had to be initiated manually. Finite element mesh was automatically done on the elements that were defined in the earlier stage. The first step for mesh generation was defining meshing attributes. Due to the CFRP layer was being modelled without assigning any material to it, now material had to be assigned to the CFRP in this step. First, SOLID46 was assigned to the CFRP layer so that system could detect that it was a layer of CFRP. The figure below shows the options in the table that had to be chosen for the material properties to define the model as shown in Figure 3.35.

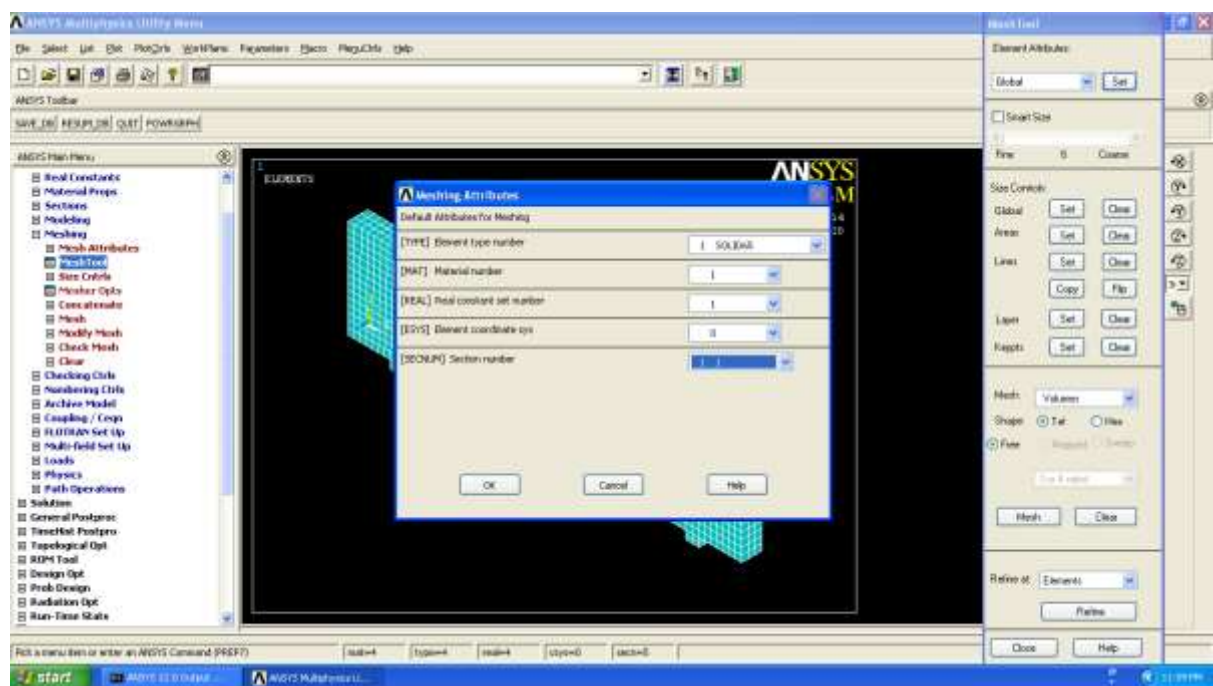


Figure 3.35: CFRP attribute was assigned to the layer during meshing

Meshing in this study was defined as 20 mm to each other. The finite element analysis were done on the intersection points of the horizontal and vertical lines. Meshing in smaller dimensions led to a more accurate result but at the same time the analysis required a longer time to complete the analysis.

3.5.2.4 Steel Reinforcement Bar

In this study, definition of steel reinforcement bars were done only after the modelling of the deep beams. In ANSYS CivilFEM 12.0, two properties were needed to define the steel reinforcement bar. The definition needed were real constant (cross sections) and element type of the reinforcement. The areas of reinforcement had to be calculated manually and keyed into the ANSYS. By referring to Figure 3.36, there were two reinforcements at the bottom and top of the deep beam, vertical shear reinforcement bars were located 300 mm apart from centre to centre while horizontal shear reinforcement bars were located 150 mm apart from each other centre to centre.

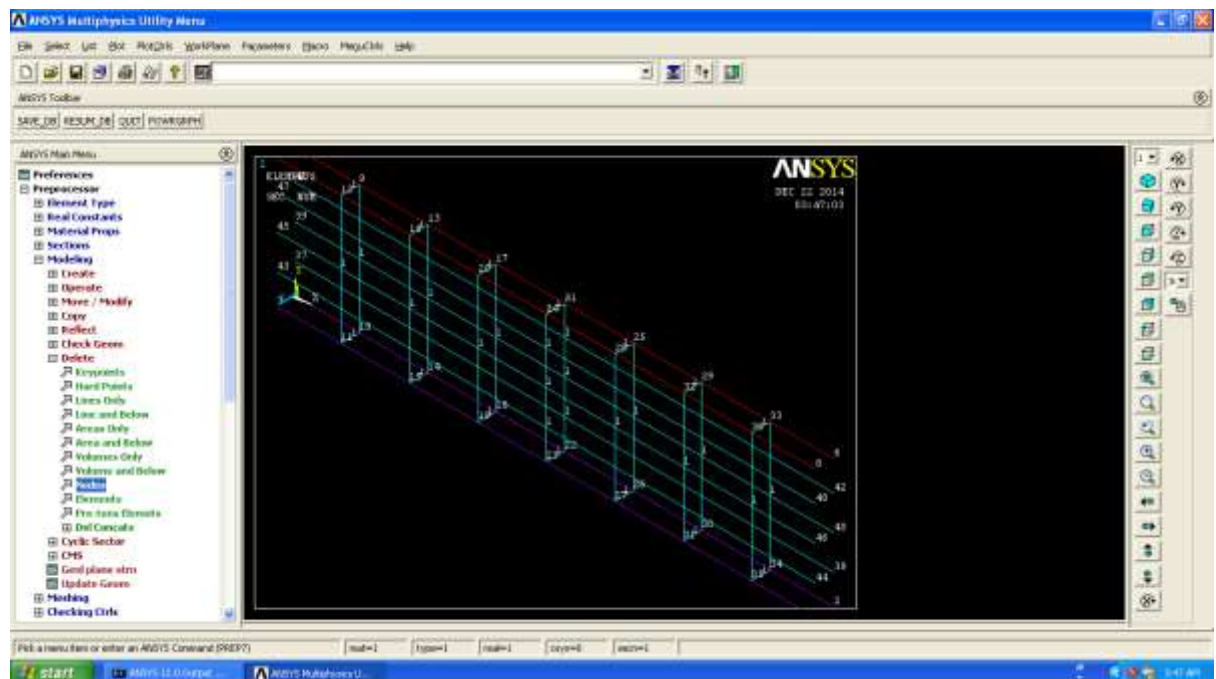


Figure 3.36: Steel reinforcement in ANSYS CivilFEM 12.0

3.5.2.5 Supports and Actions

In this study, the modelled beams were supported at the bottom. In addition, load was modelled at the top by pressure as well as to allow the load from the analysis to be uniformly applied to the simply supported deep beams. Pressure was applied through area thus it had a better uniformity of distributed load to the beams. The pressure area load was applied to the beam as shown in Figure 3.39. Incremental load was applied to the deep beams to ensure the maximum load-carrying capacity could be determined. The elements that being exerted pressure had a red colour perimeter on the top of the elements to indicate the location of load. The value also would be shown on the left side top of the window as shown in Figure 3.39. As for this study, all the deep beams were applied incremental load from the same strength that was started from zero to the maximum. The maximum load-carrying capacity different for all the deep beams.

For the supports to be concerned, one of the supports would be restrained in three degree of freedom (Figure3.37) and the other will be roller support and restrain the degree of freedom in y-direction. Since the beams were only modelled in half-length, thus the beam was only restrained at the support by all degrees of freedom and at the mid-span of the span, it was restrained for x-direction (Figure 3.38). All the restrains were modelled on the nodes of the elements.

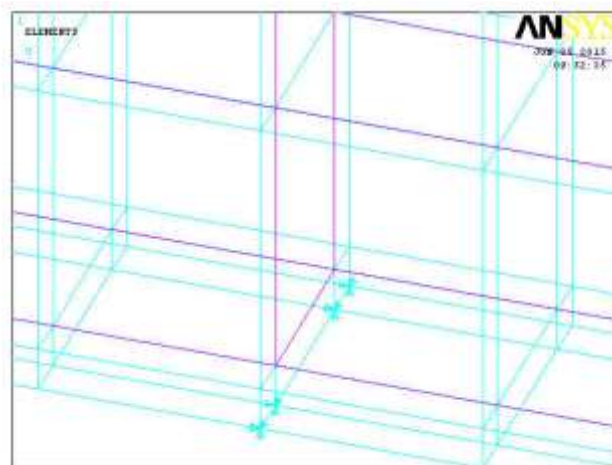


Figure 3.37: Support with all degree of freedom are restrained

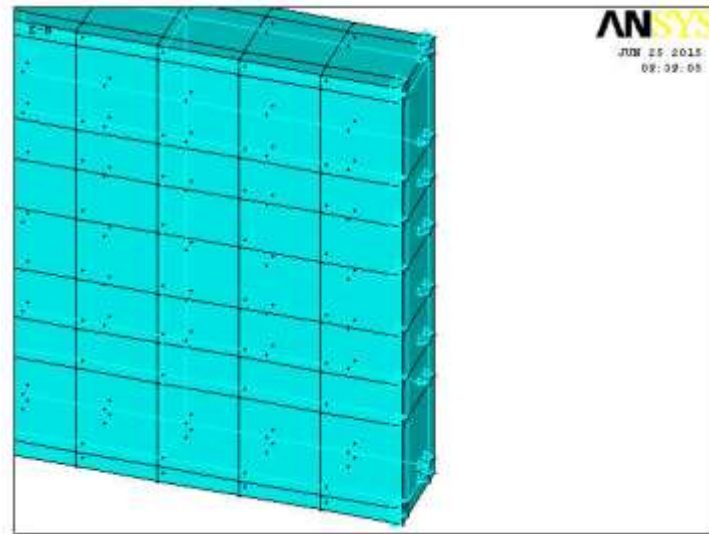


Figure 3.38: Support with restrained y-direction

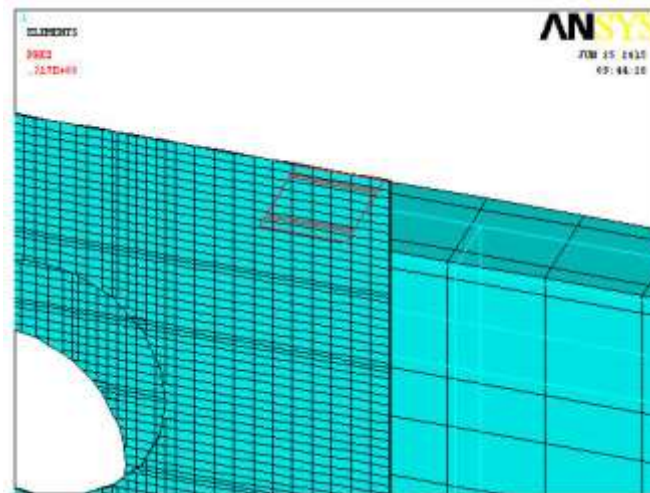


Figure 3.39: Pressure (area loads) was applied on the deep beam

3.5.2.6 Loading History and Solution Parameters

Load steps had to be defined so that the system could increase the load constantly over the time. All the numbers of load steps, loads were to be increased over time and maximum loads were defined into the system. For monitoring purpose, the load step had to be set that monitored at every load step. If this is not been set, only the last load step before the deep beam failed could be obtained. Figure 3.40 shows the monitoring window to set all the desired command to the ANSYS.



Figure3.40: Interaction window to set the option for load applying

3.5.2.7 Monitoring Points

One of the objectives of this study was to identify the load-deflection behaviour, crack pattern, stress and strain contours of the deep beams, therefore, it was very important to have monitoring on the forces, displacements and stresses in the models as the monitored data able to provide vital information about the states of the structures. In addition, the maximum load bearing capacity could be determined as well.

3.5.3 Finite Element Non-Linear Analysis

By using all the data that had been prepared in the previous steps, non-linear finite element analysis of the beam can be conducted. In ANSYS CivilFEM 12.0, before starting the analysis, the finite element mesh numbering could be viewed. It was possible to view, on or off for all the nodes, elements, and geometrical entities to ensure all the desired data inserted was all correct.

3.5.3.1 Starting Analysis

Finite element analysis could be run automatically after all the required data was filled in. Load step had to be selected initially to determine when the analysis should be terminated. The data required to be displayed in the stress and strain contours was determined. All the data was stored in the ANSYS and then the data was extracted from the output and result for further analysis.

3.5.3.2 Interactive Window

After clicking the ‘Solve current LS’ button in the dialog box, the actual finite element analysis was initiated and the analysis progress could be monitored through the interactive window. Figure 3.41 shows the initializing of analysis.

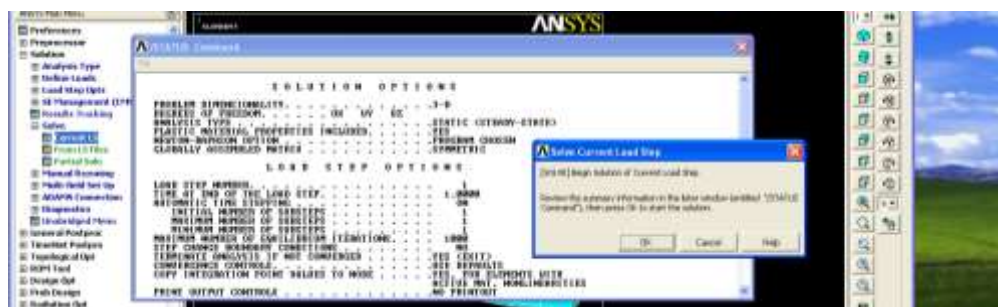


Figure 3.41: Interactive window of initializing the analysis

3.6 SUMMARY OF PROCEDURES

- i. The code of practice, Eurocode 2 and International System of unit were set in ANSYS CivilFEM 12.0.
- ii. Material types were defined in the ANSYS CivilFEM 12.0, concrete as SOLID65, steel reinforcement bars as LINK8 and carbon fibre reinforced polymer as SOLID46.
- iii. Real constants were set for the LINK8 since there were three different diameters of reinforcement being used for modelling. The real constants could be differentiated by the area of the cross sections of the reinforcements.
- iv. Nodes for each elements were modelled into ANSYS by coordinates x , y , and z . Eight nodes were joined together to form a block of elements. All the nodes were joined together to form many blocks of elements. When all the elements joined, it became a model of beam. The models of the beams were in 3 – dimensional.
- v. For beams that were strengthened by CFRP, the CFRP was modelled by block for square openings and then the block was meshed to define the material properties of CFRP. On the other hand, for circular opening, since there was a regular polygon to indicate circular opening, thus the CFRP had to be modelled through nodes. The nodes were modelled in the ANSYS and also eight nodes to join together to form the elements of CFRP.
- vi. Steel reinforcements were modelled by joining two nodes to form a line of reinforcement. Thus two nodes at each end of the reinforcements had to be modelled to let the elements of reinforcement to be modelled.
- vii. One support was modelled for all the RC deep beams models by applying restrain for all degree of freedom at the bottom support and restrain in x -direction at the mid-span of the beams.
- viii. Incremental pressure load was applied on the beams until the beams failed.
- ix. The behaviour of the all deep beams was obtained from the analysis. Load-deflection behaviour, crack pattern, stress and strain contours were obtained.
- x. The steps were repeated for a few models to identify the most effective method of strengthening for RC deep beams with openings.
- xi. The results from ANSYS CivilFEM 12.0 were compared to the result from experimental work to validate both of the result.

3.7 METHODOLOGY CHART

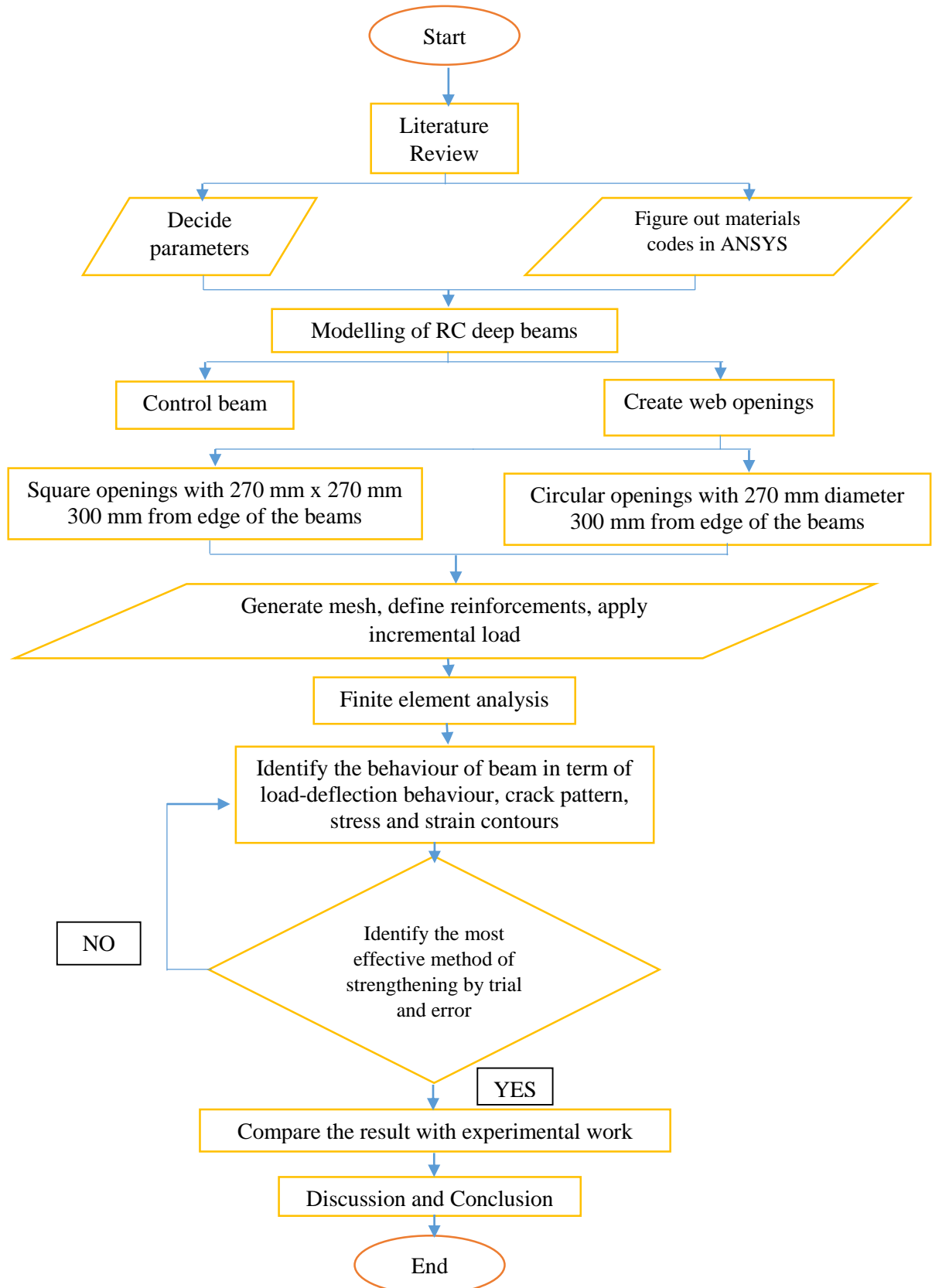


Figure 3.42: Methodology chart of work flow

CHAPTER 4

RESULTS AND DISCUSSION

4.1 INTRODUCTION

Results from FEA were discussed in the later section. Results were extracted from FEA which included load-deflection behaviour, crack pattern, stress and strain contours as well as vector plot cracking. In the later section, the validation of FE results of beam models CB, DBS, DBSS7, DBC, DBCS1 and DBCS3 with the experimental results were discussed. Bonding of interface between concrete and CFRP was assumed to be perfect bonding. Different shapes and strengthening method provided different behaviours and results.

4.2 LOAD-DEFLECTION BEHAVIOUR

In engineering, deflection refers to the structural elements displaced under a load. The displacement may refer to an angle or a distance in horizontal or vertical direction. The deflection distance of a member under a load is directly related to the slope of the deflected shape of the member under that load and can be calculated by integrating the function that mathematically describes the slope of the member under that load. The deflection of beam elements is usually calculated on the basis of the Euler–Bernoulli beam equation. The following sections discussed the load-deflection behaviour for all the modelled RC deep beams.

4.2.1 Control Beam

Control beam acted as the reference for all the other modelled beams to determine the behaviour of the deep beams e.g. the reduction of load capacity of beams and the recovery of load capacity after strengthening by CFRP.

Control beam had the highest load capacity among all the fourteen beams. Load capacity of the control beam from numerical analysis was 425.04 kN at 2.62 mm deflected from its original position as shown in Figure 4.1. Control beam showed a very stiff behaviour as it had a small displacement under a heavy load. CB showed elastic behaviour at the beginning of the time until 50 kN. The arrangement of steel stirrups in regular spacing and adequate numbers of steel reinforcements made the control beam had a very stiff behaviour. The load path of the control beam did not experience any disturbance thus the load was transferred well to the support and all the other parts of the control beam. Uniform distribution of the load successfully made the control beam had a very high load capacity. Control beam always show the highest load capacity among all the beams modelled and analysed in this study.

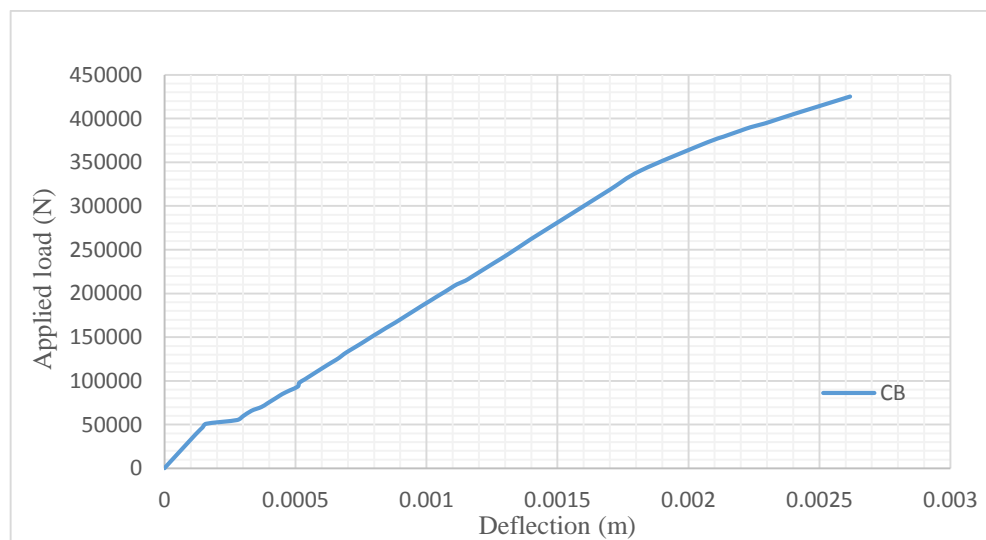


Figure 4.1: Load-deflection curve of control beam (CB)

4.2.2 RC Deep Beams with Openings

RC deep beams with openings included deep beams with square and circular openings, DBS and DBC respectively. DBS and DBC were used to determine the percentage of reduction of load capacities compared to the control beam.

Deep beams with openings showed a significant reduction in the load capacity as shown in Figure 4.2. The load-deflection curve also showed that the deep beams with openings were more brittle than the control beam. DBS and DBC experienced more displacements when the modelled beams withstood the same amount of load. However, DBC showed a better result in load capacity and displacement as compared to DBS. This was due to the effect of the shapes of the openings. Square openings which had four sharp edges and the edges greatly affected the load capacity of the modelled deep beams. The load path of the deep beams were disturbed by the openings.

DBC had a maximum load capacity of 207 kN at 1.71 mm while DBS experienced a maximum load capacity of 162 kN at 2.26 mm. The difference between the load capacity of DBC and DBS were almost 25%. This showed that square opening weakened the deep beams much critically than circular opening as the stress was concentrated at the sharp edge while smooth circular opening distributed the stress better around its circumference. As compared to control beam, the reduction of load capacities for square and circular openings were 61.9% and 51.3% respectively.

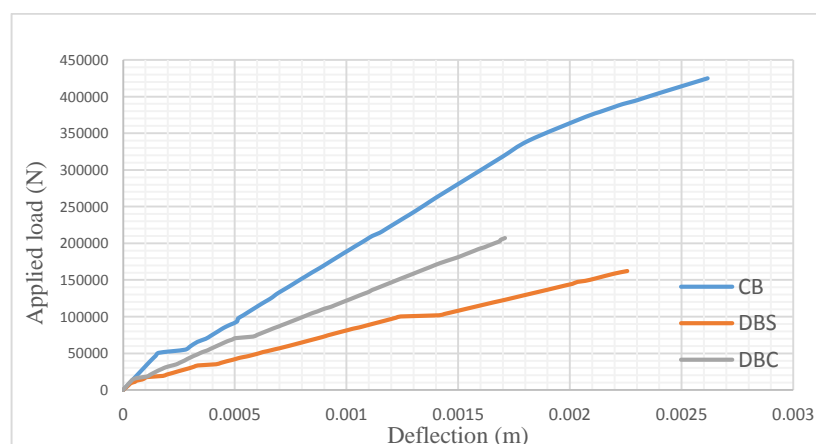


Figure 4.2: Load-deflection curves for CB, DBS and DBC

4.2.3 RC Deep Beams with Openings Strengthened by CFRP

The most effective method to strengthen the modelled RC deep beams had been identified through trial and error method. Two strengthening method had been done to determine the most effective method which were surface strengthening and U-wrap strengthening. Strengthening of the RC deep beams helped in recovery of load capacity of the deep beams with openings. The behaviours of the deep beams were discussed at the following sections.

4.2.3.1 Surface Strengthening for Deep Beams with Square Openings

Surface strengthening which was surface bonded between the concrete surface and the CFRP laminates. The CFRP was bonded to the concrete by epoxy and in FEA, the bonding was assumed to be perfect-bonding. There were four RC deep beams were modelled to simulate the behaviours of strengthened deep beams with square openings by surface strengthening. Results from DBSS1, DBSS2, DBSS3 and DBSS4 are shown in Figure 4.3.

Deep beams with square openings showed a lower recovery although the strengthening method was done by the same way as to strengthen the deep beams with circular openings. The CFRP that was pasted in vertical alignment (90°) showed a better recovery than those pasted in horizontal alignment (0°). DBSS1 and DBSS3 which were pasted in vertical alignment showed a recovery of 37.7% from 162 kN to 223 kN and 31.1% from 162 kN to 212.4 kN respectively. For the CFRP in horizontal alignment, it showed a recovery of 36.2% and 29.6% for DBSS2 and DBSS4 respectively. The load capacities after strengthening were 221 kN for DBSS2 and 210 kN for DBSS4. DBSS1 and DBSS2 showed a better result when compared to DBSS3 and DBSS4 because the performance of CFRP. The cut strips in DBSS3 defeated the performance of the CFRP as there were more cut between the CFRP itself and between the concrete. CFRP could not show its ultimate performance as the CFRP was cut and then joined together by epoxy which was weakened during the process.

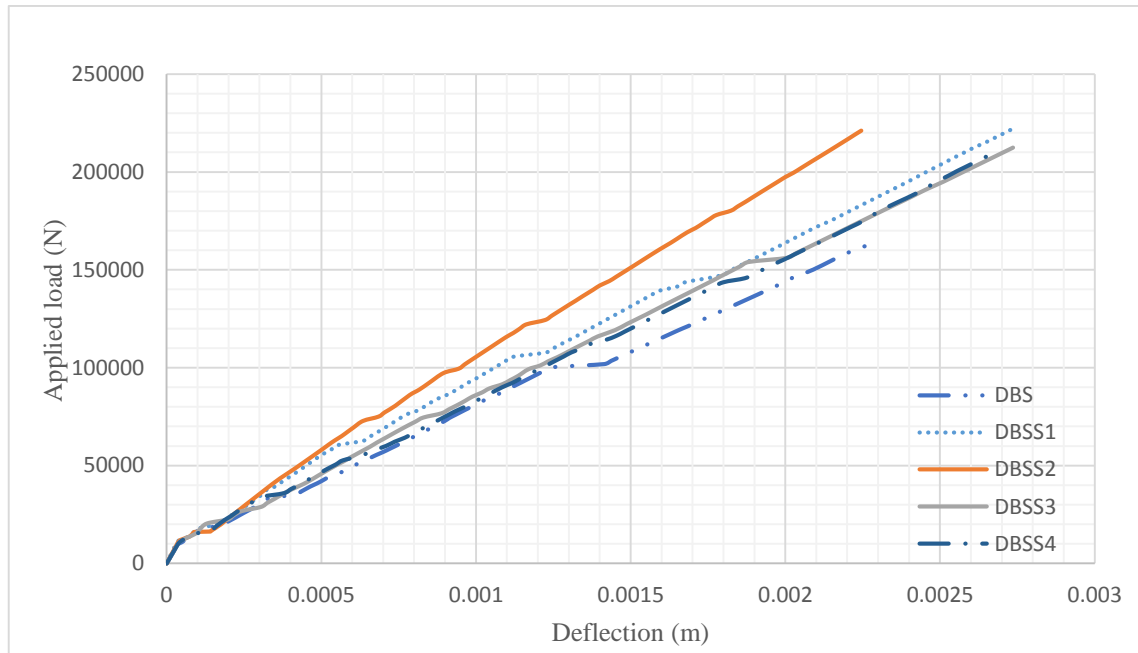


Figure 4.3: Load-deflection curve of deep beams with square openings

4.2.3.2 Surface Strengthening for Deep Beams with Circular Openings

Deep beams with circular openings were also strengthened by CFRP to recover the load capacity of the beams. DBCS1 showed a better recovery of load capacity than DBCS2 due to the direction of alignment of CFRP. DBCS1 recovered the deep beams with openings about 15.6% while strengthening in DBCS2 successfully regain around 14.5% of load capacity. Load-deflection curve in Figure 4.4 demonstrates the difference between DBCS1 and DBCS2 which represented alignment of vertical and horizontal respectively. The vertical alignment gave a better result due to the openings were created at the critical shear zone. The failure of the beams were due to shear failure, thus the CFRP in vertical alignment could greatly increase the resistance for the beams to be failed in shear. Horizontal alignment usually used to recover the beams due to flexural failure. The CFRP resisted the beams to have great deflection or displacement by holding the concrete firmly to increase the load capacity of the beams. Since vertical alignment could resist the displacement in y-direction in the shear zone better than horizontal alignment, thus vertical alignment gave a better recovery of load capacity.

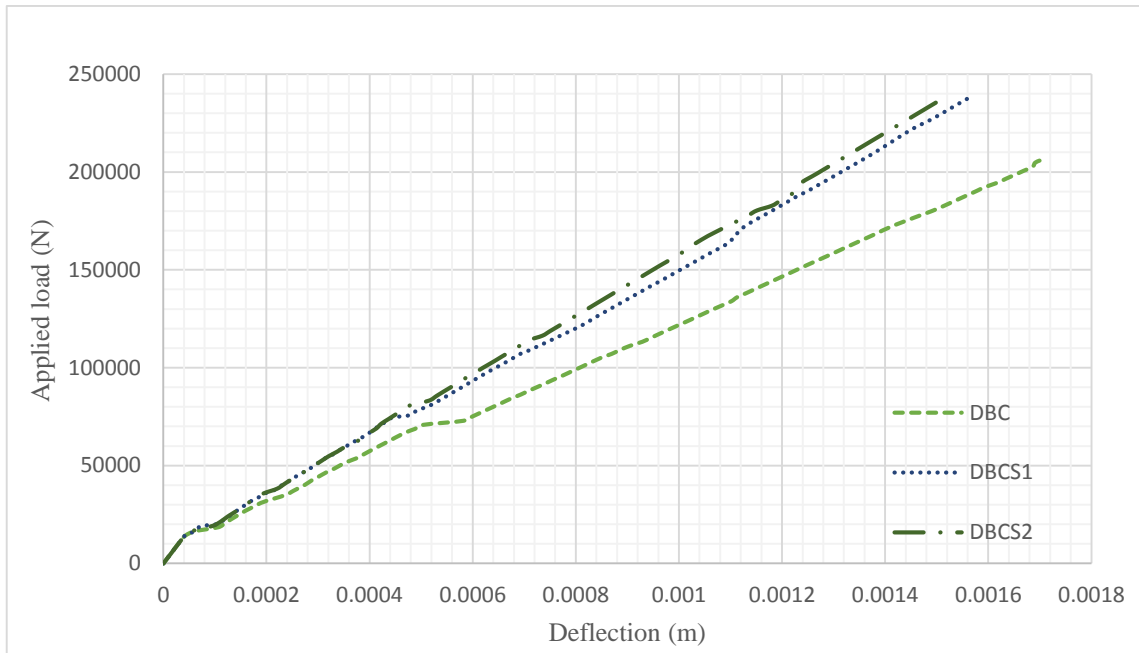


Figure 4.4: Differences in the recoveries of load capacities of DBCS1 and DBCS2

Although the beams were analysed to regain the load capacities as much as possible yet the deep beams with openings could not restore to the original load capacity as behaved by control beam. Once the load path was disturbed, the load capacity decreased significantly even though circular openings did not have sharp edge that was extremely weak against shear failure and cracking.

By comparing the strengthened beams to the control beam, the strengthened deep beams with openings were only acquired half around half of the load capacity of the control beam except DBCS1 which were 52.5%, 52%, 50.0%, 49.4%, 63.4% and 55.8% for DBSS1, DBSS2, DBSS3, DBSS4, DBCS1 AND DBCS2 respectively. The load-deflection curve in the figure below shows that the stiffness of the deep beams with openings dropped significantly.

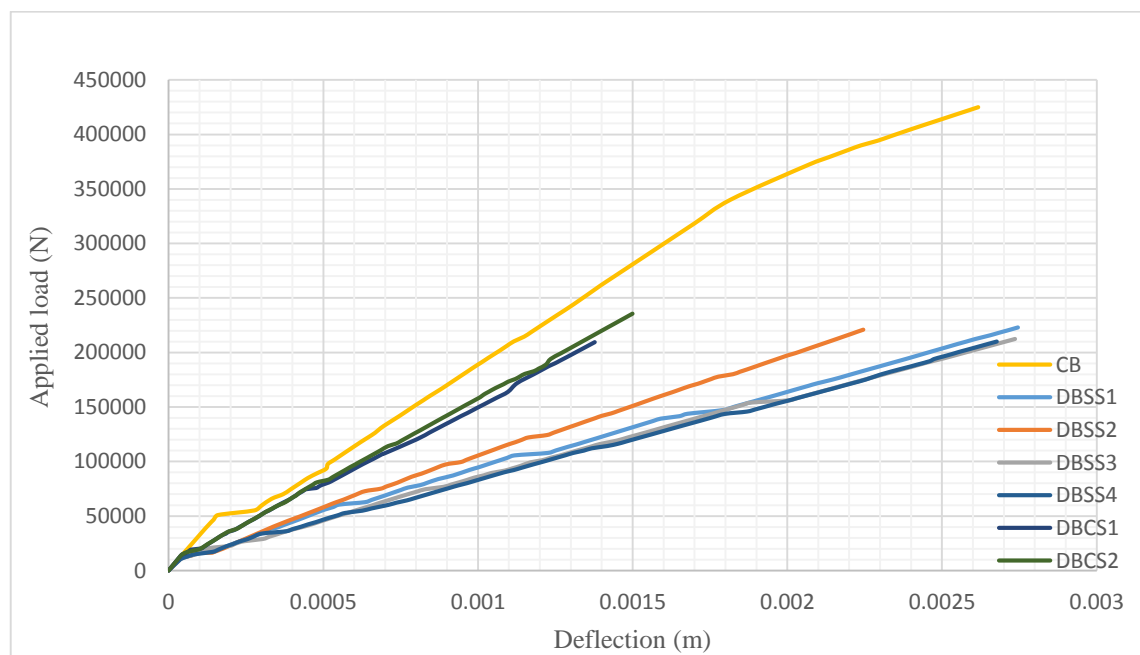


Figure 4.5: Comparison of control beam and all the beams strengthened by surface strengthening method in square and circular openings

4.2.3.3 U-wrap Strengthening (Square & Circular Openings)

Another method being analysed in this study was U-wrap strengthening method. The CFRP was pasted along three sides which included the bottom to ensure the deep beams with openings were fully strengthened. DBSS5, DBSS6 and DBSS7 were modelled in U-wrap strengthening method to simulate the recovery of load capacities. Figure 4.6 shows the load-deflection curves of DBSS5, DBSS6, DBCS3 and DBCS4.

Yet the square openings showed a lower load capacity after strengthening by CFRP when compared to the circular openings. Deep beams with square openings showed recovery of 63.0% and 61.7% for DBSS5 and DBSS6 respectively while 85.0% and 83.6% of recoveries were obtained for DBCS3 and DBCS4.

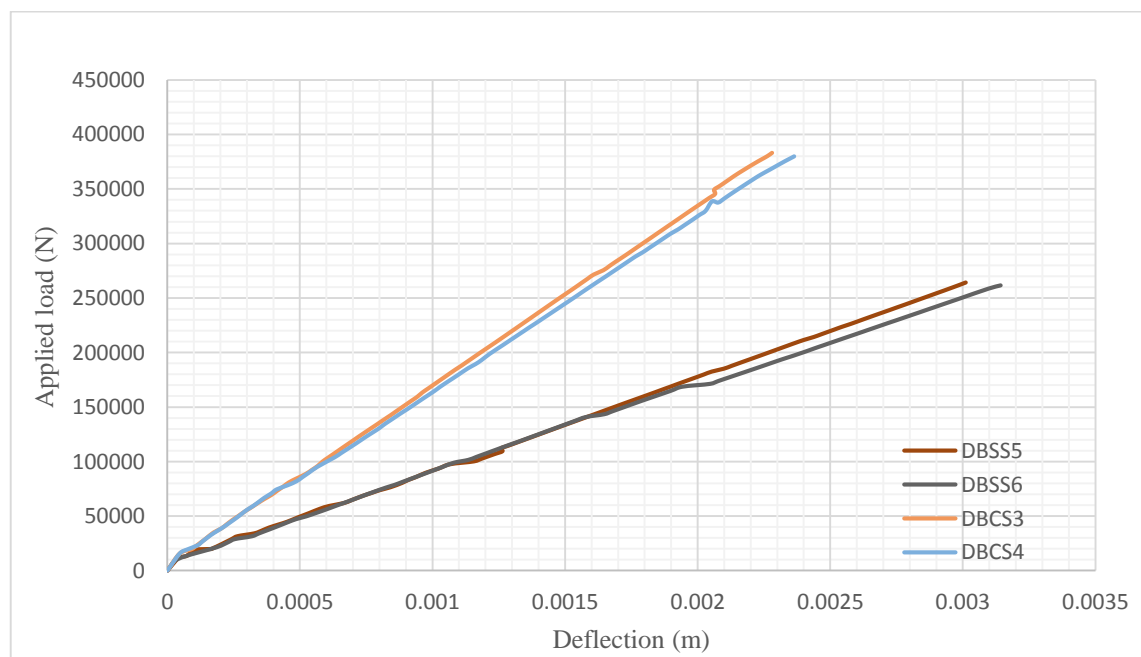


Figure 4.6: Load-deflection curves of DBSS5, DBSS6, DBCS3 and DBCS4

4.3 CRACK PATTERN

Cracking was also being analysed to study the behaviour of the deep beams with openings. The cracking of deep beams were obtained after the analysis of the deep beams were done. The cracking patterns were captured and discussed in this section. Cracking is influenced by the material property and does not depend on the size of the structures. Fracture energy is defined as the energy required to open unit area of crack surface. Fracture energy is a function of displacement and not strain. Fracture energy deserves prime role in determining ultimate stress at crack tip.

Crack patterns of all the beams analysed in this study. The crack patterns were almost the same for all the beams and the beams were failed due to shear failure. First crack was determined and the crushing of the beams also were captured and compared among all the beams. The meaning of symbols of crack patterns used in ANSYS were included shear crack, flexural crack, compressive crack and secondary crack. All the cracks were possible to happen on a beam. The figure in Appendix A shows all the types crack failure as referred to explain the crack patterns in this study of ANSYS CivilFEM 12.0.

The symbols used for cracking pattern were easily to be differentiated as the small line indicated the directions of the cracks occurred along the line, small circles illustrated where the concrete had cracked and small octagon showed where the concrete had crushed as shown in Figure 4.7. Principal tensile stresses occurred mostly in the longitudinally which shown by the small red line. When the principal stresses exceeded the ultimate tensile strength of the concrete, circle as cracking signs appeared perpendicular to the principal stresses.

Figure 4.8a and b also show the regions that cracking occurred due to the different failure mode. There are basically four failure modes which were shear crack, flexural crack, compressive crack and secondary crack.

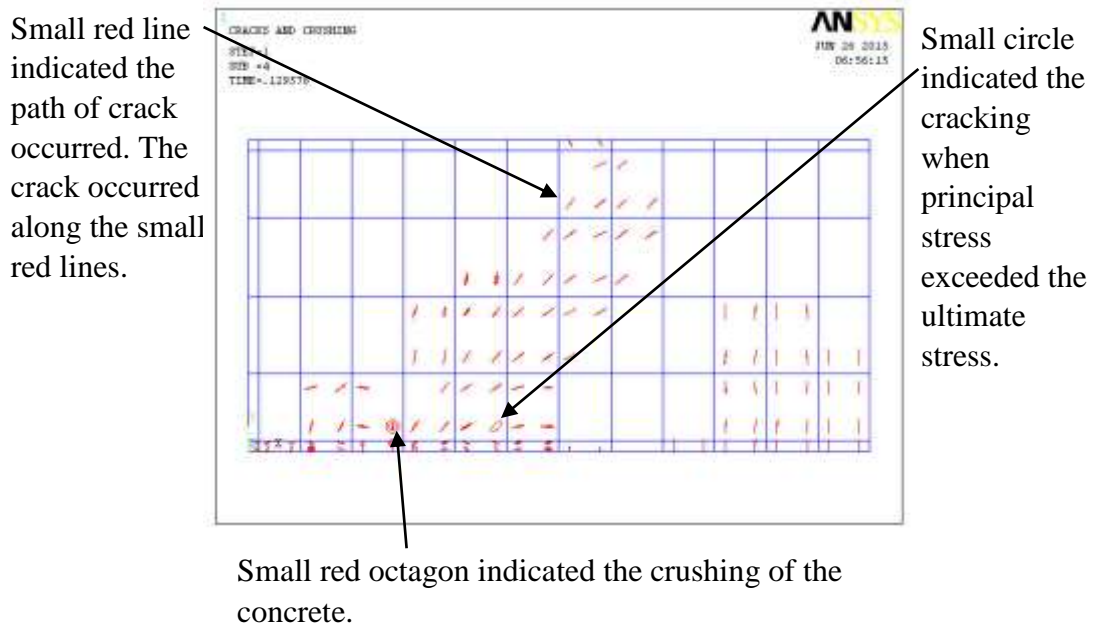


Figure 4.7: Symbols of crack pattern

4.3.1 Control Beam

Figures 4.8a and b show the crack pattern of the control beam at the initial step. At sub-load step 4 the crack pattern was already obviously observed. The crack was started at two locations where the supports of the beams and moved diagonally to the location where load was applied and at the mid span of the modelled beams. The crack at the support was seem to be more critical compared to other location. Shear cracking as usual occurred from the support of the beam and then diagonally to the location of applied load. At the same time, flexural cracking at the mid span started due to the excessive deflection at the mid span. The top side of the beam experienced the compressive cracks as the load increased from time to time. Secondary cracks occurred at the region where the concentration of stress was very high and finally led to crushing of the concrete beam.

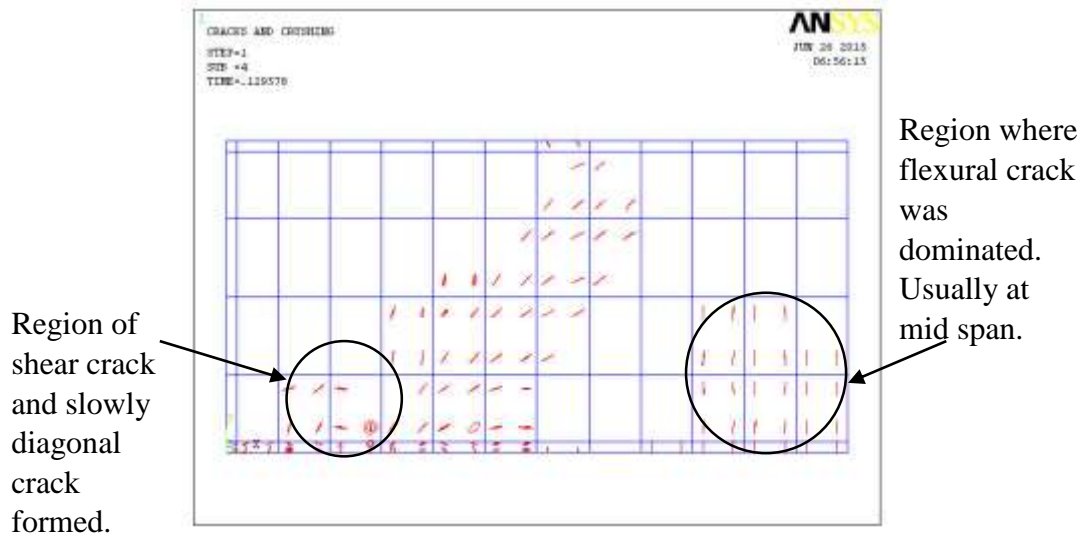


Figure 4.8a: Crack pattern of control beam

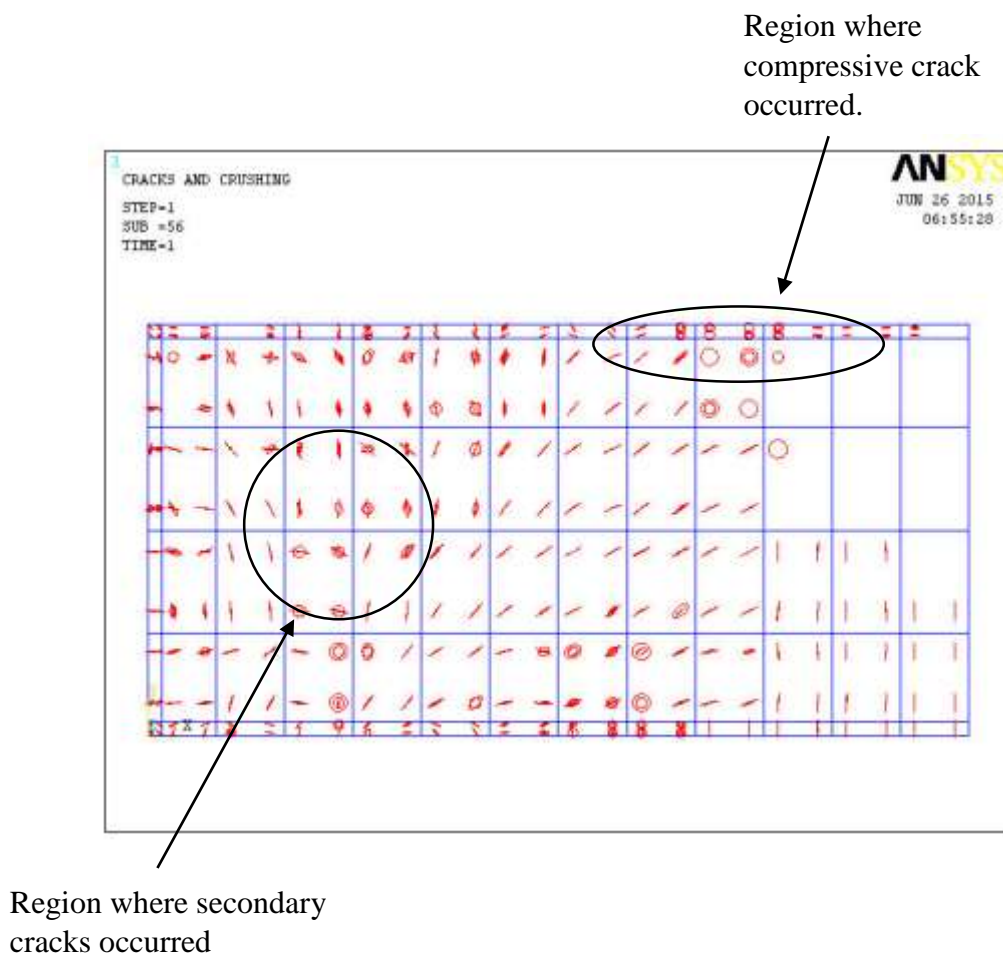


Figure 4.8b: Crack pattern of control beam at the last load step

4.3.2 RC Deep Beams with Square and Circular Openings

Crack patterns were also analysed for all the modelled deep beams with openings. Figure 4.9 shows the crack pattern of DBS while Figure 4.10 illustrates the crack pattern of DBC.

From Figure 4.9a, obviously the crack started at the edge of the square opening because the stress concentrated at the edge of the openings. The crack pattern started at the edges that near to the location of load and support. This was due to the edges were nearer to the actions thus the edges experienced larger force than other edges. Sharp edge always have the highest stress thus cracks were easily formed. Then the crack was slowly experienced by the other two edges and moved towards the edge of the beam. The beam also failure due to shear failure as the last load step also indicated that the beam experienced large amount of shear cracking around the opening and form a diagonal cracking pattern towards the support and location of the applied load.

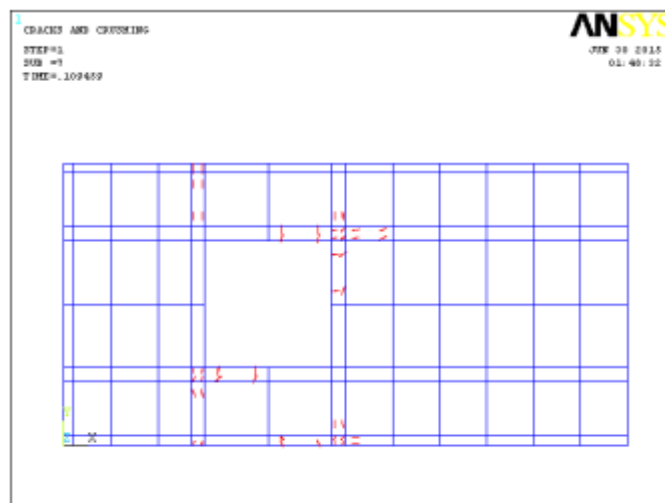


Figure 4.9a: Crack pattern of DBS at the initial step

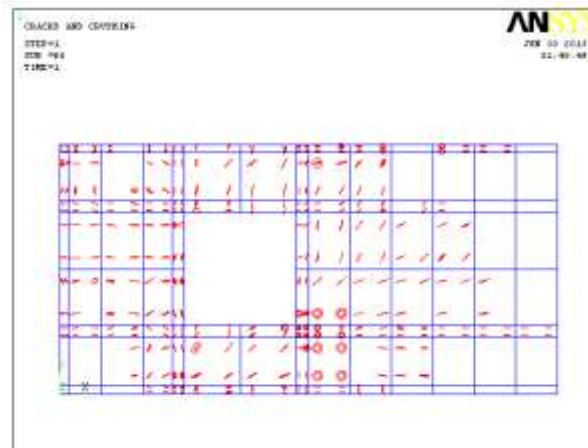


Figure 4.9b: Crack pattern of DBS at the last load step

Figure 4.10a illustrated that the crack pattern also formed in diagonal path. Although the circular opening did not have sharp edge, the beam was weakened due to the large opening and crack could easily formed by passing through the large opening. DBC showed that the cracking at support was quite critical as it also experienced compressive cracking at the support. Besides that, secondary cracking also could be observed at the bottom part of the opening. When the DBC crushed, it was mainly due to shear cracking and compressive cracking.

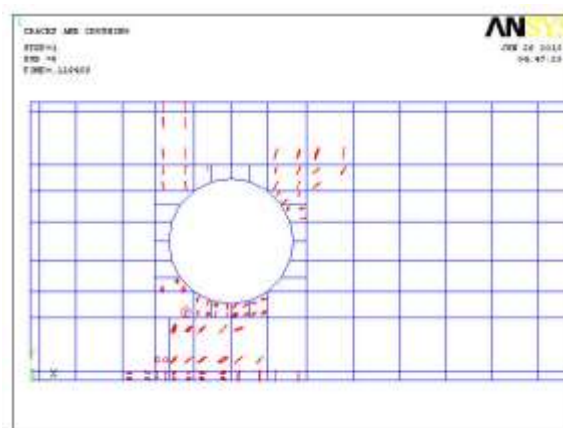


Figure 4.10a: Crack pattern of DBC at the first load step

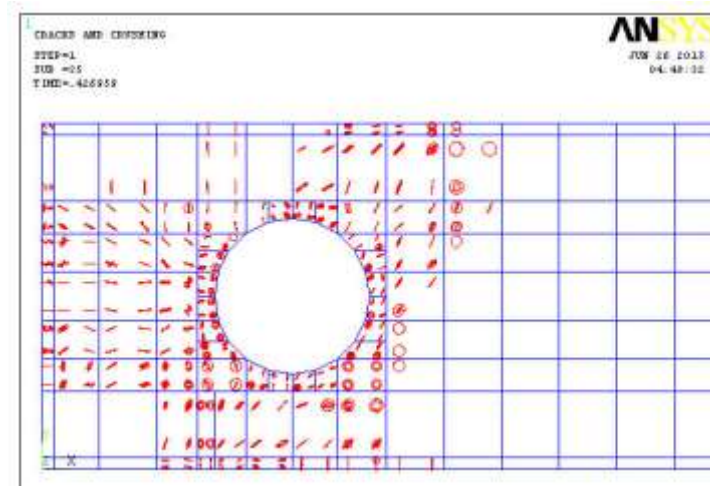


Figure 4.10b: Crack pattern of DBC at the last load step

4.3.3 RC Deep Beams with Openings Strengthened by CFRP

All the deep beams with openings strengthened by CFRP were also analysed for the crack pattern. The crack pattern of each of the beams were shown in the respective subsections.

4.3.3.1 Surface Strengthening – Deep Beams with Square Openings (Initial Step)

Figures 4.11b to e show the crack patterns of the deep beams with square openings strengthened by CFRP at the initial step. Figure 4.11a shows the crack pattern of deep beams with square openings for comparison purpose. Similarly, all the first crack happened at the edges near to the support and locations of applied loads although the beams were strengthened by CFRP. The crack pattern formed a diagonal crack pattern for all the beams. The performance of CFRP affected a lot by the method of applying CFRP on the surface of the deep beams with square openings.

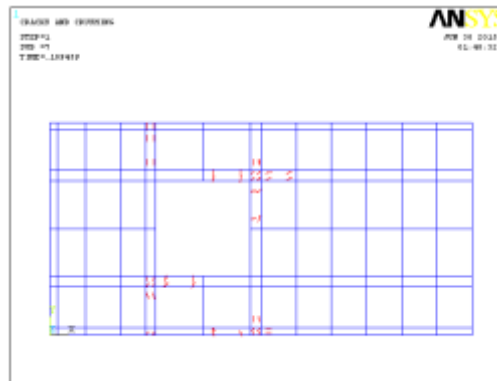


Figure 4.11a: Crack pattern of DBS at the initial step

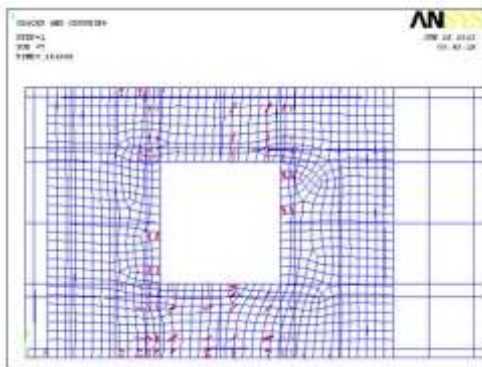


Figure 4.11b: Crack pattern of DBSS1 at the initial step

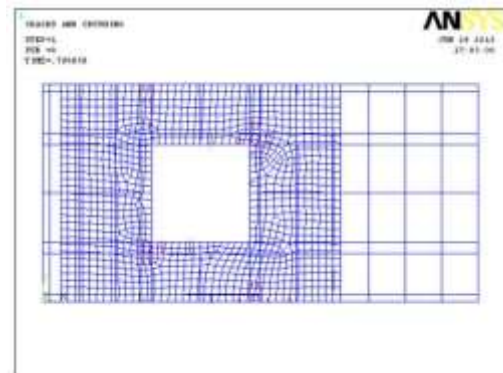


Figure 4.11c: Crack pattern of DBSS2 at the initial step

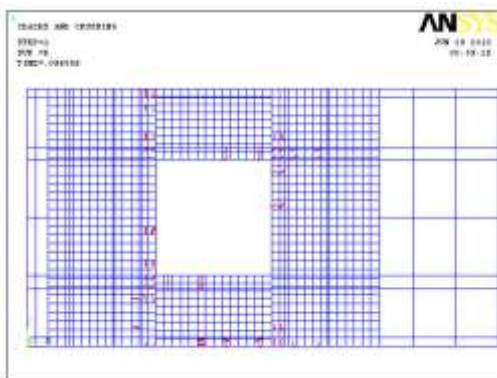


Figure 4.11d: Crack pattern of DBSS3 at initial step

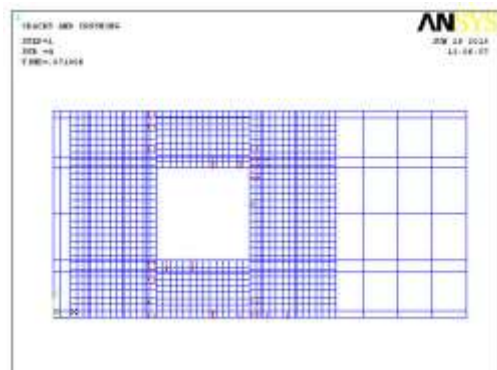


Figure 4.11e: Crack pattern of DBSS4 at initial step

4.3.3.2 Surface Strengthening – Deep Beams with Square Openings (Final Step)

Figure 4.12a to 4.12d show the crushing of the deep beams with square openings at the last load step of the beams. Although the beams were failed due to the shear cracking, the cracks were obviously much lesser than that in DBS. The crack also being dispersed out from the surrounding square openings by CFRP. The cracking was less critical at the area of recovered by CFRP as compared to the DBS which experienced the mess of cracking all around the opening.

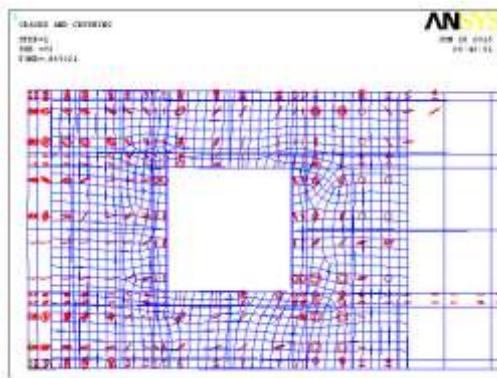


Figure 4.12a: Crack pattern of DBSS1 at the final step

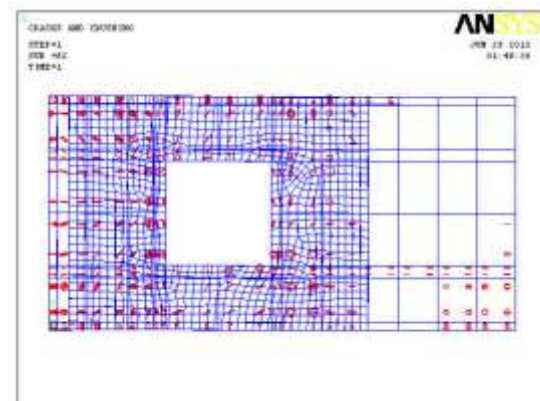


Figure 4.12b: Crack pattern of DBSS2 at the final step

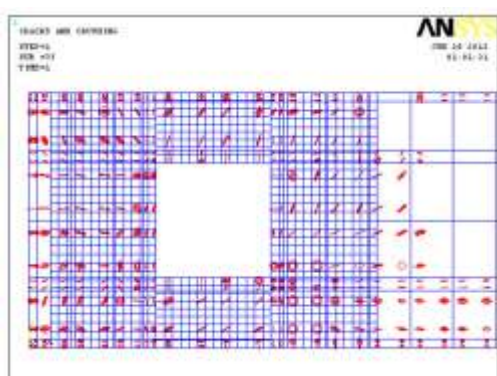


Figure 4.12c: Crack pattern of DBSS3 at the final step

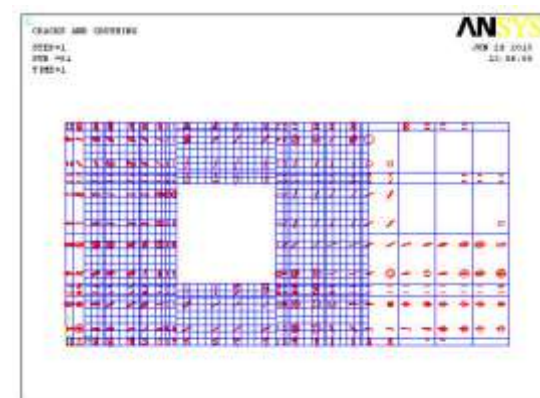


Figure 4.12d: Crack pattern of DBSS4 at the final step

4.3.3.3 Surface Strengthening – Deep Beams with Circular Openings

Similarly, Figure 4.13 shows the initial crack while Figure 4.14 shows the crushing of the deep beams with CFRP surface strengthening in vertical alignment (DBCS2) and deep beams with CFRP surface strengthening in horizontal alignment (DBCS3) at the last load step of the beams. The initial crack was still happened at the around the circular opening but the final load steps showed a different result when compared to the DBC. The cracks were dispersed away from the circular opening and from Figure 4.14b, the crack pattern was observed that concentrated at the area that did not strengthened by CFRP which was near to the side of the beam. The crack pattern around the circular opening was much lesser as compared to DBC.

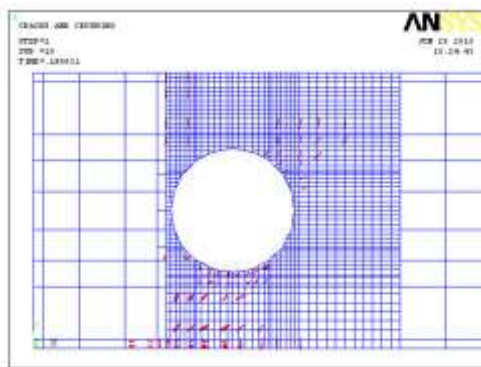


Figure 4.13a: Crack pattern of DBCS1 at the initial step

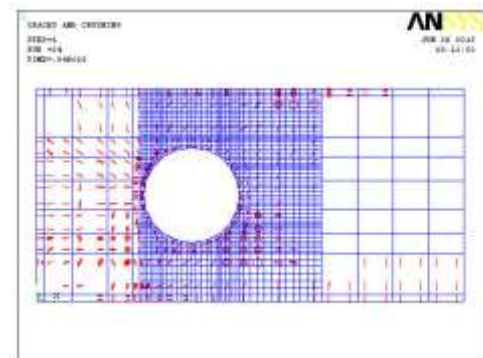


Figure 4.13b: Crack pattern of DBCS1 at the final step

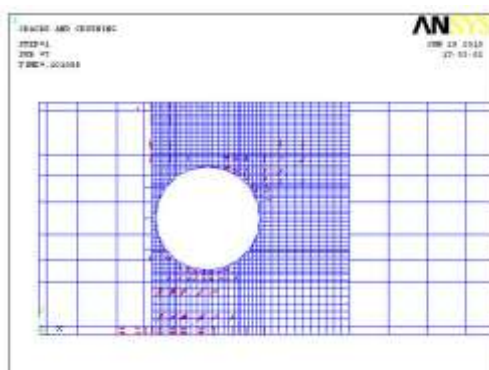


Figure 4.14a: Crack pattern of DBCS2 at the initial step

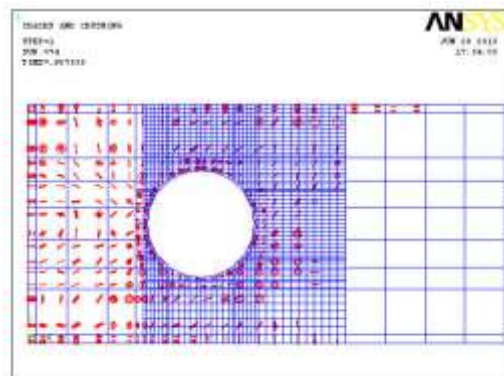


Figure 4.14b: Crack pattern of DBCS2 at the final step

4.3.3.4 U-wrap Strengthening

By referring to Figure 4.15a and c, the crack patterns started at circumference of the square opening strengthened by CFRP. This showed that the U-wrap method was really improved the behaviour of the deep beams with openings that it could withstand more load without forming any cracking pattern at the initial step. U-wrap method even showed more clearly that the crack pattern was dispersed from the square openings and to the area that did not strengthened by CFRP. The observation was shown in Figure 4.15b and c.

Figures 4.16a and b show the deep beams with circular openings strengthened by U-wrap method showed the similar behaviour. The crack initiated at the edges of the square opening and the crack was also dispersed away from the opening as the opening was protected by the CFRP as similar to those occurred in square openings. For the direction of alignment of CFRP in different orientation, it did not show significant difference between the crack patterns.

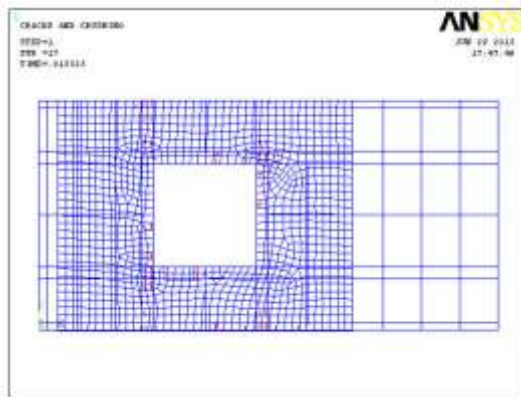


Figure 4.15a: Crack pattern of DBSS5 at the initial step

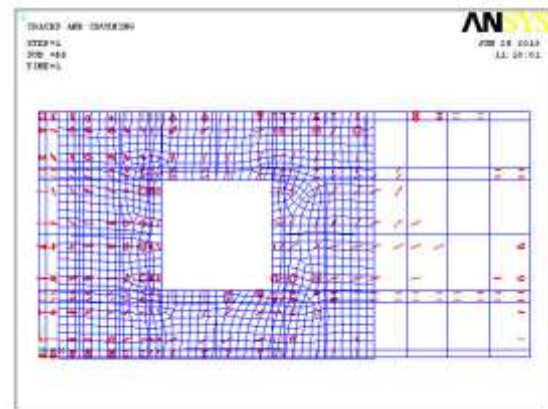


Figure 4.15b: Crack pattern of DBSS5 at the final step

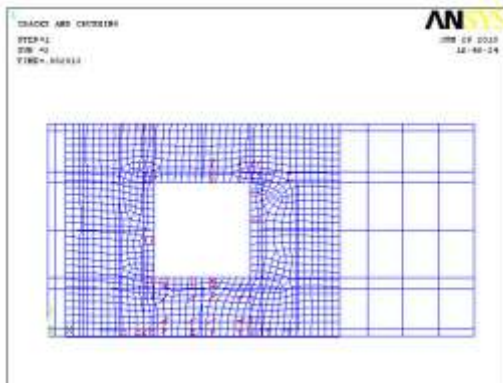


Figure 4.15c: Crack pattern of DBSS6 at the initial step

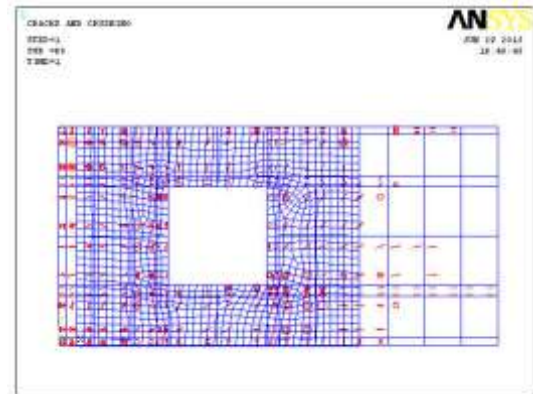


Figure 4.15d: Crack pattern of DBSS6 at the final step

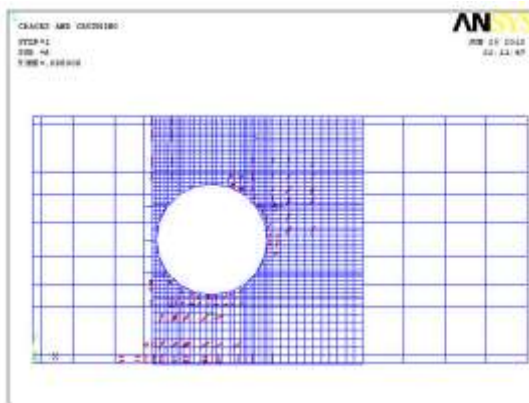


Figure 4.16a: Crack pattern of DBCS4 at the initial step

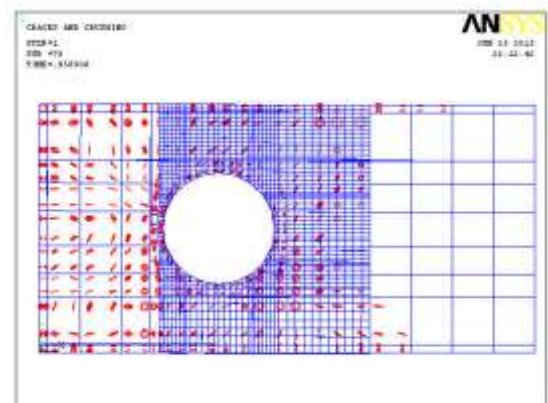


Figure 4.16b: Crack pattern of DBCS4 at the final step

4.4 STRAIN CONTOUR

Strain contour indicated the values of the crack happened at the deep beams. As mentioned in the previous section, crack was due to material property and not because of the size, thus strain is the rate of change in strain or deformation of a material with respect to time. Thus it could be used to show the value of crack. Strain compromises both the rate at which the material is expanding and shrinking and also the rate at which it is being deformed by progressive shearing without changing its volume or commonly known as shear rate.

4.4.1 Control Beam

Figure 4.17 shows the strain contour of control beam at initial step and critical step. It also related to the crack of the control beam. It had the same deformation path as the cracking. As shown in the figure, the most critical part was at the support and had the maximum value of strain. The deformation at the support was critical. The maximum value of the strain value was 0.020767 and minimum value was 0.101E-5.

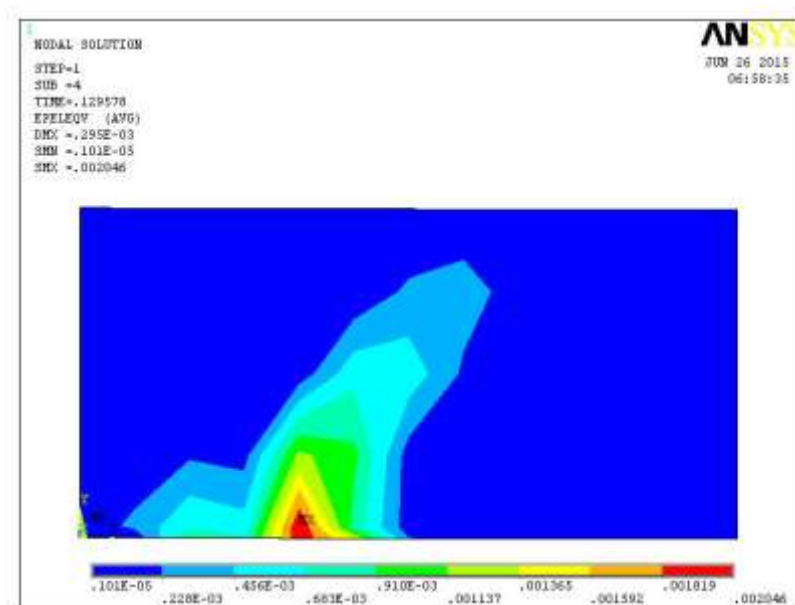


Figure 4.17a: Strain contour of control beam at initial load step

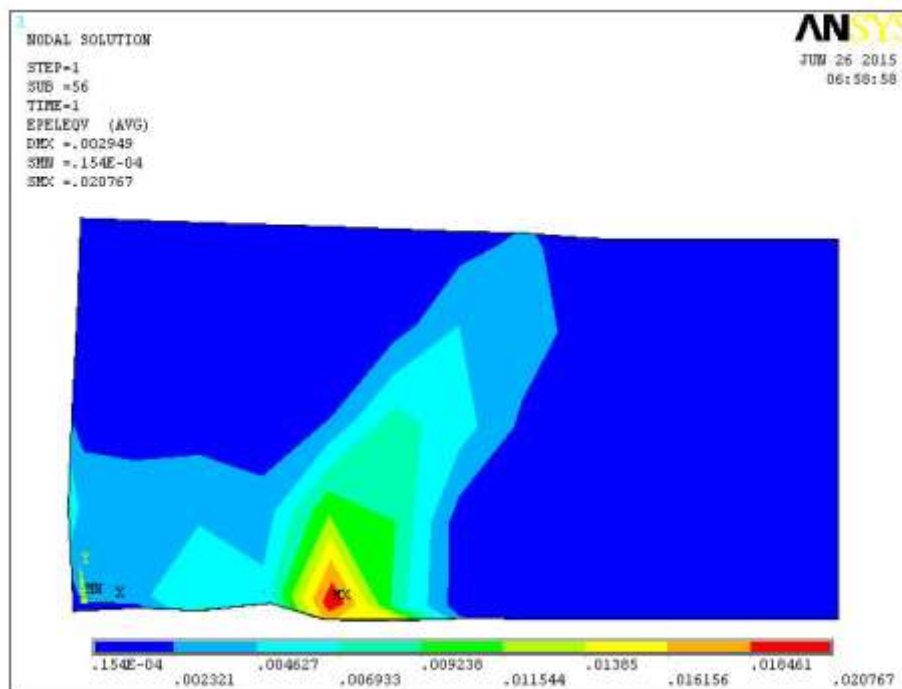


Figure 4.17b: Strain contour of control beam at ending load step

4.4.2 RC Deep Beams with Openings (DBS and DBC)

Figures 4.18a – d show the strain contour of deep beams with square openings (DBS) and circular opening (DBC) at initial step and critical step. As shown in the figures, the most critical part was at the support and had the maximum value of strain. The deformation at the support was critical. The maximum value for DBS was 0.003518 as shown in red colour contour and 0.022767 as represented in blue colour contour for DBC.

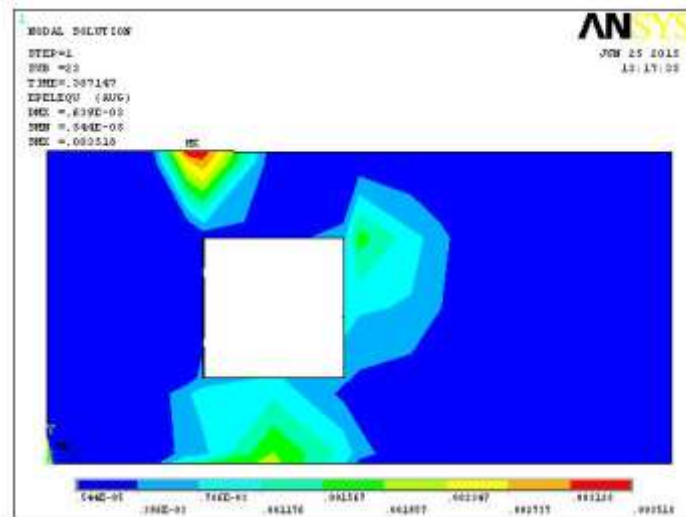


Figure 4.18a: Strain contour of DBS at initial load step

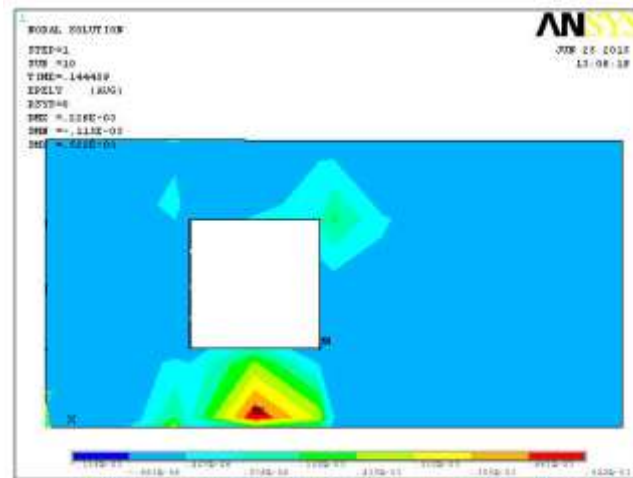


Figure 4.18b: Strain contour of DBS at critical load step

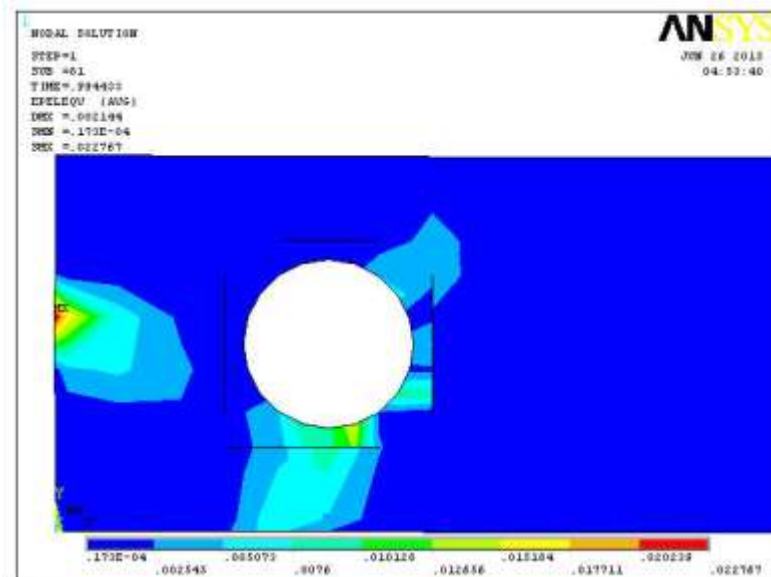


Figure 4.18c: Strain contour of DBC at initial load step

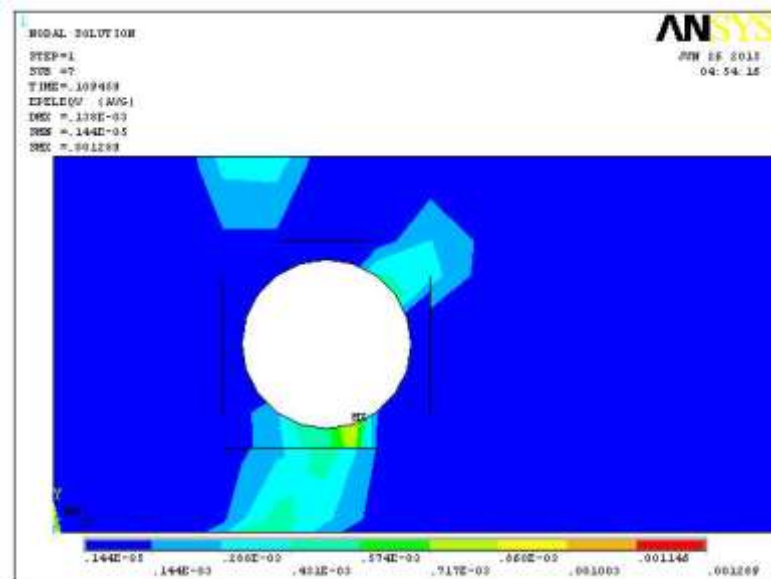


Figure 4.18d: Strain contour of DBC at critical load step

4.4.3 RC Deep Beams with Openings Strengthened by CFRP

i. Square Opening

Figures 4.19a to b show the strain contours for surface strengthening in vertical alignment (DBSS1) and U-wrap strengthening in vertical alignment (DBSS5). The strain also showed the critical or maximum value at the support of the beams.

Figures 4.19a shows that the strain was started around the edges of the opening and with maximum value of 0.001647. CFRP took all the strain thus the strain was congested at the support where CFRP was presented and then then overall of the beam experienced the uniform of strain value which was $0.364E-5$ as shown in Figure 4.19b. The side of the beam experienced high value of strain as well due to the CFRP was too close to the edge of the beam.

Figures 4.19c clearly shows that the edges experienced the largest strain with value of $0.738E-3$ and towards the direction of the support of the beam. CFRP performed well that absorbed all the strain and ensured the beam experienced the uniform strain.

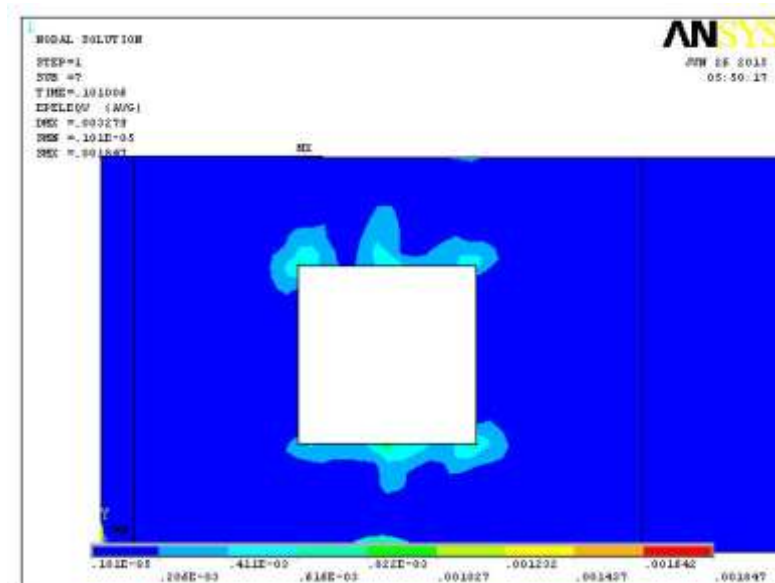


Figure 4.19a: Strain contour of DBSS1 at initial load step

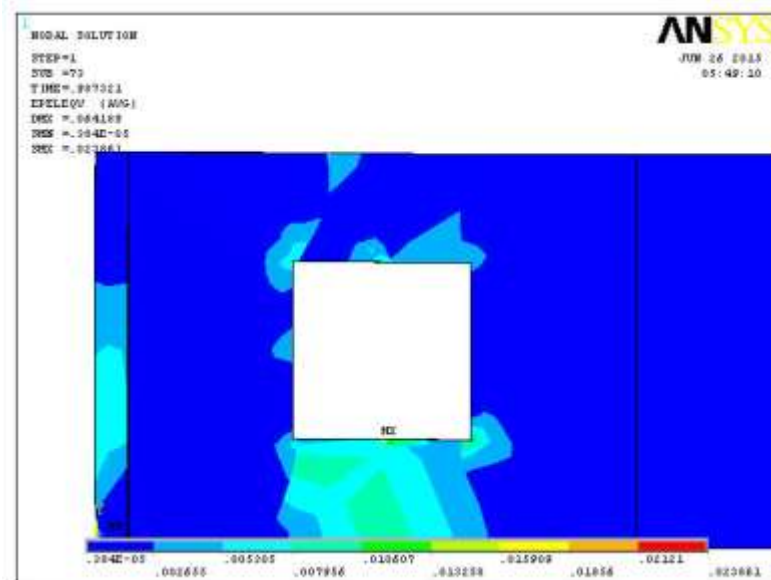


Figure 4.19b: Strain contour of DBSS1 at critical load step

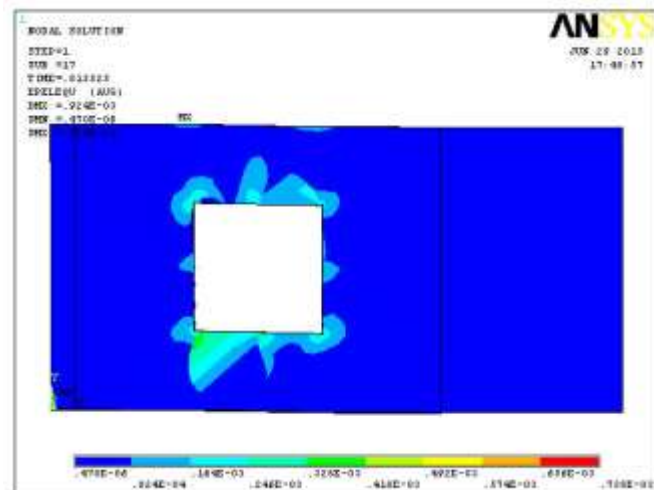


Figure 4.19c: Strain contour of DBSS5 at initial load step

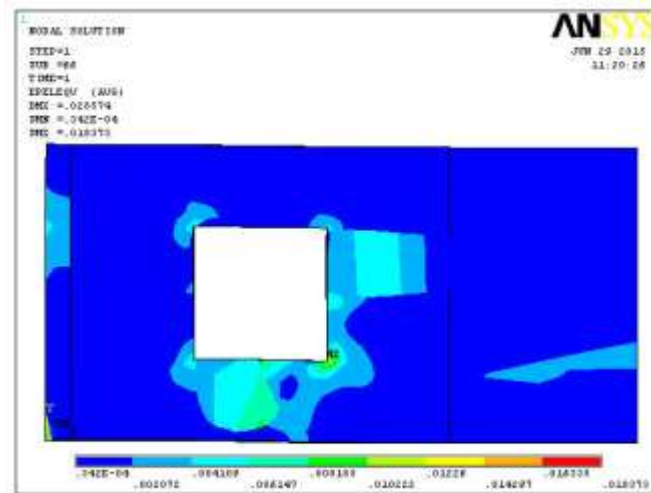


Figure 4.19d: Strain contour of DBSS5 at critical load step

ii. Circular Opening

Figures 4.19e and 4.19f show the strain contour in deep beams with circular openings strengthened at the surface in the orientation of 90° (DBCS1). The strain also started at the circumference of the circular opening and slowly moved to the support of the beam. The value increased from 0.00295 to 0.04342.

Beam strengthened by U-wrap method in vertical alignment (DBCS3) always show a better result as the CFRP covered the beam by three sides as shown in Figures 4.19g and h. At the critical state, the CFRP protected the beam well by having the most critical strain within the area covered by CFRP thus the beam experienced a balanced strain value. The maximum value of strain at the critical stage was 0.05676.

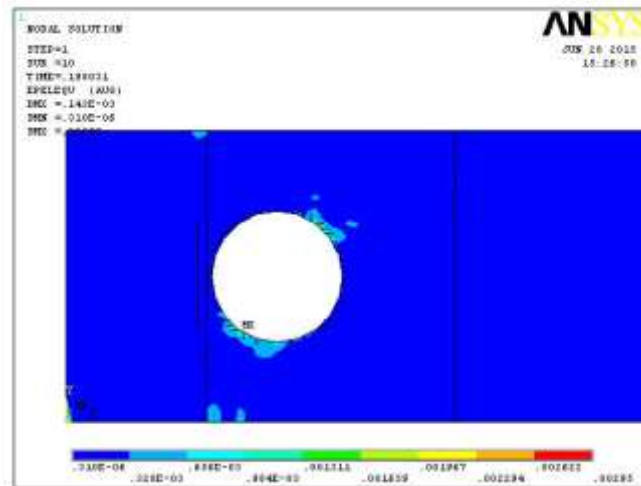


Figure 4.19e: Strain contour of DBCS1 at initial load step

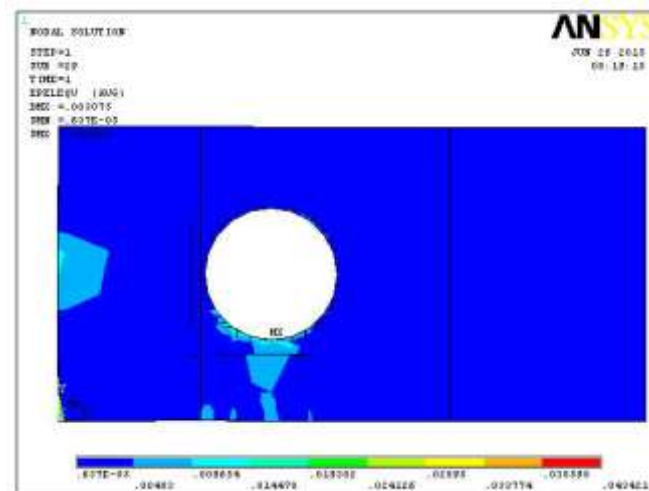


Figure 4.19f: Strain contour of DBCS1 at critical load step

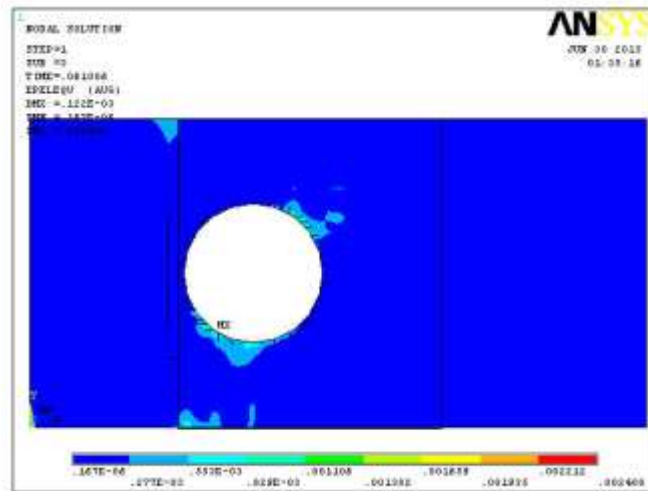


Figure 4.19g: Strain contour of DBCS3 at initial load step

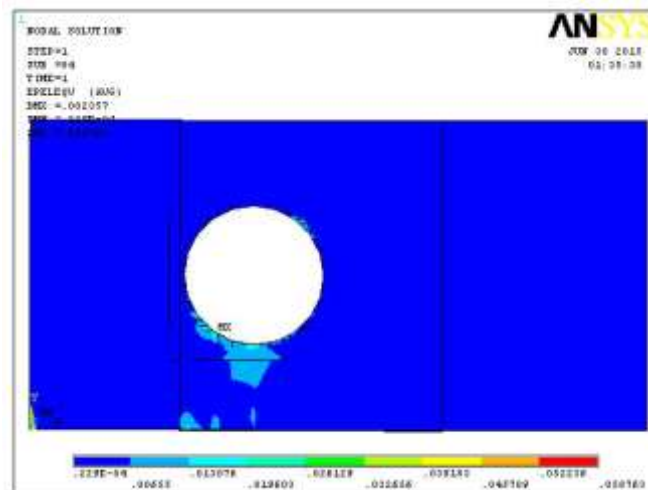


Figure 4.19h: Strain contour of DBCS3 at critical load step

4.5 STRESS CONTOUR

Stress contour suggested that the yielding of materials begin when the second deviatoric stress invariant reaches a critical value. Prior to yield, material responses is assumed to be elastic. A material is said to start yielding when its stress reaches a critical value known as the yield strength. The stress contour is used to predict the yielding of materials under any loading condition from results of simple uniaxial tensile tests.

4.5.1 Control Beam

Figures in 4.20 show the load path of control beam as presented in stress contour. The load path also showed in diagonal path which was the failure path of the control beam. The value of stress increased from $21.5E6$ Pa to $151E6$ Pa.

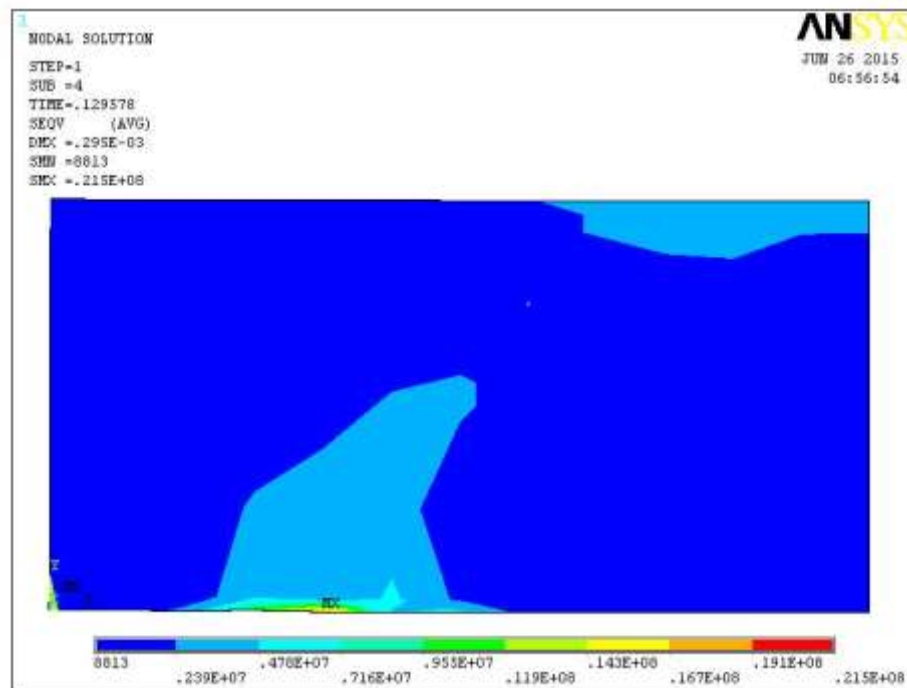


Figure 4.20a: Stress contour of CB at initial load step

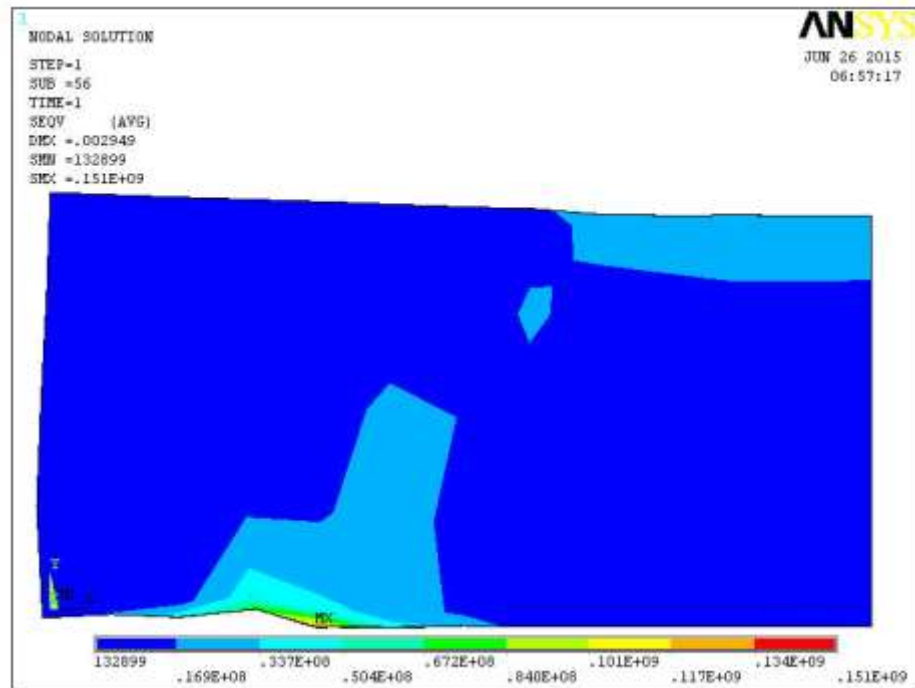


Figure 4.20b: Stress contour of CB at critical load step

4.5.2 RC Deep Beams with Openings

Figures in 4.21 illustrated the stress contour of DBS and DBC. Square opening showed a larger area that experienced higher value of stress as compared to circular opening where also the location of applied, support of the beam and the circumference of the beam experienced higher value of stress. This could be explained that the square opening had sharp edges that disturbed the load path significantly and the stress had to be experienced by the whole beam. The stress contour showed that the stress was from the support to the location of applied load through the diagonal edges of the square opening. The minimum value of stress in DBS was 3.77 kPa as illustrated in blue colour and the maximum value was up to 3.43E3 kPa while the maximum value of DBC was up to 6.67E3 kPa as shown in red colour contour.

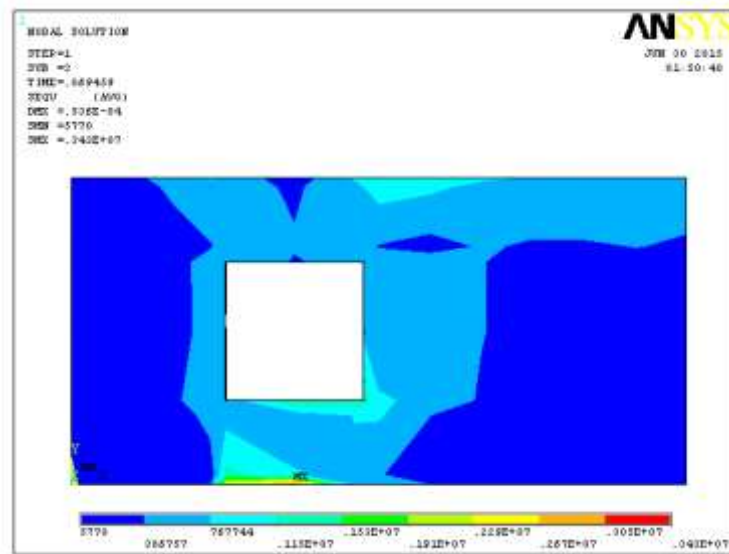


Figure 4.21a: Stress contour of DBS at initial load step

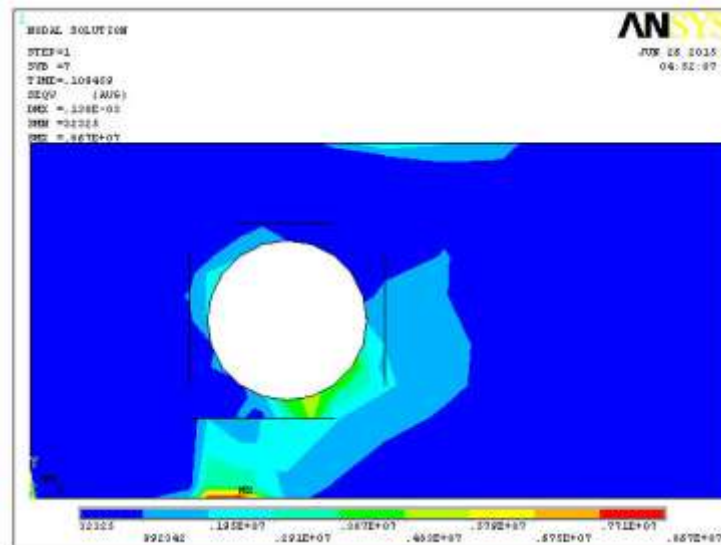


Figure 4.21b: Stress contour of DBC at initial load step

4.5.3 RC Deep Beams with Openings Strengthened By CFRP (Surface Strengthening)

Figures in 4.22 show the ultimate stress contour at critical state of strengthened RC deep beams with openings. After strengthening by CFRP, the beam experienced a uniform of stress although it was in critical state. Figure 4.22a shows the stress around the opening strengthened by surface method in vertical alignment DBSS1 and 4.22b shows the stress around the opening strengthened by U-wrap method in vertical alignment (DBSS5). The area of experienced critical stress was slightly lesser in U-wrap method. The value for DBSS1 was 646E3 kPa and DBSS5 was 551E3 kPa.

Figures 4.22c and 4.22d show the stress contour of circular opening strengthened by CFRP. The value of stress of DBCS1 was 1.05E6 kPa while DBCS3 was 2.06E6 kPa. Both showed the similarity that the higher stress values only showed at the support of the beam and around the circumference near to the support. Location of the applied load just experienced same value of stress as other part of the beams.

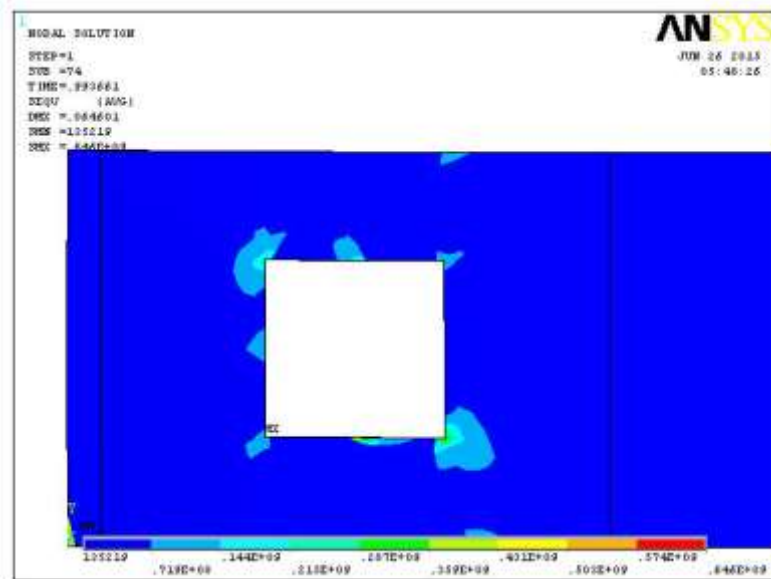


Figure 4.22a: Stress contour of DBSS1 at critical load step

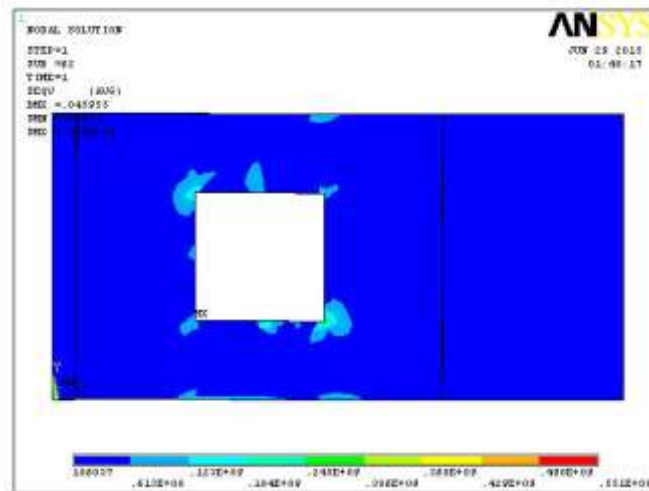


Figure 4.22b: Stress contour of DBSS5 at critical load step

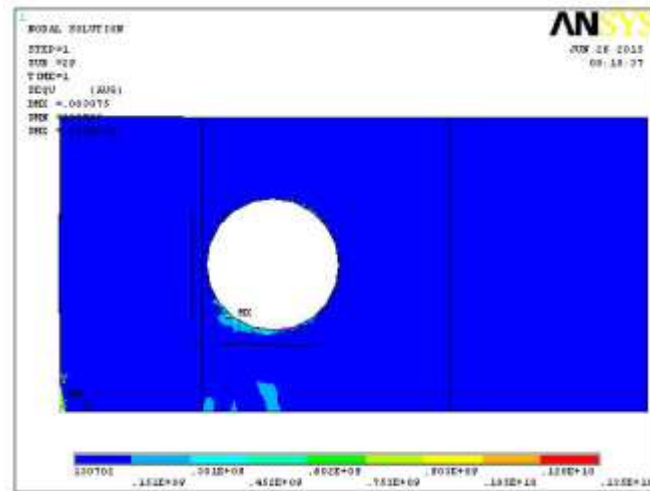


Figure 4.22c: Stress contour of DBCS1 at initial load step

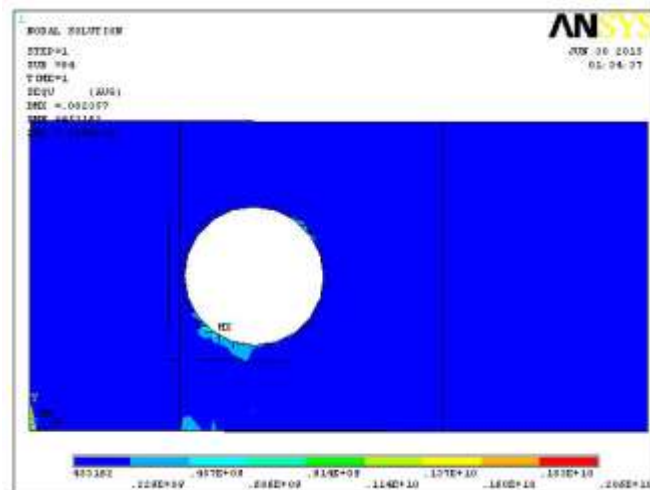


Figure 4.22d: Stress contour of DBCS3 at critical load step

4.6 VALIDATION OF FINITE ELEMENT ANALYSIS RESULTS WITH EXPERIMENTAL RESULTS

It is commonly accepted that RC deep beams with large openings will experience a significant reduction in its load capacity. Strengthened by CFRP externally is the latest technology to recover the load capacity of deep beams with openings. Different shapes are modelled in this study to determine how these parameters affect the beam capacity. Various types of strengthening methods are tried in this study to identify the most effective strengthening method for RC deep beams with openings. Finite element analysis is adopted in this study to analyse all the beams.

4.6.1 Control Beam

The load capacities for all the RC deep beams in FEA results showed an excellent agreement with the experiment results. The load capacities differed within 5% between the experimental and FEA results. FEA by ANSYS estimated the results for all the beams in this study lower than the experimental results. This was more conservative as safety factor had to be taken into account as well. Load-deflection curves also could be used to validate the FEA results. Figure 4.23 showed the load-deflection curve of control beam in both FEA and experiment.

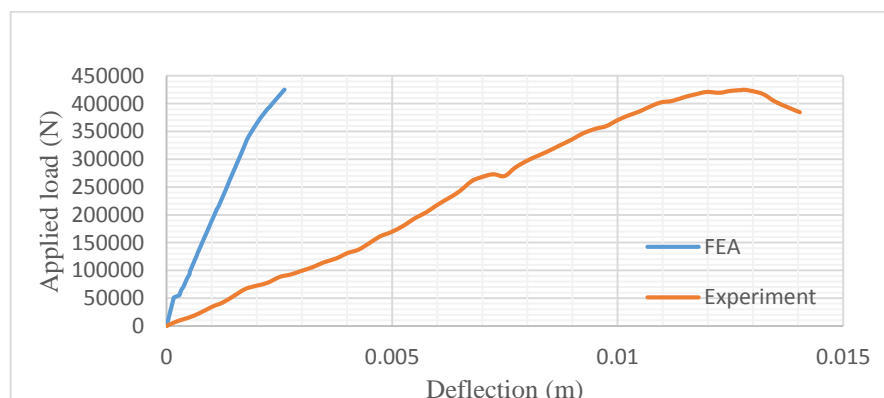


Figure 4.23: Comparison of the load-deflection curve of control beam between FEA and experimental results

Figure 4.24 shows comparison of the crack pattern of control beam in FEA and experiment. Both of the models showed the same diagonal crack pattern. The crack started from the support in experiment and it was just exactly the same with FEA. FEA also showed that the crack started at the support of the beam and lastly diagonal crack was formed. Figure 4.24b shows the pattern of cracking of the modelled control beam. The arrow shows that the crack was along the diagonal path and the crack was to the direction of arrows.

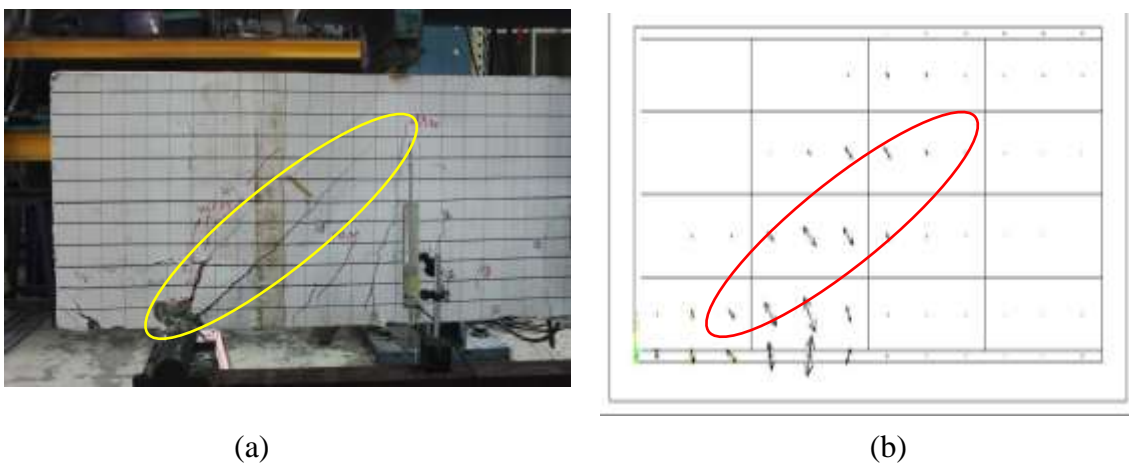


Figure 4.24: Validation of crack pattern in experiment (a) and FEA (b)

4.6.2 RC Deep Beams with Openings (Square and Circular)

Deep beams with openings without strengthening were validated with experiment results. Figure 4.25 shows the load-deflection curve of deep beams with square openings without strengthening of CFRP. Both the beam had similar ultimate load capacity which were 162.56 kN for experiment result and 162 kN for FEA result.

Crack pattern for both results are shown in the following figure. The crack pattern showed the similar trend that the crack was started at the sharp edge of the opening, slowly formed towards the location of applied load and the support. The crack pattern at the sharp edges of both results are clearly shown in Figure 4.26.

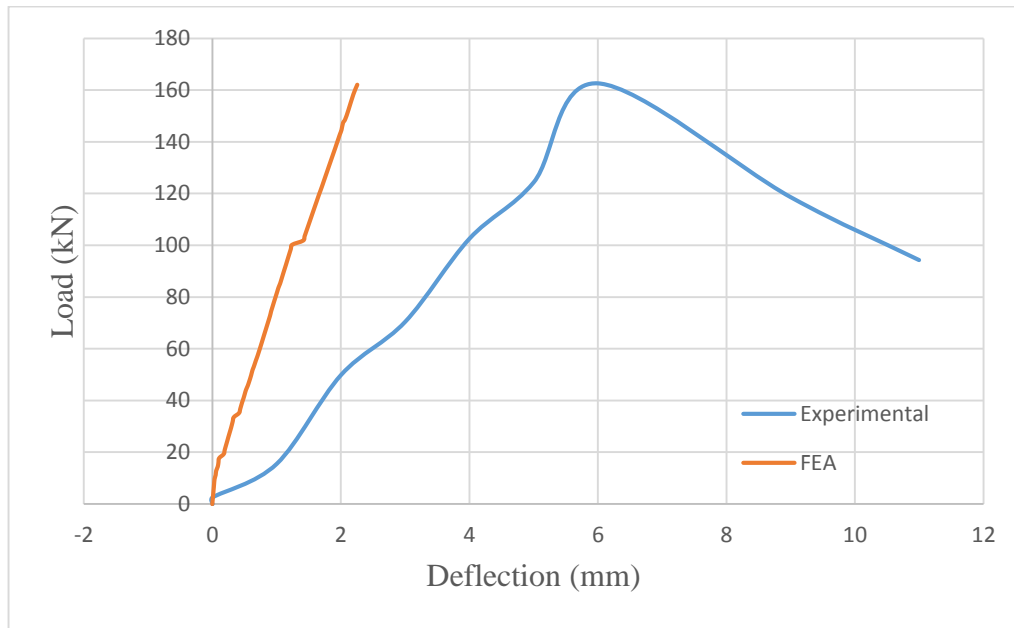


Figure 4.25: Load-deflection curve of deep beams with square openings

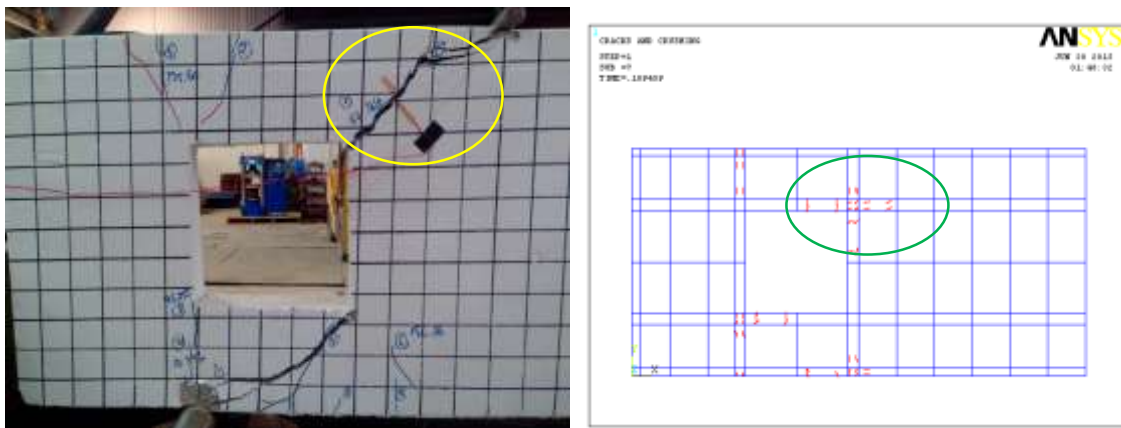


Figure 4.26: Load-deflection curve of deep beams with square openings without strengthening of CFRP

Deep beams with circular openings without strengthening were validated with experimental results. Figure 4.27 shows the load-deflection curve of deep beams with circular openings without strengthening of CFRP. Both the beam had similar ultimate load capacity which was 207.47 kN for experiment result and 207 kN for FEA result. Figure 4.28 shows comparison of the crack pattern of DBC1 in FEA and experiment.

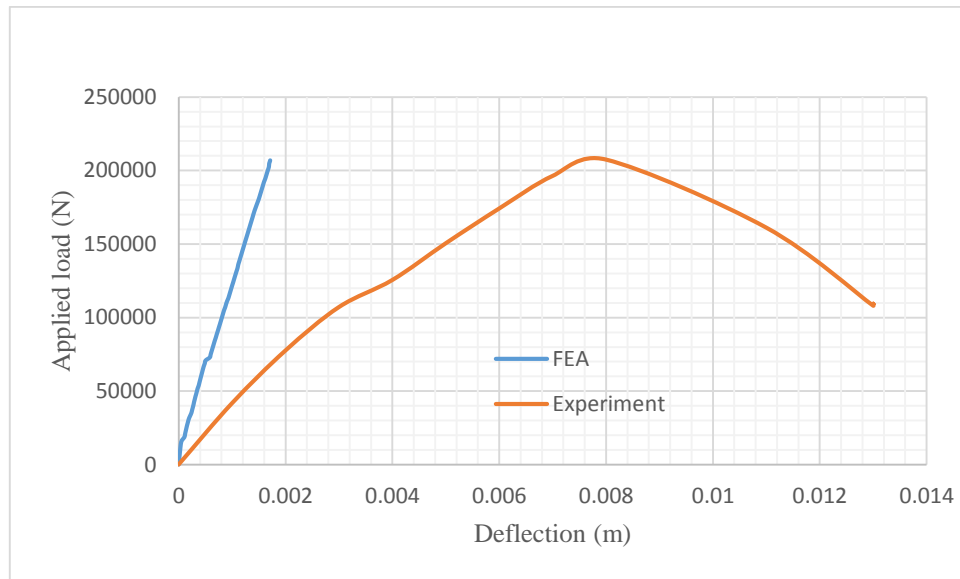


Figure 4.27: Load-deflection curve comparison for deep beams with circular openings in FEA result and experimental result

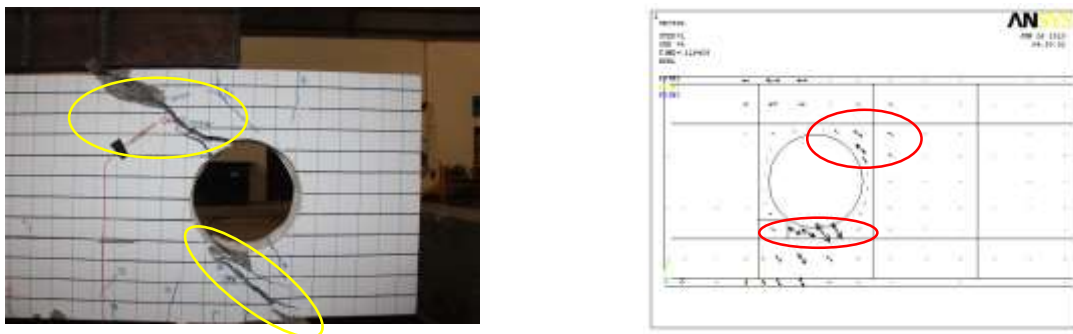


Figure 4.28: Crack patterns between FEA and experiment

4.6.3 Strengthened RC Deep Beams

4.6.3.1 Surface Strengthening for RC Deep Beams with Circular Openings (DBCS1)

Surface strengthening method was validated by comparing the DBCS1 to the experimental result. Load-deflection curve and crack pattern were compared to validate the result. The maximum load capacity of DBCS1 was 238.1 kN and experimental result gave a slightly lower load capacity of 238 kN. Figure 4.30 shows the similarity of the FEA result and experimental result between the crack patterns.

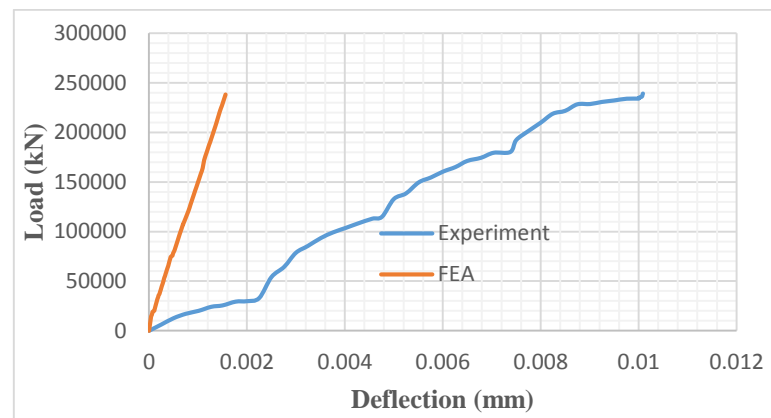


Figure 4.29: load-deflection curve between experimental and FEA results

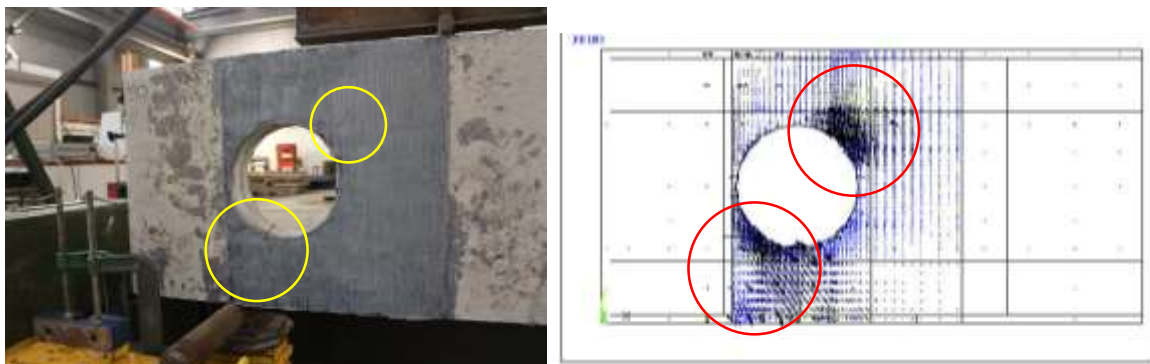


Figure 4.30: Crack patterns between experimental and FEA results

4.6.3.2 U-wrap Strengthening of DBSS7 and DBCS3

U-wrap strengthening method was validated by experimental results as well. Deep beam with square opening strengthened by CFRP was validated by using deep beams with square openings strengthened by U-wrap cut strips CFRP in vertical alignment (DBSS7). Load-deflection curve and crack pattern were shown in the figures below.

Figure 4.31a shows the comparison between the FEA and experimental result in term of load-deflection behaviour. The load-deflection curves showed that the maximum value of FEA was 264 kN which was very close to the experimental result (264.6 kN). Figure 4.31b shows the crack pattern of both FEA and experimental results. Both figures indicated the same crack pattern at the initial step. FEA showed that there was a crack between the side CFRP and top CFRP and this was proven by experimental result that the crack was initiated at the same location.

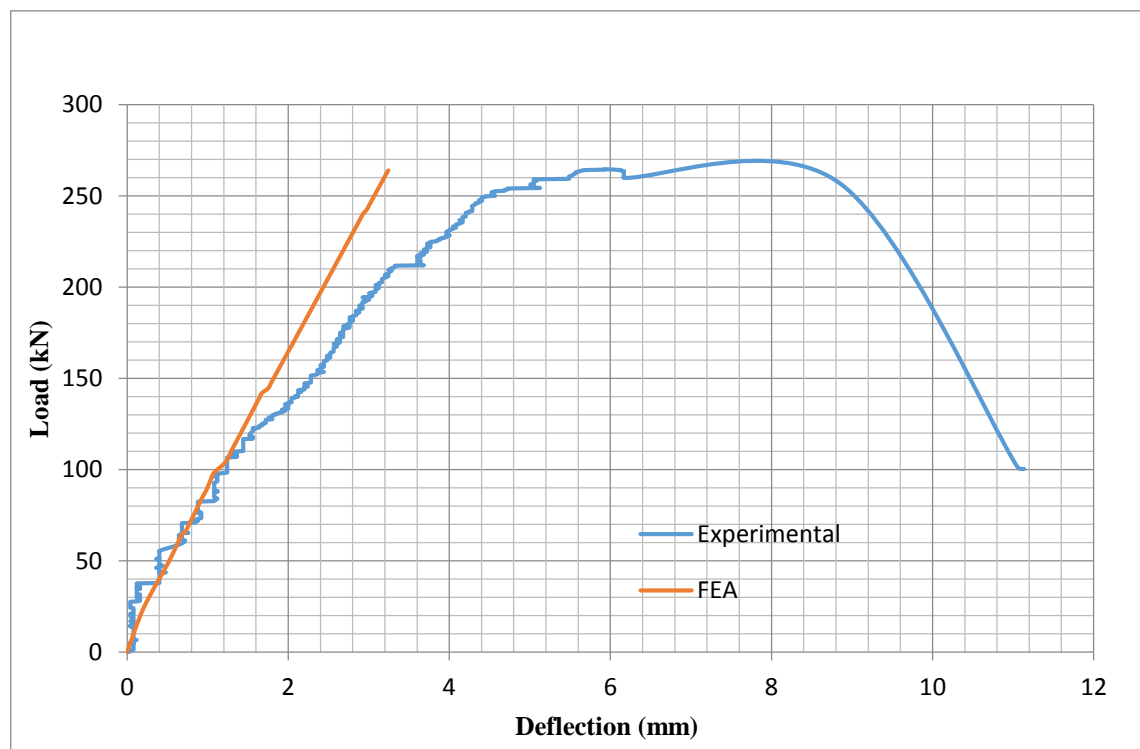


Figure 4.31a: Load-deflection curves of DBSS7 as compared to experimental result

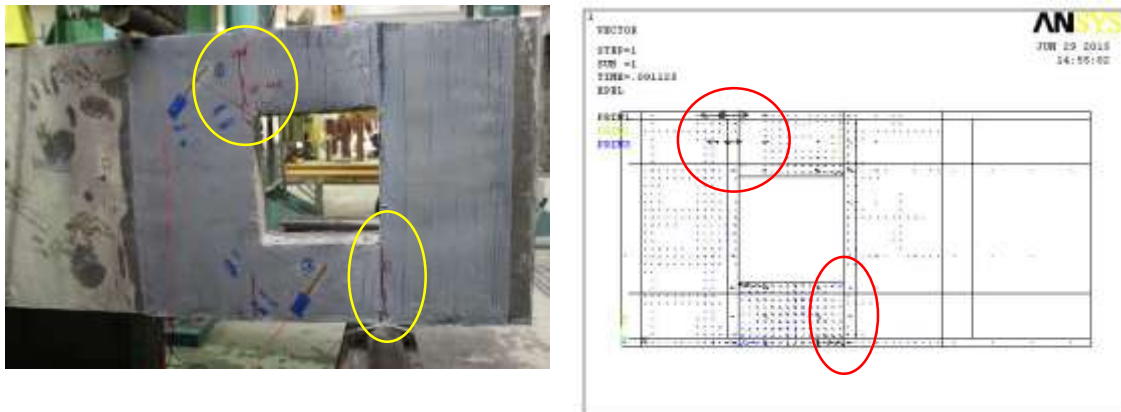


Figure 4.31b: Crack pattern of DBSS7 in FEA and experimental crack

Figure 4.32a shows the crack pattern of DBCS3 and from the experimental result. Both crack pattern also showed that the crack initiated from the circumference and then move towards the support and location of applied load. Figure 4.32b shows the load-deflection curves of both FEA and experimental result for strengthened deep beams with circular openings by U-wrap method in vertical alignment. The maximum value for FEA was 383.04 kN while the maximum value of experimental result was 383.8 kN. FEA load-deflection showed a very stiff behaviour while experimental load-deflection curve showed a more brittle behaviour.

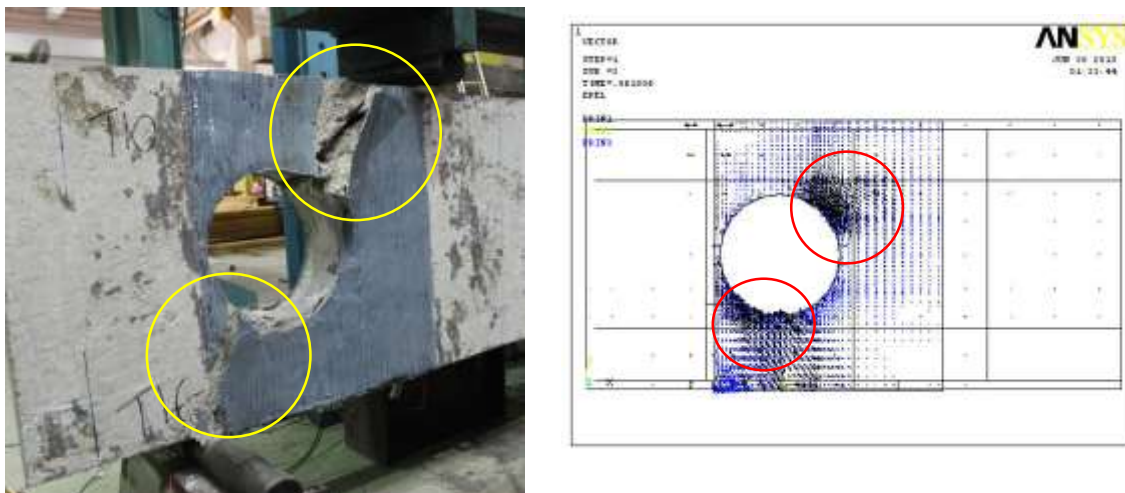


Figure 4.32a: Crack pattern of DBCS3 and experimental crack

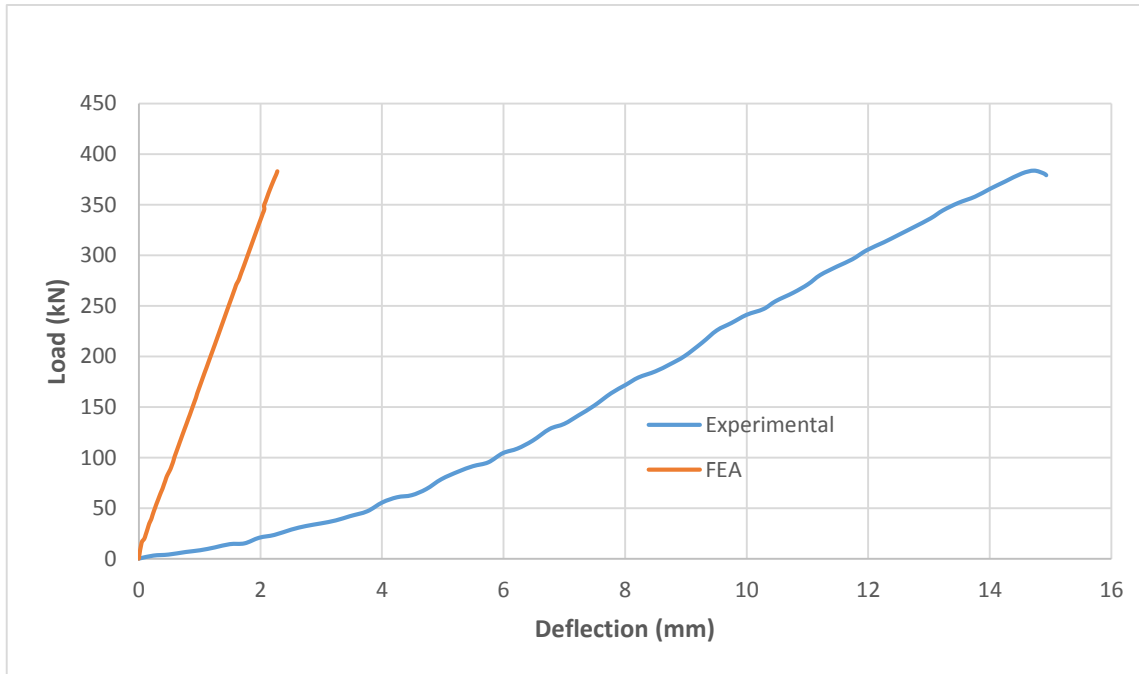


Figure 4.32b: Load-deflection curve of DBCS3 and experimental crack

4.7 SUMMARY OF THE RESULTS

Table 4.1 summarizes all the load from the FEA and compared to the experimental result. The reduction of load capacity significantly dropped for both openings and the dropped was up to 61.9% for the square openings. The recovery of the load capacity in U-wrap methods showed an excellent results as the maximum recovery was 83.6%. From the finding, the load capacity of the beams were not recovered to the original load capacity of the beams as the large openings gave a magnified effect to the load path.

Table 4.1: Comparison of FEA and experimental results and percentage of the beams

Beam	Finite Element Result (kN)	Experimental Result (kN)	Percentage of Reduction (%)	Percentage of Recovery (%)	Percentage from the Control Beam (%)
CB	425.0	425.12	-	-	-
DBS	162.0	162.56	61.9	-	38.1
DBSS1	223.0	-	-	37.7	52.5
DBSS2	221.0	-	-	36.4	52.0
DBSS3	212.4	-	-	31.1	50.0
DBSS4	210.0	-	-	29.6	49.4
DBSS5	264.2	-	-	63.0	62.1
DBSS6	262.0	-	-	61.7	61.6
DBSS7	264.0	264.60	-	63.0	62.1
DBC	207.0	207.47	51.3	-	48.7
DBCS1	238.1	238	-	15.0	56.0
DBCS2	237.1	-	-	14.5	55.8
DBCS3	383.1	383.80	-	85.0	90.1
DBCS4	380.1	-	-	83.6	89.4

CHAPTER 5

CONCLUSION AND RECOMMENDATION

5.1 CONCLUSION

In conclusion, FEA showed a comparable agreement on the load-deflection behaviour and an excellent agreement on the crack patterns obtained by FEA analysis and experimental work. Deep beams with openings failed due to shear crack because the load path had been disturbed. Opening shapes with sharp edges even worsened the load capacity of the beams. External strengthening was successfully analysed in this study to identify the most effective method of strengthening for the weakened RC deep beams.

The objectives of this study were successfully achieved and the conclusion can be drawn as follow.

- i. Load-deflection curves were obtained for all the modelled beams and analysed to determine the stiffness and behaviours of the beams. Load capacity of control beam was found to be 425 kN. Reduction of 62.0% and 51.3% in load capacity for square and circular openings respectively. The load capacity dropped significantly were basically due to two majors reasons which the size of the openings were considered as large opening (45% of the depth) and the openings were located at the most critical shear zone. The openings were located 300 mm from the edge of the beams which the positions of supports were located. Crack patterns were obtained for two stages which were the initials step and critical steps to identify the failure mode of the modelled beams. The crack patterns all showed the cracking started at the edges of the openings, supports and the location of

applied load. The cracks formed a diagonal crack at the end of the analysis. The crack patterns in FEA matched with the experimental cracks similarly. Stress and strain contours were used to study the load path and deformation of crack of the RC deep beams. The stress contour showed that the stress was concentrated at the sharp edges and formed diagonally.

- ii. Two different shapes were adopted in this study to identify the effect of shapes. Through this study, it was found that the opening shape with sharp edge e.g. square openings, weakened the deep beams more critically as the reduction was around 62.0% from 425 kN to 162.0 kN. Opening shape with sharp edge not only disturbed the load path but also weakened the load capacity of the beams by allowing the cracks easily to form at the sharp edges. The load capacity of deep beam with circular openings was 207.0 kN. Reduction of 51.3% from the control beam. Circular openings showed a higher load capacity due to the circular openings distributed the stress around the openings more uniformly. The concentration of stress was lower than that in the square openings. The load capacities of deep beams without strengthening proved that the different shapes affected the deep beams with different of degree and sharp edges worsen the deep beam more.

- iii. From the result obtained, it was found that the most effective method to strengthen the RC deep beams with openings was U-wrap strengthening method with whole piece in 90° orientation. The recoveries of the load capacity were 63.0% and 83.6% for square openings and circular openings, respectively. It was 25.3% higher than that surface strengthening method as compared DBSS7 to DBSS1. U-wrap method managed to disperse the crack patterns more to the outside of the area of strengthening uniformly when compared to surface strengthening. A minimum deflection showed when both method of strengthening experienced the same amount of load.

5.2 RECOMMENDATION

There are a few precaution and improvement have to be taken into consideration for further study in similar approach. With the recommendations given below, better and more accurate results can be obtained from the finite element analysis.

- i. Strengthening method should be diversified and more methods should be considered in the study e.g. numbers of layers of CFRP applied on beams, CFRP wrapped in inclined method and etc.
- ii. Values, parameters and materials properties from the experiments have to be tested and obtained. Then the values should be used for the FEA to obtain a more convincing results.
- iii. Epoxy of the CFRP have to be correct because the bonding between the concrete and CFRP plays a significant role in the study.
- iv. Yielding stress of the beams in ANSYS had to be identified to reduce the stiffness of the modelled beams to show a better non-linear results.

References

- Alemdar, F., Matamoros, A., Bennett, C., Asce, M., Barrett-gonzalez, R., Rolfe, S. T., ... Asce, H. M. (2012). Use of CFRP Overlays to Strengthen Welded Connections under Fatigue Loading, 420–431. doi:10.1061/(ASCE)BE.1943-5592.0000230.
- Al-Mahaidi, R., Lee, K., & Taplin, G. (2001). Behavior and Analysis of RC T-Beams Partially Damaged in Shear and Repaired with CFRP Laminates, 1–8.
- Alsaeq, H. M. (2014). Enhancing the Structural Behavior of R . C . Deep Abstract :, (2).
- Amin, H. M., Agarwal, V. C., & Aziz, O. Q. (2013). Effect of Opening Size and Location on the Shear Strength Behavior of R . C Deep Beams without Web Reinforcement Continuous Deep Beams to evaluate the Shear Strength with, (7), 28–38.
- Badawi, M., & Soudki, K. (2005). Control of Corrosion-Induced Damage in Reinforced Concrete Beams Using Carbon Fiber-Reinforced Polymer Laminates. *Journal of Composites for Construction*, 9(2), 195–201. doi:10.1061/(ASCE)1090-0268(2005)9:2(195)
- Badawi, M., & Soudki, K. (2010). CFRP Repair of RC Beams with Shear-Span and Full-Span Corrosions, (June), 323–335.
- Ban, L., & Abduljalil, S. (2014). With Opening Strengthened By CFRP Strips Abstract :
فأبلاً ذ وبر اكلا تيريميلوبلا تمواقم ص قلا تابتعلا تيناسر خلا تحلسما تقيمعا تاذ تاحتقلا ةواقملا حنارشيد
18(1), 14–32.
- Birrcher, D., Tuchscherer, R., Huizinga, M., & Bayrak, O. (2009). Depth Effect in Reinforced Concrete Deep Beams, 1595–1603.
- Birrcher, D., Tuchscherer, R., Huizinga, M., Bayrak, O., Wood, S., & Jirsa, J. (2008). Strength and Serviceability Design of Reinforced Concrete Deep Beams, 7. Retrieved from <http://trid.trb.org/view.aspx?id=891084>
- Campione, G., & Minafò, G. (2012). Behaviour of concrete deep beams with openings and low shear span-to-depth ratio. *Engineering Structures*, 41, 294–306. doi:10.1016/j.engstruct.2012.03.055
- Dadvar, B. (2014). Design and Modeling of Slender and Deep beams with Linear Finite Element Method, (March).
- El Maaddawy, T., & Sherif, S. (2009). FRP composites for shear strengthening of reinforced concrete deep beams with openings. *Composite Structures*, 89(1), 60–69. doi:10.1016/j.compstruct.2008.06.022

- El-maaddawy, T., & El-ariss, B. (2012). Behavior of Concrete Beams with Short Shear Span and Web Opening Strengthened in Shear with CFRP Composites, (February), 47–59. doi:10.1061/(ASCE)CC.1943-5614.0000237.
- Elsafty, A., & Graeff, M. K. (2013). Optimum CFRP Configuration to Efficiently Repair Laterally Damaged, Simply Supported Rectangular Reinforced Concrete Beams, (August), 165–176. doi:10.1061/(ASCE)SC.1943-5576.0000150.
- Farghaly, A. S., & Benmokrane, B. (2013). Shear Behavior of FRP-Reinforced Concrete Deep Beams without Web Reinforcement. *Journal of Composites for Construction*, 17(6), 04013015. doi:10.1061/(ASCE)CC.1943-5614.0000385
- Flaga, K. (2000). Advances in materials applied in civil engineering. *Journal of Materials Processing Technology*, 106(1-3), 173–183. doi:10.1016/S0924-0136(00)00611-7
- Godat, A., Neale, K. W., & Labossière, P. (2007). Numerical Modeling of FRP Shear-Strengthened Reinforced Concrete Beams. *Journal of Composites for Construction*, 11(6), 640–649. doi:10.1061/(ASCE)1090-0268(2007)11:6(640)
- Hafiz, R. B., Ahmed, S., Barua, S., & Chowdhury, S. R. (2014). Effects of Opening on the Behavior of Reinforced Concrete Beam. *IOSR Journal of Mechanical and Civil Engineering*, 11(2), 52–61. doi:10.9790/1684-11275261
- Hawileh, R. a., El-Maaddawy, T. a., & Naser, M. Z. (2012a). Nonlinear finite element modeling of concrete deep beams with openings strengthened with externally-bonded composites. *Materials and Design*, 42, 378–387. doi:10.1016/j.matdes.2012.06.004
- Hawileh, R. a., El-Maaddawy, T. a., & Naser, M. Z. (2012b). Nonlinear finite element modeling of concrete deep beams with openings strengthened with externally-bonded composites. *Materials & Design*, 42, 378–387. doi:10.1016/j.matdes.2012.06.004
- Hemanth, K. (2012). Experimental and numerical studies on behavior of FRP strengthened deep beams with openings, (May). Retrieved from <http://scholar.google.com/scholar?hl=en&btnG=Search&q=intitle:Experimental+and+numerical+studies+on+behaviour+of+frp+strengthened+deep+beams+with+openings#0>
- K.W. Neale, P. L. and M. T. (2000). FRPs for Strengthening and Rehabilitation: Durability Issues. *Concrete*, 8000(x 2119), 1–8.
- Khalifa, A., Gold, W. J., Nanni, A., & M.I., A. A. (1998). Contribution of Externally Bonded FRP to Shear Capacity of RC Flexural Members. *Journal of Composites for Construction*, 2(4), 195–202. doi:10.1061/(ASCE)1090-0268(1998)2:4(195)
- Kim, S.-W., & Vecchio, F. J. (2008). Modeling of Shear-Critical Reinforced Concrete Structures Repaired with Fiber-Reinforced Polymer Composites. *Journal of*

- Structural Engineering*, 134(8), 1288–1299. doi:10.1061/(ASCE)0733-9445(2008)134:8(1288)
- Kong, F. (2006). *Reinforced concrete deep beams*. (F. K. Professor Kong, Ed.) *Zhurnal Eksperimental'noi i Teoreticheskoi Fiziki*. Van Nostrand Reinhold. Retrieved from <http://scholar.google.com/scholar?hl=en&btnG=Search&q=intitle:No+Title#0>
- Masuelli, M. A. (2013). Introduction of Fibre-Reinforced Polymers – Polymers and Composites : Concepts , Properties and Processes, 3–40. doi:<http://dx.doi.org/10.5772/54629>
- Mohamed, A. R., Shoukry, M. S., & Saeed, J. M. (2014). Prediction of the behavior of reinforced concrete deep beams with web openings using the finite element method. *Alexandria Engineering Journal*, 53(2), 329–339. doi:10.1016/j.aej.2014.03.001
- Moreno, M. Á., Monteagudo, E., Maia, I., & Ingeciber, S. A. (2001). ANSYS + CivilFEM : High -End Solution For Advanced Civil Engineering Projects.
- Patel, M. R., & Tank, T. (2014). Finite element modeling of RC deep beams strengthened in shear with CFRP strips, (August), 69–76.
- Roylance, D. (2001). *Finite element analysis*. Retrieved from http://books.google.com/books?hl=en&lr=&id=JsCg-QWUT28C&oi=fnd&pg=PA1&dq=Finite+Element+Analysis&ots=jRtwXTsAgQ&sig=EjAO16TH9QzX0LbZLqBX-V3_P2U
- Saiedi, R., Eng, P., Green, M. F., Fam, A., & Asce, M. (2013). Behavior of CFRP-Prestressed Concrete Beams under Sustained Load at Low Temperature, 27(1), 1–15. doi:10.1061/(ASCE)CR.1943-5495.0000045.
- Seo, S.-Y., Yoon, S.-J., & Lee, W.-J. (2004). STRUCTURAL BEHAVIOR OF R/C DEEP BEAM WITH HEADED. In *13th World Conference on earthquake Engineering*. Vancouver, B.C., Canada.
- Sezen, H. (2012). Repair and Strengthening of Reinforced Concrete Beam-Column Joints with Fiber-Reinforced Polymer Composites, (October), 499–506. doi:10.1061/(ASCE)CC.1943-5614.0000290.
- Shaw, M. (n.d.). Structural Strengthening with external plate bonding. Welwyn Garden City. Retrieved from http://www.bath.ac.uk/cwct/cladding_org/icbest97/paper24.pdf
- What is a beam? | Tata Steel Construction. (n.d.). Retrieved December 7, 2014, from <http://www.tatasteelconstruction.com/en/reference/teaching-resources/architectural-teaching-resource/elements/design-of-beams-structural-steel/what-is-a-beam>

APPENDIX A

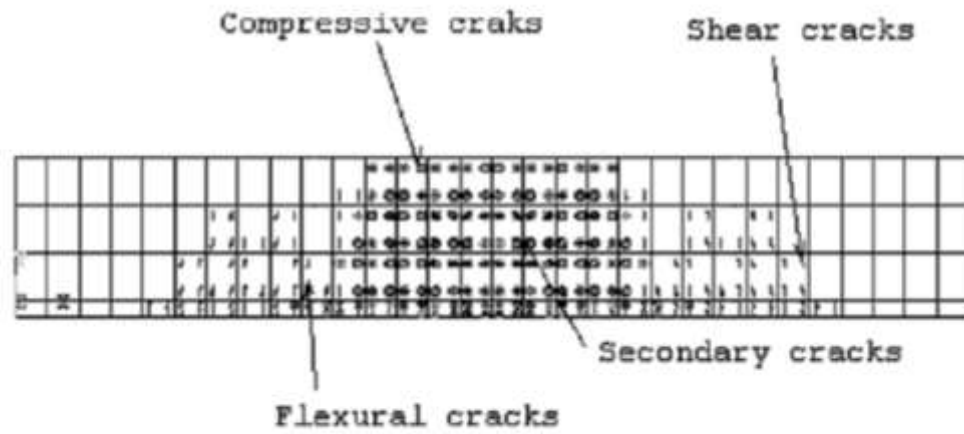


Figure A1: Types of crack patterns in ANSYS

APPENDIX B

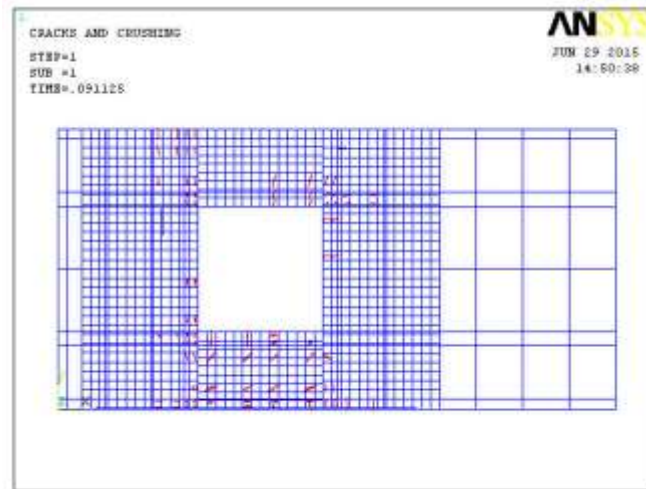


Figure B1: Crack pattern of DBSS7 at initial step

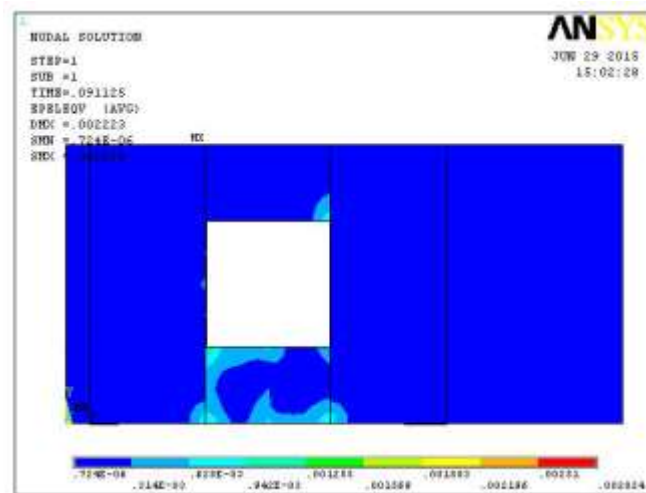


Figure B2: Strain contour of DBSS7 at initial step

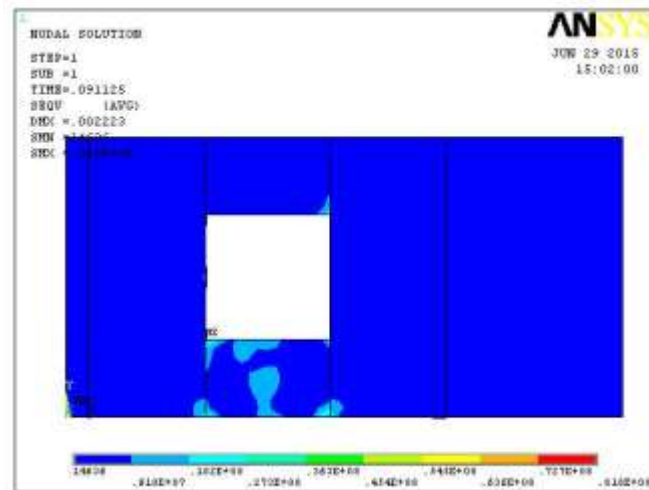


Figure B3: Stress contour of DBSS7 at initial step

APPENDIX C

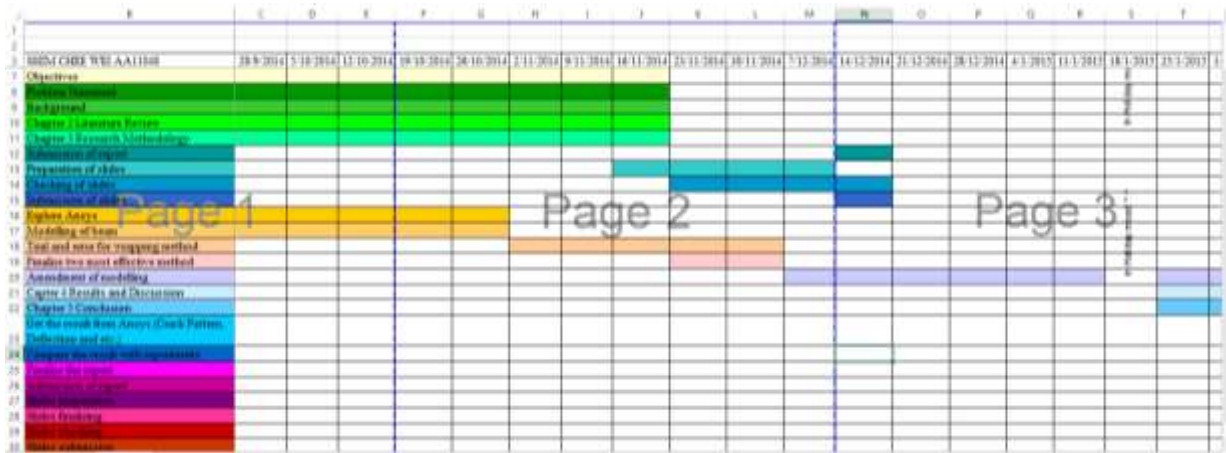


Figure C1: Gantt chart of the study